An-Najah National University

Faculty of Graduate Studies

EXPLORING THE RELATIONSHIP BETWEEN THE DEFLECTION AMPLIFICATION FACTOR AND THE TIME PERIOD OF REINFORCMENT CONCRETE – MOMENT RESISTING FRAME STRUCTURES

By

Murad Ribhy Hussin Bsharat

Supervisors

Dr. Monther Dwaikat

Dr. Munther Diyab Ibrahim

This Thesis is Submitted in Partial Fulfillment of the Requirements for the Degree of Master of Structural Engineering, Faculty of Graduate Studies, An-Najah National University, Nablus, Palestine.

2024

EXPLORING THE RELATIONSHIP BETWEEN THE DEFLECTION AMPLIFICATION FACTOR AND THE TIME PERIOD OF REINFORCMENT CONCRETE – MOMENT RESISTING FRAME STRUCTURES

By

Murad Ribhy Hussin Bsharat

This thesis was Defended Successfully on 12/06/2024 and approved by

Dr. Monther Dwaikat	
Supervisor	Signature
Dr. Munther Diyab Ibrahim	
Co-Supervisor	Signature
Dr. Abdulsamee Halahla	
External Examiner	Signature
Dr. Mohammad Samaaneh	
Internal Examiner	Signature

Dedication

This thesis is dedicated to my dear parents who have encouraged and supported me. Also, to my great family and friends.

Acknowledgment

First of all, I am thankful to the almighty God for granting me good health, strength and peace throughout the research period.

I would like to thank everyone who has contributed to accomplishing this thesis.

I would want to express my heartfelt gratitude to my academic advisor Dr. Monther Dwaikat and Dr. Munther Diyab Ibrahim. for their extraordinary support in this project process. I think the completion of this project would not have been possible without their guidance and support.

I would like to sincerely thank my family and friends for their endless support and encouragement throughout the project.

Declaration

I, the undersigned, declare that I submitted the thesis entitled:

EXPLORING THE RELATIONSHIP BETWEEN THE DEFLECTION AMPLIFICATION FACTOR AND THE TIME PERIOD OF REINFORCMENT CONCRETE – MOMENT RESISTING FRAME STRUCTURES

I declare that the work provided in this thesis, unless otherwise referenced, is the researcher's own work, and has not been submitted elsewhere for any other degree or qualification.

Student's Name: **Murad Ribhy Hussin Bsharat**

Signature: Murad Ribhy Hussin Bsharat

Date: **2024/06/12**

List of Contents

List of Tables

List of Figures

List of Appendices

EXPLORING THE RELATIONSHIP BETWEEN THE DEFLECTION AMPLIFICATION FACTOR AND THE TIME PERIOD OF REINFORCEMENT CONCRETE -MOMENT RESISTING FRAME STRUCTURES

By
Murad Ribhy Hussin Bsharat
Supervisors
Monther Dwaikat
Dr. Munther Diyab Ibrahim

Abstract

The deflection amplification factor (C_d) is an important parameter in seismic design. C_d is essential in seismic design according to the American Society of Civil Engineers minimum design load standards (ASCE7-16) especially for the drift check and for the calculation of the seismic separator distance.

Contractors face difficulty in implementing seismic separation, especially in high-rise buildings. The seismic separator is computed in ASCE7-16 depending on the C_d factor by calculating the inelastic displacement, which is crucial for calculating the seismic separation.

C_d remains constant for the same structural system, as per ASCE7-16, regardless of the building characteristics such as (time period which depends on span length, story height and numbers of bays). The goal of this work is to obtain a C_d value for each building based on the building's characteristics, which helps in reducing the width of the seismic separator, especially for high-rise buildings.

To achieve this goal, various parameters associated with building characteristics that may influence C_d value were studied. 36 case studies of square-shaped building models with varying numbers of floors, floor height, span length, and the number of bays were analyzed using both linear and nonlinear time history analysis. Three-time history records that match the response spectrum in SAP2000 and seismomatch are used to compute C_d. On the other hand, the computer software, ETABS was used for the structural design considering both gravity and seismic loads.

Results from the analysis show that ASCE 7-16 is conservative in presenting C_d values and that $C_{d\ varies}$ depending on the characteristics of the building. The results show that

the value of C_d decreases with increasing span length, story height, number of bays, and time period (T_n). The results of this study were used to develop an equation to estimate C_d based on the building characteristics.

Keywords: Deflection amplification factor, C_d, SMRFs, Time history, Response Spectrum, nonlinear displacement, liner displacement, fiber hinge.

Chapter One
Introduction

1.1 Overview

In regions prone to earthquakes, ensuring the safety and structural integrity of buildings is crucial. Designing structures that can withstand earthquakes involves various factors, including the deflection amplification factor (C_d).

C_d value is very important for high-rise buildings because it's used to determine the seismic separator and check drift.

C_d is crucial for calculating inelastic displacement. Engineers use C_d by multiplying it with elastic displacement to find the resulting inelastic displacement. This value is then utilized to calculate the seismic separation between two buildings. Construction of high-rise buildings based on may conservative C_d values taken from ASCE Code 7-16, which do not take into account the characteristics of the building. A challenge arises from the role that the Cd value plays in determining the seismic separator, as it gives a large distance between two adjacent buildings that is difficult to apply when carrying out building construction.

Previous research and insights from books on the dynamics of structures suggest that the C_d factor may decrease as the building height (and hence the period of the building) increases (Chopra, 2017). If an equation is developed to obtain a C_d value that takes into account the building properties, a specific C_d value can be calculated for each building. This is in contrast to the ASCE7-16 code, which adopts precise values for the identical structural system. This approach can reduce the distance of the seismic separation between buildings if the Cd value is less than ASCE7-16 code, as a result addressing an assignment that engineers face at some point of the implementation of constructing construction.

The improvement of an equation (mathematical expression) governing the Cd value represents a large advancement in displacement-based layout methodologies. This development complements the precision and reliability of seismic design, supplying engineers worldwide with the ability to fine-tune designs to achieve targeted performance levels.

1.2 Definition of Deflection Amplification Factor (C_d)

Cd, which referred to as the deflection amplification issue, is a critical parameter used in structural engineering to assess the quantity to which the deflection of a building is multiplied mainly occasions. Indeed, it assists engineers in comprehending and forecasting how expertise and predicting how a shape will reply to external forces. Further, by using taking Cd into consideration and controlling the degrees of deflection, engineers can make certain that homes continue to be safe.

Cd represents the ratio of the expected displacement, throughout a seismic occasion (most inelastic displacement) to the deflection determined the usage of elastic evaluation (ASCE7-sixteen, 2017). It quantifies how a great deal the buildings movement is magnified for the duration of an earthquake compared to its motion beneath ordinary conditions.

This parameter performs a function in layout and assessment presenting insights, into structures dynamic behavior in the course of earthquakes and helping in designing buildings to withstand seismic forces effectively.

1.3 Research Significance

This study seeks to address a major engineering hurdle of seismic separation, especially when designing high-rise buildings. The hurdle revolves around a critical factor known as C_d. Engineers usually rely on C_d to check the drift and determine the separation distance between two adjacent buildings. In high-rise buildings, structural seismic separation becomes a large distance when using ASCE7-16, which creates challenges for implementation. C_d value remains constant in ASCE7-16 for same structural system regardless of the specific characteristics of the building. Hence, the aim is to obtain a specific C_d value for building based on it is characteristics, which value may be less than the code value based on previous studies suggested that the C_d coefficient tends to decrease with increasing building height which will be discussed in the chapter two. This enables the hurdle seismic separator solution, which is affected by the value of the C_d.

The aim of this thesis is to understand how structure characteristics (span length, story height, number of bays, and time period (T_n)) effect on the C_d for buildings with the RC-SMRF structural system. It also aims to explain the effects of building characteristics on

C_d by creating an empirical equation through which the value of C_d is calculated based on the building's characteristics, if the results of the analysis allow.

1.4 Objectives

The primary goal of this study is to reevaluate the C_d, in conventional Reinforced Concrete Special Moment Resisting Frames (RC-MRFs) that commonly used in Palestine. This reassessment involves using nonlinear time history analysis tools to investigate how the C_d is influenced by structural time periods (related to mass and stiffness) and structural geometry (span length, story height, and the number of bays).

To achieve this goal, the research begins with a thorough literature review to examine recent studies on the C_d, aiming at gaining insights into the subject. Subsequently, nonlinear time history analysis is applied to understand the relationship between the deflection amplification factor for RC-MRFs and the structural geometry and time period. A simplified equation has been devloped for the defliction amplification factor (C_d). using statistical regression.

1.5 Structure of the Thesis

This thesis unfolds by way of presenting distinctive chapters, every contributing to the overall exploration.

Chapter One: Introduction and Literature Review:

The thesis opens with a short but comprehensive introduction in the first chapter. This Chapter This chapter seeks to address the research problem and highlight its importance within this field. On the other hand, presents an in-depth examination of the associated challenges with modeling (specifically issues pertaining to simulating fiber hinges) using linear or non-linear time-history analyses. It also treats validation and verification of the analysis tool, material nonlinearity, review literature relevant to this study.

Chapter Two: Modeling and Analysis:

In this Chapter, this thesis delves into the intricacies of modeling particularly focusing on the hurdles associated with portraying fiber plastic hinges. The chapter also delves into computing both inelastic displacements using linear and nonlinear time history analyses to determine the C_d value.

Chapter Three: Proposed Equation for C_d :

The Chapter Three holds significance within the thesis framework. It showcases the effects of the analysis for 36 scenarios highlighting the Cd particular characteristics of each parametric study. An examination of the collected records is carried out to explain how every parametric study (each building characteristic) influences Cd, observed with the aid of a formulation for locate the Cd value based based on building characteristics.

Chapter Four: Conclusions and Recommendations:

Acting as a repository for discoveries within the thesis Chapter Four consolidates research findings into conclusions and offers evidence-based totally suggestions critical, for seismic engineering.

1.6 Overview

Understanding seismic engineering is understanding how structures perform under dynamic forces, especially those caused by earthquakes. The Deflection Amplification Factor is a key parameter in this understanding of structural dynamics, which depends on for the most part about C_d. The need for C_d and its importance in seismic design, especially in drift and seismic separator is explains extensively by this thesis.

Through linear and nonlinear time-history analysis, a software like SAP2000 will calculate the C_d value by getting elastic and inelastic displacement.

Cd value is an important parameter in seismic design. screening drifts that govern the dimensions of concrete sections and the distance between adjacent buildings (seismic separator). This chapter examines the various methods of calculating Cd from engineering codes and literature. After that the design criteria of Special Moment Resisting Frames (SMRFs) are collected based in ACI-318. Also, linear and non-linear time-history analyses are carried out.

1.7 Special Moment Resisting Frames (SMRF)

SMRFs (Special Moment Resisting Frames) are utilized to withstand under the influence of lateral loads such as wind or earthquake force. Generally, composed of beams and columns interconnected by strong joints that allow them to transfer lateral loads from the building down through connections all the way driven into ground.

SMRFs add a measure of stability and stiffness to the building, especially in Seismic regions because they help it sustain multiple loads that result from lateral movement respectively.

In Guidelines for ACI detailing of special moment resisting frames, designing criteria are given with respect to material properties, Proper reinforcement detailing, including column and beam reinforcement, ensures adequate ductility and confinement for concrete by ties under seismic loading. Beam-column joint design is crucial, requiring sufficient strength and ductility through special detailing like confinement and shear reinforcement.

1.8 Deflection Amplification Factor by Different Codes.

The deflection amplification factor is crucial in design, so engineers refer to engineering codes to find the factor value. However, each code has its own method for determining this factor value. This section will explain how to find the factor value in the main engineering codes.

1.8.1 ASCE 7-22

For seismic analysis and design, seismic force-resisting systems are categorized in ASCE-7-16's Table 12.2-1, further divided for different types of vertical elements. FEMA P-695 (2009b) establishes a methodology for quantifying seismic system performance, addressing parameters like R, over-strength factor (Ω0), and deflection amplification factor (C_d). These are collectively termed "seismic design coefficients." Future systems are likely to adopt this methodology, with existing coefficients subject to review. Height limits, specified for over 50 years, have evolved based on expert judgment from organizations like the NEHRP Provisions Update Committee and the ATC-3 project team, adjusting over time based on observations and testing, albeit with subjective values (ASCE7-16, 2016).

To Compute C_d, determine the values of $\Delta\, max$ and Δe for the specific seismic loading scenario under consideration from liner and non-liner time history.

Shown (Uang, 1991) that the force reduction and deflection amplification factors for strength design can be expressed by the following formulas, and Figure B .30 in Appendix B explain the General Structural Response :

$$\frac{C_d}{R} = \frac{\mu_S}{R_\mu} = \frac{\left(\frac{\Delta max}{\Delta y}\right)}{\left(\frac{C_e}{C_y}\right)} = \frac{\left(\frac{\Delta max}{\Delta y}\right)}{\left(\frac{\Delta e}{\Delta y}\right)} = \frac{\Delta max}{\Delta_e} \quad (1)$$

Where:

Δ_{max}: maximum inelastic drift.

Δ_e: maximum elastic drift

Δ_e: maximum yielding drift.

C_e: elastic base Shear Ratio.

C_y : yielding base Shear Ratio.

Divide the maximum inelastic displacement (δi) by the maximum elastic displacement(δe):

$$C_d = \delta i * I / \delta e \quad (2)$$

Where:

- (δi): the maximum inelastic displacement
- (δe) :maximum elastic displacement divided on reduction force factor (R).
- I: Important Factor

1.8.2 UBC97 standard

The UBC code obtained the C_d value for SMRFs through a comprehensive analysis of structural behavior data, empirical correlations, and engineering expertise, similar to the approach followed by other seismic design codes like ASCE.

Within the UBC97 standard, the calculation for the nonlinear displacement value is outlined as follows (International Code Council, 1997).

$$\Delta m = \beta Ru \Delta s \quad (3)$$

$$\Delta m = 0.7\, Ru \Delta s \quad (4)$$

The equation No.4 simplify to find C_d to Equation No. 5, where β is set at 0.7, and it can be formulated as:

$$C_d = 0.7Ru \quad (5)$$

Δs: Maximum inelastic displacement of the structure.

Δm: Maximum elastic displacement of the structure.

$R\mu$: Coefficient of ductility behavior.

1.8.3 Eurocode 8

Euro code 8, the deflection amplification factor (often denoted as q) is used to account for increased deflections in structural elements during seismic events, taking into consideration the nonlinear behavior of the structure. The calculation of C_d is a bit more complex and may involve several steps. Here is a simplified overview of how to compute the deflection amplification factor in Eurocode 8 (Solomos, Pinto, & Dimova, 2008):

The Deflection Amplification Factor (C_d) which called (q) can be calculated according Eurocode 8 using in the following equation:

$$q = (Sd / Sa) * (T / To) * \mu \quad (6)$$

Where:

- *Sd*: is the design response spectrum acceleration at the structure's period T.
- *Sa*: is the design ground acceleration.
- *T*: is the fundamental natural period of the structure.
- T_o: is the reference period, usually taken as 1 second.
- μ : Ductility Reduction Factor

Table A.1 in Appendix A displays the usage of C_d in the NEHRP Recommended Provisions.

The subsequent table provides a visual representation of deflection amplification factors within a range of building codes explain in table A .2 in Appendix A.

1.9 Seismic loading

1.9.1 Palestine Seismicity

Palestine is an active seismic region with seismic foci concentrated in areas influenced by the Arabah Valley, the Jordan Rift Valley, the Dead Sea vicinity, and the southern extent of the Sea of Galilee. These seismic influences are connected to fault lines associated with the Depression Zone, demarcating regions between Palestine and Jordan. Noteworthy fault lines include the Fara'a Rift occurring in 1759 (El-Hussain, Sader, & Juhari, 2018). multiple seismic foci are situated, with up to five epicenters located about 10 to 12 kilometers beneath the surface (Meghraoui, 2015). Also, the Carmel Fault, impacting cities like Nablus, Ramallah, and Jerusalem. Near the Dead Sea, Carmel region exhibits activity every 200 to 300 years, with the most recent destructive earthquake.

Palestine experiences recurring earthquakes in various regions. The northern Tiberias region and the Galilee Finger encounter earthquakes approximately every 800 years (Marco et al. 2003). Recent earthquake engineering studies reveal that Palestine region has a medium or medium-high level of seismic hazard (Monteiro, Dursun, & Andrade, 2016).

Analyzing the Earthquake Acceleration (PGA) map for Palestine provides insights into ground shaking intensities' distribution.] This map outlines peak ground accelerations resulting from seismic events, helping identify zones with varying seismic hazard levels (Zones 1, 2A, 2B, and 3) (Filippou, 2013).

The Palestinian Engineers Association mandates earthquake-resistant building design following international codes and local codes like UBC97 or IBC 2012. Figure B.1 in Appendix B illustrates the Seismic Hazard Map and Seismic Zone Factor (Source: ESSEU, Earth Sciences and Seismic Engineering Unit at NNU).

1.9.2 Response Spectrum

The response spectrum, as defined in ASCE 7-16, is a graphical representation depicting the maximum response of a structure to seismic ground motions across different frequencies. It gives engineers the basics of how to analyze and design structures that are safe for seismic forces. This picture is very important to measure the dynamic response

under seismic, which helps practical research in earthquake engineering for construction safety and durability.

Some key parameters for design spectral acceleration in ASCE 7-16 SDS stands for short-period design spectral response acceleration (usually 0.2 seconds). SD1 indicates the spectral response acceleration at 1 second-period, corresponding to a segment of steady velocity in the spectrum. TL marks the transition from this constant-velocity segment to the constant-displacement segment. Understanding these parameters is very vital for seismic analysis and designing which helps an engineer to know the behavior of a structure under earthquake loads and making it safe in case of all earthquakes (Ghosh, 2014).

Figure B.2 in Appendix B shows the ASCE-7-16 design response spectrum.

1.9.3 Time History Records

In the realm of earthquake engineering and structural dynamics, time-history records are datasets that capture ground motion during seismic events. They provide information on ground acceleration, velocity and displacement for instruction on how to move during earthquakes. They help us understand the impacts of earthquakes on structures by telling us how long they last. Besides, they involve frequency content that tells us about energy distribution at different frequencies thus affecting response of a structure. Amplitude measurements in the records quantify the strength of shaking experienced during earthquakes.

The ASCE7-10 code, which is section 16.14, prescribes specific requirements for seismic analysis. These include the use of at least three ground motion record sets in order to ensure a comprehensive evaluation of structural response to ground motions. This means that a minimum of three sets of ground motion records must be used in any analysis. If there are less than seven sets, the design parameters will be based on the maximum values obtained from all the analyses. Conversely, where seven or more records are involved in an analysis, design can be based on average values derived from the analysis. Although using seven or more ground movements is useful, for the sake of more case studies and available technical capabilities, only three combinations are used.

Figure B.3 in Appendix B illustrates the earthquake record format adopted by the International Building Code (IBC).

Table A.3 in Appendix A shows the characteristics of three ground records used in both linear and nonlinear time-history analysis.

1.9.4 Time History Matching to Response Spectrum

In seismic engineering and analysis, aligning ground motion time records with specific response spectra is crucial, particularly in Palestine where the seismic hazard is different from other locations. In order to better understand how structures interact with potential seismic loads. It requires selecting and modifying time history records to accurately simulate local seismic events. This involves utilizing software tools like SeismoMatch and SAP2000, which facilitate the matching of temporal structural response profiles to response spectra. SeismoMatch uses specialized algorithms for spectral matching, while SAP2000 reconciles the process involves refining chronological data by iteratively comparing it with response spectra. Figure B .4 in Appendix B demonstrates successful times the alignment between the time-history and response spectram.

The procedure for Spectrum Matching has shown that achieving a good match is easier when extending the matching period beyond the period range of interest. This is why spectrum matching is required within the range of 0.8 times the lower period (Tlower) to 1.2 upper period (Tupper). Hence, a good match achieved is when the average acceleration spectrum computed from the matched records in each direction stays within 10% above or below the target spectrum across the period range of interest (ASCE7-16, 2017).

1.10 Modeling Nonlinear Behavior

1.10.1 Fiber Hinges

The fiber hinge concept divides a reinforced concrete section into individual fibers, each following a non-linear stress-strain curve based on its material type (such as unconfined concrete, confined concrete, or steel reinforcement). This concept employs fiber hinges to distribute plasticity throughout the section, allowing for a comprehensive representation of its behavior. The section's overall response is determined by summing up the contributions of all fibers. In SAP2000, fiber hinge model can use, and calculates

non-linear deformations in response to internal forces within the section using advanced numerical methods and algorithms based on finite element analysis (FEA).

Figure B.5 in Appendix B illustrates the behavior of fibers and materials under cyclic load.

1.10.2 Material

1.10.2.1 Concrete

Understanding the behavior of concrete in reinforced concrete sections involves considering confined and unconfined concrete models. Various models are available to study both types of concrete behavior simultaneously, while some focus solely on confined concrete. Examples include models developed by Cusson & Paultre (1995), Hoshikuma et al. (1997), Sheikh & Azumiri (1982), Martinez et al. (1984), Ahmed & Shah (1982), Al-Dash & Ahmed (1995), and Asa et al. (2001). Additionally, widely used and accurate models for selecting the most appropriate one for research purposes include those by Kent & Park (1971), Razvi & Satcioglu (1999), and Mander, Priestley, & Park (1988).

Confined and Unconfined Models for Reinforced Concrete section:

Confinement models examine how lateral reinforcement (such as hoops, spirals, and ties) affects the stress-strain characteristics of concrete. They are designed to capture the increased strength, ductility, and energy absorption capacity observed in confined concrete. These models utilize parameters like the confinement ratio, details of lateral reinforcement, and concrete strength to forecast stress-strain relationships. Both empirical and theoretical models can be used to provide accurate estimations of concrete confined stress-strain behavior.

On other hand, Unconfined models study how stress and strain change without considering lateral reinforcement. They take into account factors such as the concrete compressive strength, tensile strength, and other material properties. These models are helpful for predicting how elements behave when they aren't heavily confined laterally.

Figure B.6 in Appendix B demonstrates Concrete area with effective confinement concret.

The most popular methods for modeling both confined and unconfined concrete are:

Kent & Park (1971) proposed that the maximum strength for both confined and unconfined concrete is the same, denoted as f'_c. They suggested a curve, as shown in Figure B.7 in appendix B, which starts from the origin and increases parabolically (known as Hognestad's Parabola) until reaching the peak at f'_c and the corresponding strain εco at 0.002. Then, it descends with one of two different straight lines. For confined concrete, which is more ductile, it descends until the point ($0.5\,f'_c$, ε50c) and continues descending to $0.2\,f'_c$ followed by a flat plateau. For unconfined concrete, it descends until the point ($0.5\,f'_c$, ε50u) and continues descending to $0.2\,f'_c$ without a flat plateau. Kent and Park assumed that confined concrete could sustain strain indefinitely at a constant stress of $0.2\,f'_c$ (Scott, 1980).

Mander's model is widely used because it's simple yet effective at accounting for the effects of confinement. The study is a look into the improvement of strength and flexibility, which occur in reinforced concrete members when they are confined. For instance, this model is often used to evaluate the strength of columns when encased with stirrups (Mander, Priestley, & Park, 1988).

Additionally, Also, Mander's model is an earthquake engineering method that focuses on confined concrete which deals with circular spiral reinforcement and hoops and rectangular ties among others. These confinement methods are studied to determine how they influence concrete performance when subjected either to cyclic or monotonic type of loadings. One important point noted is the effective lateral confinement pressure coefficient (k_e) which improves both strength and ductility in concrete. Also, Mander's model is concerned with the complex interactions between reinforcing elements such as materials that are used to bind together the pertaining structures and thus it gives insight in relation to the mechanics of closed-in concretes structures.

When concrete is confined laterally in, its compressive strength (f'_{cc}) and corresponding strain (ε_{cc}) are significantly higher than those of unconfined concrete (f'_{co} and ε_{co}), as depicted in Figure B.8 in appendix B. Here, f'_t, f'_{co}, f'_{cc}, ε_t, ε_{co}, ε_{cc}, ε_{cu}, ε_{sp}, E_c, and E_{sec}

represent the tensile strength of concrete, the compressive strength of unconfined concrete, the compressive strength of confined concrete, the tensile rupture strain of concrete, the concrete strains corresponding to peak strength of unconfined concrete, the concrete strains corresponding to peak strength of confined concrete, the ultimate compressive strain of confined concrete, the strain at which the concrete cover is considered completely spalled, the modulus of elasticity of concrete, and the secant modulus of confined concrete at peak stress, respectively (Mosheer, Khamail Abdul-Mahdim, 2016).

Saatcioglu & Razvi (1992) found that the lateral pressure from expanding concrete and the restraining effect of transverse reinforcement may not always be consistent. After testing concrete with strengths ranging from 30 to 130 MPa, they introduced a new model Figure B.9 in appendix B showing an exponential relationship between lateral confinement pressure and peak confinement strength. Their experiments involved changing factors like the volume ratio, spacing, yield strength, layout of transverse reinforcement, concrete strength, and section shape.

Confined concrete models are created using physical engineering, empirical, and combined methods. Notably, Mander et al. (1988) and Saatcioglu & Razvi's (1992 & 1999) models are known for their effectiveness and accuracy. Mander et al. (1988) model it is practical and reliable. This model provides a straightforward yet efficient method to understand how confinement affects concrete. It accurately reflects the strength and flexibility improvement in reinforced concrete when confined. Moreover, Mander's model is commonly used to assess the strength of columns confined by stirrups.

In this study, Mander et al. (1988) approach will use to determine the stress-strain relationships of both confined and unconfined concrete in different structural elements like columns and beams. The materials will use are Concrete Grade B350 and Grade 60 reinforced steel in confind concrete modal .

Table A.4 in Appendix A showes Comparison of models for confined and unconfinedconcrete for by Kent & Park (1971), Razvi & Satcioglu (1999), and Mander, Priestley, and Park (1988).

1.10.2.2 Mander et al. (1988) Model for Tension Behavior

The tension behavior according to the Mander model is divided into two linear segments as show in Figure B.8 in Appendix B : linear elastic behavior and linear behavior beyond the yield point. The linear elastic behavior is described by an equation No. 8 where stress is directly proportional to strain within the elastic range. Additionally, the model may include linear behavior beyond the yield point, described by equations No.9 and 10 that detail the stress-strain relationship under tension. (Huang, Wang, Yang, & Wei, 2023)

$$f_t{}' = E \cdot \epsilon_t{}' \tag{8}$$

$$\sigma_t = \begin{cases} \frac{f_t\,\epsilon_t{}'}{2\times10^{-4}} & \epsilon_t{}' \le 2\times10^{-4} \quad (9) \\ \frac{f_t\,(8\times10^{-4}-\epsilon_t{}')}{6\times10^{-4}} & \epsilon_t{}' \le 2\times10^{-4} \quad (10) \end{cases}$$

where:

E: represents the modulus of elasticity (21 000 , MPa)

f_t: tensile strength of con- crete.

$\epsilon_t{}'$: corresponding strain.

σ_t: tensile stress

The equation represents how concrete behaves elastically in a linear fashion, with stress being directly proportional to strain within the elastic range. For non-linear behavior beyond the yield point, Mander's model has a linear segment and possibly more sophisticated equations that can be used to describe stress-strain relationship under tension. Such equations might incorporate terms for strain hardening or softening and also ultimate stress and strain values at failure. Tensile Strength of Concrete.

1.10.2.3 Steel Rebar

Steel reinforcement Grade 60, known as ASTM A615 Grade 60 is a standardized specification for deformed and plain carbon steel bars that are used in reinforcing concrete structures. The construction industry uses this specification to enhance the tensile and yield properties of the steel bars in question. The table below gives an insight into mechanical properties specifically for ASTM A615 Grade 60. In addition to that, kinematic hysteresis loops are applied to expound on rebar behavior mechanism in

mechanics of materials. This is described by figure B10 page 146 (Appendix B) showing Stress-Strain Curve for Steel Reinforcement.

1.10.3 Hysteresis Loops

Hysteresis loops are commonly seen in materials such as reinforced concrete or steel when they undergo cyclic loading, such as during earthquakes (Pozo, Martínez, & Martínez, 2009). When hysteresis loops are nonlinear, it means that the structural response does not directly correspond to the applied load due to the material or structural behavior. This nonlinearity occurs when the relationship between the applied load and the resulting deformation or displacement of the structure is not linear. In other words, as the load increases or decreases, the deformation or displacement of the structure does not change proportionally, leading to a nonlinear hysteresis loop. This behavior is often observed in structures subjected to large deformations, yielding, or other nonlinear effects, where the relationship between stress and strain is not linear throughout the loading and unloading cycles, often because of factors like material yielding, stiffness reduction, or frictional effects within the structure.

Various types of Hysteresis Loop Models exist, such as the Elastic, Kinematic, Degrading, Takeda, Pivot, Concrete, BRB Hardening, and Isotropic Hysteresis Models. In this study, Takeda and Kinematic Hysteresis Models will use .

1.10.3.1 Takeda Hysteresis Loops

Takeda model is similar to the kinematic model but incorporates a degrading hysteresis loop based on Takeda's work, as outlined in Takeda, Sozen, & Nielsen (1970). Takeda model is simpler and does not require additional parameters, making it well-suited for analyzing reinforced concrete rather than steel due to its lower energy dissipation compared to the kinematic model . Therefore, this study will use the Takeda Hysteresis Model in SAP2000. (Sabah, Öztorun, & Sayin, 2022).

Takeda model during reloading , it follows a secant line to the backbone curve in the opposite direction, starting from the maximum deformation observed in previous load cycles. This results in reduced energy dissipation as deformations increase. The accompanying Figure B.11 in Appendix B illustrates this behavior (Sengupta & Li, 2017).

1.10.3.2 Kinematic Hysteresis Loops

Kinematic hysteresis loops are well-suited for studying the behavior of steel, such as steel bars in concrete reinforcement because the kinematic modeldissipates a lot of energy. Kinematic hysteresis behavior occurs when a material shows a delay in its response to an applied force or deformation. This means that the material's behavior is affected by its previous loading and unloading history. For instance, when a material experiences cyclic loading, like during earthquakes, it may deform during loading but not fully return to its original shape when the load is removed. This delayed response is called hysteresis, and when it's related to a material's behavior, it's called kinematic hysteresis. Figure B.12 in Appendix B depicts the configuration of kinematic hysteresis loops.

According to SAP2000 software the Kinematic Hysteresis Model, a commonly observed behavior in metals where plastic deformation in one direction affects deformation in the other direction. Under kinematic hardening rules, plastic deformation in one direction influences the behavior in the other direction. Symmetrical pairs of points on the multi-linear curve are linked, even if the curve is not symmetrical, allowing some control over the shape of the hysteresis loop (Sabah, Öztorun, & Sayin, 2022) . one direction influences the behavior in the other direction. Symmetrical pairs of points on the multi-linear curve are linked, even if the curve is not symmetrical, allowing some control over the shape of the hysteresis loop (Sabah, Öztorun, & Sayin, 2022) .

1.11 Literature Review

Many studies have been conducted on deflection amplification factor (Cd) and differences in the actual behavior of structures as compared to those predicted by ASCE7-16 among others. These works were majorly focused with regards to multi-storey buildings which present unique challenges in terms of earthquake design. The objective of this part is to highlight the significant contributions made by some authors on the improvement of knowledge in this area.

In this study, five different moment-resisting frames with varying numbers of stories ware analyzed by Sap20000 : three, five, seven, nine, and twelve. A nonlinear static analysis to determine their capacity curve was conducted. From these curves, the overstrength factor and ductility ratio ware derived. Finally, the deflection amplification factor was calculate. The study illuminated the comparative behaviors of Special Moment Resisting

Frames (SMRF) and Ordinary Moment Resisting Frames (OMRF). Specifically, SMRFs displayed higher ductility ratios and overstrength factors when juxtaposed with OMRFs. Interestingly, In both Ordinary Moment Resisting Frames (OMRF) and Special Moment Resisting Frames (SMRF), the overstrength factor specified in ASCE 7-10 is higher than the overstrength factor obtained from our analysis. As a result, ASCE 7-10 is slightly conservative.

Moreover, an evident correlation emerged between the deflection amplification factor and the structure's ductility ratio. It is noteworthy that the calculated deflection amplification factors for structures with fewer than eight stories were found to be below the stipulated values in the ASCE 7-10 code. However, as the number of stories escalated, the calculated deflection amplification factors aligned more closely with the values dictated by the code. Figure B.13 in Appendix B explain Deflection amplification factor for different story levels in ordinary and special MRF.

Anil K. Chopra (2012) claimed that the earthquake-induced inelastic response of a system is affected by the relative values of u_m (maximum inelastic displacement) and u_o (peak elastic displacement resulting from earthquake-induced resisting deformation). These values rely on the system's natural vibration period (T_n) and the ground motion characteristics, with damping in the system playing a secondary role. Therefore, as it is the deflection amplification factor depends on both the elastic and maximum inelastic displacements, indicating that the factor is related to the time period of the structure.

Through the case study conducted by Anil K. Chopra on Single –degree freedom system shown in the Figure B.24 in Appendix B. The graph shown in Figure B.25 in Appendix B was obtained which ductility demand for elastoplastic system due to El Centro ground motion; ζ=5% and normalized yield strength (f_y) = 1, 0.5, 0.25, and 0.125. it is evident that there's a Relationship between ductility demand μ (the ratio of maximum deformation to yield deformation) and the time period (T_n). This suggests a potential relationship between C_d and (T_n). The ductility demand is notably high for shorter time periods and decreases as the time period increases. This observation supports the conclusion be quoted from Chopra's book " The ductility demand on very-short-period systems may be very large even if their strength is only slightly below that required for the system to remain elastic. Thus extremely-short-period systems ($T_n < T_a$) should be designed for a

yield strength (f_{-y}) the same as the strength (f_o). required for the system to remain elastic; Otherwise, the inelastic deformation and ductility demand may be excessive".

The study centers on the buckling-restrained brace (BRB), a new technique used to improve the ductility capacity of standard steel braced frames. Understanding the nonlinear response of BRBs in estimating maximum displacements during earthquakes is crucial for structural designers. The study investigates the deflection amplification factor (C_d) in BRBs, recently introduced in seismic design provisions as a lateral-resisting system. Five BRB models of varying heights (3, 5, 7, 10, and 15 stories) are created in OpenSees software. Ground motion simulation is created conducted using scaled earthquake records, and elastic and ultimate displacements are computed through pushover and nonlinear time-history analyses.

The research results revealed that the deflection amplification factor recommended in well-known building codes (like ASCE-7-16) may, in certain cases, be overestimated for assurance, while in other conditions, it may be underestimated. Indeed, the results suggest that the Cd value in these systems is closely linked to the building's height.

This research find the deflection amplification factors are highest on the lower floors in dynamic analyses, but they decrease as the number of floors in a building with BRBFs increases. This suggests that the constant coefficient provided by ASCE-7-16 (C_d = 5) is very cautious for upper levels but doesn't accurately estimate the actual displacement of the lower floors in such steel buildings.

On the other hand, this research provid Some math formulas are suggested to estimate deflection amplification factors in short to mid-rise buildings with BRBFs. These formulas are based on data from nonlinear time-history analyses and define this factor in relation to the number of stories in such structures.

where $1 \leq n \leq 15$

$$C_d = 6.572e^{0.111\,n} \qquad R^2 = 0.958 \tag{11}$$

$$C_d = 7.194\ln(\mathrm{n}) \qquad R^2 = 0.976 \tag{12}$$

$$C_d = 8.8194\,n^{0.635} \qquad R^2 = 0.961 \tag{13}$$

Based on the studies above , there is inconsistency in how the deflection amplification factor is affected by both the height and time period of a building .Some studies, such as those by Anil K. Chopra and Mahmoudi, Mussa, and Mohammad Jalili Sadr Abad, suggest that the factor may decrease with building height. Conversely, other literature, such as the research by Ramin Taghinezhad et al. (2017) proposes that the coefficient could increase with the number of floors. This study seeks to examine divergent perspectives and potentially formulate an equation that elucidates the relationship between building period, building dimensions, and the deflection amplification factor.

1.12 The Fundamental Period Value

Three distinct methodologies are employed to compute the structural time period. Specifically, two of these methodologies are codified within ASCE7-16, and they are designated as Equation No. 14 and Equation No. 15. The third methodology is sourced from the SAP2000 program, and a comparative analysis will be undertaken to assess their concurrence .

Equation No. 14 represents an empirical relationship derived from statistical analysis of building structures' responses to small- to moderate-sized earthquakes and wind effects (Goel & Chopra, 1997, 1998). Figure B.14 in Appendix B illustrates data gathered from various building structures with steel and reinforced concrete moment-resisting frames. As the empirical expression is derived from the lower bound of the data, it provides a conservative estimate of the period for a building structure of a given height (ASCE7-16, 2017).

$$Tn = Ct\ h^{0.9} \tag{14}$$

Where:

h: Structural height

C_t: Coefficient with a fixed value of 0.0466 for moment-resistant frame configurations.

Formula number fourteen or Equation 14 in ASCE7 is a simplified empirical equation that can be used to estimate the period of a building structure, conservatively. Derived from historical data and practical judgments based on observed structural dynamics, this simple approach might be applicable where the dynamic analysis of non-complex structures may not be desirable or possible (ASCE7-16, 2017). Although it may not cover

all aspects of dynamic behavior of any given structure, it serves as a useful tool for preliminary design and assessment purposes particularly for low-rise or simple structures.

For equation No. 15 of the code to be applicable, the seismic force-resisting system must comprise solely concrete or steel moment-resisting frames, and the average story height should be at least 10 feet (3 meters).

$$Tn = 0.1\ N \tag{15}$$

Where:

N: Number of stories

Different methods are implemented by SAP2000 in the determination of the time period. They are mainly related to modal analysis and response spectrum analysis. The modal analysis features the calculation of natural frequencies and corresponding mode shapes for a structure. Thus, the time period for modal analysis is defined as the inverse of the natural frequency of the fundamental mode. On the other hand, the response spectrum analysis allows the evaluation of the time period as the structure's response to the seismic excitation which is defined by a spectrum curve. It follows that the value of the time period is mainly dependent on the dynamic characteristics of the structure and the input of the ground motion. The predominant period of the vibration of the structure is being calculated by a set of advanced numerical algorithms that consider the following modifications: the geometry of the structure, the properties of the material, the site conditions, the type of loading, boundary conditions, and the presence of the reinforcement (MANUAL, ANALYSIS REFRANSE MANUAL. "SAP2000®." 2023).

1.13 Analysis tool (SAP 2000 software)

For structural analysis and design purposes, SAP2000 is a key software tool that focuses on nonlinear time history analysis. It encompasses a wide variety of tools for structurally analyzing dynamic time-history systems.

By simulating complex non-linear behaviors such as material nonlinearity, large deformations and interaction effects, SAP2000 provides more accurate representation of structural performances.

SAP2000 has the ability to inform us what structures do when they are subjected to ground motions in seismic engineering. Through actual earthquake records in terms of time histories, engineers can examine the dynamic characteristics of a structure and its interplay with moving forces thus identifying weak points or vulnerabilities within it. This knowledge facilitates development of focused retrofit strategies thereby enhancing resistance to earthquakes.

SAP2000 utilizes the Newton-Raphson method to solve nonlinear equations in structural analysis. This method is an iterative process that aims to find the roots of a system of equations by successive approximations.

In this scientific study, the SAP2000 program, designed for structural analysis, underwent verification and validation to confirm the accuracy of its results and validate the input data. The verification phase included using various methods.

1.13.1 Verification through comparison with Anil K. Chopra textbook:

- Validation through a Single Degree of Freedom (SDOF) Approach:

To initiate the process of verifying the reliability of the analysis tools represented by SAP2000 . The case study began by selecting a single degree of freedom system and ensuring its stability with fixed support. The system's characteristics were then determined to achieve a single degree of freedom with a time period of 0.5 seconds. that enabled a for comparing the elastic and inelastic displacement values outlined in Chapter 7 of Anil K. Chopra's book with analysis results by SAP2000.

The comparison shown in Figure B.15 in Appendix B significant agreement between the results obtained from analysis by SAP2000 software and the presented in Anil K. Chopra's book . For instance, with a normalized yield strength (f_y) equal 1 , Chopra's book indicates a displacement of 5.72 cm at 0.5 seconds time period , while SAP2000 computes a displacement of 5.27 cm at 0.497 seconds time period. Similarly, at a normalized yield strength (f_y) equal 0.25, Chopra's book reports a displacement of 4.45 cm at 0.5 seconds , whereas SAP2000 calculates a value of 4.74 cm at 0.497 seconds time period.

The preceding findings indicate a very close convergence between the two models. While there exists a small disparity, it can be attributed to the slight difference in the time period between the two models. This difference may arise if the book designates the time period as 0.5 seconds, whereas in the SAP2000 model, it is 0.497 seconds.

- Validation via Analysis of a Concrete Frame:

A similar validation procedure was conducted on a concrete frame structure, consisting of two columns and a single beam. The previous methodology employed for comparing the elastic and inelastic displacement values outlined in Chapter 7 of Anil K. Chopra's book with analysis results by SAP2000. The results obtained from this analysis closely matched the anticipated values, as depicted in Figure B.16 in Appendix B.

At precisely 0.5 seconds, we analyze the displacement values. When a normalized yield strength (f_{-y}) is set to 1, Chopra's reference notes a displacement of 5.72 cm, while under the same fy setting, SAP2000 calculates a displacement of approximately 5.6045 cm at a time close to 0.5 seconds. Similarly, with a normalized yield strength (f_{-y}) equal 0.25, Chopra's reference indicates a displacement of 4.45 cm, whereas SAP2000 a displacement equal to 4.05 cm at an equivalent time point.

1.13.2 Validation through A Closer Look at the Vecchio & Emara (1992) Framework Modal (Vecchio & Emara, 1992):

To enhance the credibility of the SAP2000 analysis tool, employed a model Vecchio & Emara 1992. The experiment involved applying force to a laboratory single-bay, two-story reinforced concrete (RC) plan frame. This frame was tested at The University of Toronto where the effects of shear on frame deformation, load carrying capacity and the failure mechanism was investigated. The test frame was large-scale to represent real possibilities. The frame had a center-to-center span of 3500 mm. The story height and overall height of the frame was 2000 mm and 4600 mm respectively. The geometry and sectional properties are shown in figure No1.. The selected dimensions will represent common practice configurations compares between The the results from Vecchio & Emara (1992) test and SAP2000 pushover analysis.

To ensure the agreement between the physical experiment's outcomes and the computational predictions from the SAP2000 program, we meticulously analyzed using

the static pushover method. The aim was to validate the program's accuracy against real-world experimental data.

Figure 1

The Vecchio and Emara (1992) frame

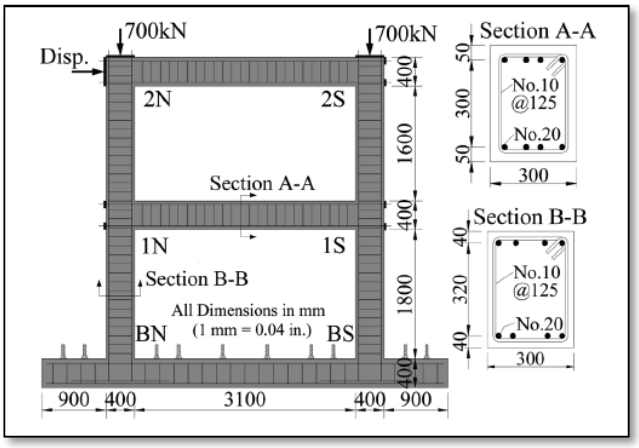

a) Structural details

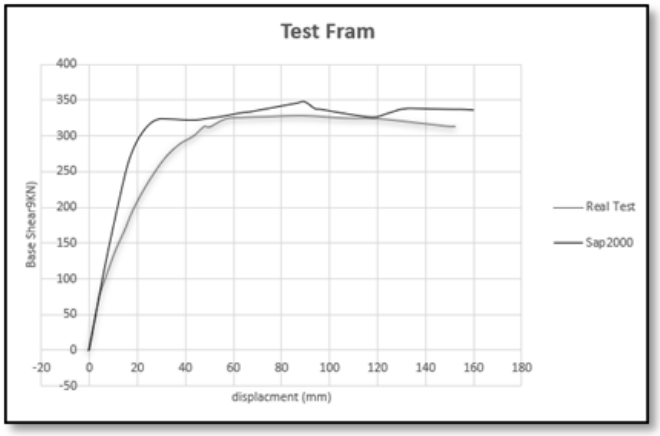

b) Comparing frame and SAP2000 pushover

A significant level of concurrence is observed between experimental data and results obtained from the SAP2000 software concerning inelastic displacements. However, disparities are noted to a extremely extent within the elastic domain, This is primarily due to the fact that the effects of cracking within SAP2000 are different from those in the real test.

1.13.3 Validation through Real Testing: A Study for Rizwan et al

The aim of this study is to assess how reinforced concrete frame structures with inadequate beam-column connections respond to seismic damage. To accomplish this,

shake table tests were carried out using 1/3rd scale models of two-story frame structures. Two different models were chosen for the experiments, and their geometric layout is illustrated in Figure No. 2 .

Figure 2

Geometric and design layout of prototype RC farm a) concrete reinforcement and sections b) real modal for testing

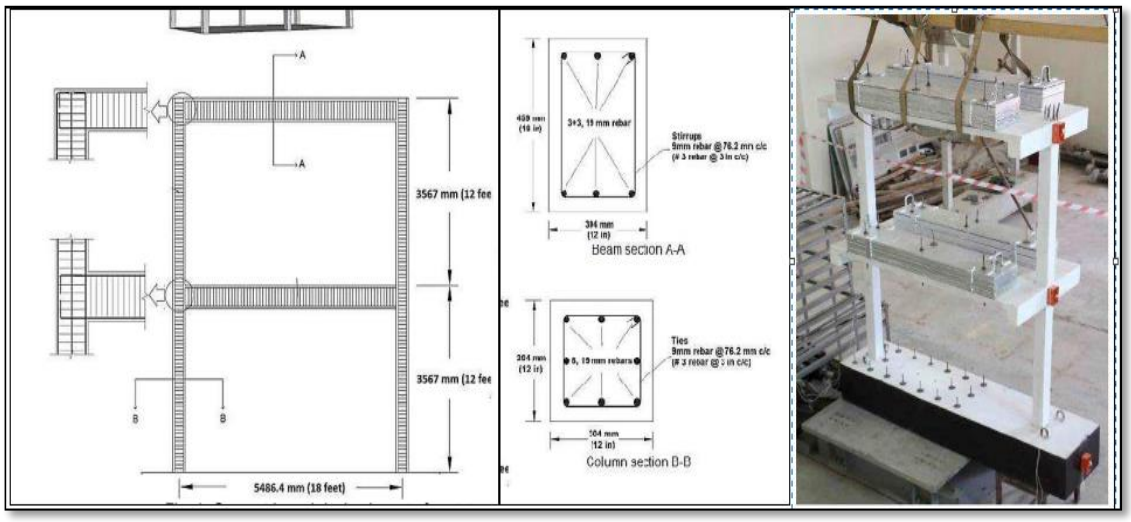

Table A.5 in Appendix A provid presents the dimensional parameters of both the prototype and reduced-scale models, along with the similitude conversion factors.

After simulating the experiment within the Sap2000 software, a comprehensive analysis was conducted considering material properties, dimensional characteristics of structural elements, such as story height and span length. The analysis employed nonlinear time-history methods, and the resultant findings are presented in figure B.17 in appendix B.

The graphical representation above shows a significant similarity between the results obtained from the real-world experiment and the SAP 2000 program model. The experimental data indicates a minimum displacement of about 142 mm and a maximum displacement of 152 mm, whereas the non-linear time-history analysis performed in the SAP 2000 software suggests a minimum displacement of around 140 mm and a maximum displacement of 162 mm.

1.14 Parameters Affecting on the Deflection Amplification Factor

The According to of Anil K. Chopra (2012) Values of Maximum displacement (u_m) which play role to find C_d depend on values the system's natural vibration period (T_n) and the

ground motion characteristics. Damping in the system plays a secondary role. On the othor hand, Taghinezhad, Ramin, et al. (2017) and Mahmoudi, & Sadr, Abad, (2022) consider that the value of C_d is affected by the number of floors .

In summary, it was agreed in previous literature that the value of C_d is affected by the time-period (T_n) of the building, which is closely related to the height of the building . On the other hand, the effect of the damping in the system can be neglected due to its secondary effect.

The time-period (T_n) is closely related to the characteristics of the building's dimensions, basically the number of floors, secondary role of height of each floor , the span length, and the number of bays. The natural period is also influenced by the properties of the materials used in the structure. However, this effect is minimal because the material characteristics are generally consistent.

1.15 Literature Review summary

To achieve the objectives of this thesis, the concrete structure was chosen, which is the most common in the State of Palestine. On the other hand, most of the West Bank belongs to seismic design category D, which means the need to use special moment resisting frames (SMRF).

The primary parameters affecting the deflection amplification factor (Cd) are related to the building's characteristics, particularly its geometry, which influences the structure's time period. This is discussed in Section 2.9. A total of 36 carefully selected case studies were analyzed, all of which feature square-shaped buildings with varying numbers of floors, floor heights, span lengths, and numbers of bays, as dimensions commonly used in Palestine.These were analyzed using linear and non-linear time history by SAP2000 for history records for three times, which were matched to the response spectrum for Seismic hazard zone Z =0.3 according coloration maps like Jericho by SAP2000 and seismomatch to compute C_d. While, ETABS used to utilized for comprehensive structural design considering both gravity load and seismic load.

For modeling nonlinearity in the structure, fiber hinges (P, M1, M3) are used. The member section is divided into three parts: steel, confined concrete, and unconfined concrete. The properties of concrete material are defined using Mander's stress-strain model. Cyclic loads are represented using kinematic hysteresis loops for steel and Takeda hysteresis loops for concrete.

Chapter Two
Modeling and Results

2.1 Overview

This research aims to investigating the parameter C_d and its relationship with the time period and various factors related to building geometry characteristics (building height, span length, story height and numbers of bays). Past research conducted by Mahmoudi et al. in 2022 suggests that C_d is influenced by the height buildings and their structural periods, This presents a promising chance to enhance our ability to address the issue of seismic separator , which may hampers the construction of tall buildings.

This chapter describes the approach taken for seismic design was done for 40 square-shaped building models, focusing on Special Moment Resisting Frames (SMRFs). It follows the guidelines from ASCE7-16 and ACI Code 318. The chapter also discusses using linear and nonlinear time-history analyses to calculate both elastic and inelastic deformations. These analyses helped compute the C_d values for all cases studied in this research using SAP2000 software.

2.2 Cases Details for Analysis

This thesis focuses on analyzing a square-shaped structure using both linear and nonlinear time-history analyses. The investigation considers variations in the number of stories, including 4, 8, 12, and 16 floors. Additionally, different floor heights of 3, 3.5, and 4 meters are explored, along with varying span lengths ranging from 5 to 7 meters. The number of structural bays is also varied, with options of 3, 4, and 5. The study comprises 36 case studies for data extraction and deriving mathematical equations, as well as four additional cases to validate the findings. .The matrix of parameters used in the study is explaine in Table No. 1.

Table 1

General properties of the RC framed structures used in Study

Parameters	range
Number of Stories	4, 8, 12, and 16 floors.
Floor Height	3, 3.5, and 4 meters.
Span Lengths	5,6, and 7 meters.
Number of Structural Bays	3, 4, and 5.

Figure B.18 in Appendix B explan the arrangement of columns in the 40 structure models analyzed in the study. In this representation, "N" represents the number of bays, "L" denotes the length of the span, and "C" symbolizes a column.

2.3 Model Description

In this study, 36 building cases were examined with variable number of floors, floor height, span length, and number of bays. This section focuses on one specific case, featuring a four-story structure with three bays in each direction. The structure has floors that are 3 meters high and5 meter long spans. This particular case serves as an illustration of the design and analysis methods employed, including linear and non-linear time-history analyses. The approach taken in this case is representative of the methodology applied to the remaining study cases. Additionally, four extra cases were selected to validate the equation derived from the data gathered in the previous 36 cases. Figure B.19 in Appendix B illustrates 3D ETABS model for desgin of parametric cases. Table A.6 in Appendix A provides the dimensions of the structure, specifying the number of floors, bay length, floor height, and number of bays.

2.4 Materials and Sections

The structural elements, including beams, columns, and slabs, were rigorously designed for both gravity and seismic loads. The dimensions of the sections were determined using the ETABS software.

Table No. 2 contains detailed information about concrete with a compressive strength of B 350 and reinforcement steel that complies with ASTM A615 standards, which is used In this thesis.

Table 2

General for Data Concrete B 350 and ASTM A615

General Data	B350 (KN, m, C)	ASTM A615
Material Type	Concrete	Steel
Material Grade	B350	A615Gr60
Weight per Unit Volume	23.56	76.
Modulus Of Elasticity, E (MPa)	24855	
Poisson, U	0.2	0.3
Coefficient Of Thermal Expansion, A	9.900E-06	1.170E-05
$f'c$, Fy (MPa)	28	413

2.5 Loads and Boundary Conditions

- Loads

The model is subjected to two types of loads: gravity loads and linear and nonlinear time-history loads. Additionally, the frame is designed to withstand earthquake loads according to ASCE7-16 using the Response Spectrum Analysis method.

The gravity loads consist of dead load and live load assigned to the slabs. The dead load includes the structure's own weight, and the live load (LL) is 4 kN/m². Furthermore, there's a superimposed dead load (SIDL) of 3 kN/m².

For the analysis to find elastic and inelastice displasment , the Time History Analysis method is used to simulate the actual time history of ground motion recorded during earthquakes. This method considers the full range of frequency content and temporal characteristics of seismic waves, providing detailed insight into the structure's dynamic response under nonlinear dynamic loads..

- Boundary conditions

Commonly considered boundary conditions in seismic analysis include fixed Suppurt, where no displacement or rotation is allowed at the boundary; roller supports, where horizontal movement is permitted but vertical movement is restricted; and pinned (or hinged) supports, where both horizontal and vertical movement are allowed.

In this thesis, the model under study is assumed to be built on rigid soil. Consequently, the boundary condition is assumed to be fixed support.

2.6 Seismic Loads for Parametric Cases

- Time history excitation

Three seismic records were chosen to represent the site's seismic hazard, ensuring a range of characteristics in terms of amplitude and frequency, as detailed in Chapter 2. According to ASCE 7-10 Code Section 16.1.4, a minimum of three distinct records is required for analytical studies. In this, design parameters should be derived from maximum values observed across all analyses.

Figure B.20 in Appendix B shows three ground motion time-history records selected for conducting linear and non-linear time history analyses using SAP2000 software.

- Response spectrum

Three earthquake time history records were used and then matched with the response spectrum using seismomatch and SAP software. The study was conducted in Zone 3 with a site class D soil and a site-specific factor (Z) of 0.3. The table No. 3 below summarizes the properties of the response spectrum.

Table 3

Response Spectrum properties

Function Name	RS
Parameters	
0.2 Sec Spectral Accel, Ss ≈ (2.5Z) *1.5	1.125
1 Sec Spectral Accel, S1 ≈ (1.25Z) *1.5	0.5625
Long-Period Transition Period	8 sec
Site Class	D
Site Coefficient, Fa	1.05
Site Coefficient, Fv	1.7375
Calculated Values for Response Spectrum Curve	
SDS = $(2/3) * Fa * Ss$	0.7875
SD1 = $(2/3) * Fv * S1$	0.6516

2.7 Designing and Analysis

The structural design was performed using ETABS software, ensuring strength, drift check, P-delta effects, and compliance with ACI building code for special-sway framed structures. After designing, section dimensions and reinforcement ued for the linear and nonlinear time history analyses.

2.7.1 Validation of the Model

After creating the model in the ETABS software, it's important to ensure it's ready for design. This verification process involves three checks outlined in Appendix C: a compatibility check, a equilibrium check, and an internal moment check.

On the other hand, ensuring buildings can withstand earthquakes requires the design process to go through four stages: designing for strength, checking drift, checking P-Delta effects, and meeting the requirements of the ACI 318 Code for detailing of the Special Sway System. These steps will be applied to all cases used in the study, as described in Appendix D on how to conduct a parametric study.

2.7.2 Analysis of Parametric Study

Once the cross sections are designed and their dimensions, along with the necessary steel reinforcement, are determined using ETABS, the analysis moves on to the SAP 2000 program. This includes performing linear and non-linear analyses using three earthquake records discussed earlier to calculate both elastic and inelastic displacements and compute the C_d value for each case. To achieve this, the model undergoes verification, similar to the design phase**.**

2.7.2.1 Define Sections Using Section Designer in SAP2000

The Section Designer tool in SAP2000 was used to define properties for three different materials: confined concrete, unconfined concrete, and steel rebars, with clear specifications of their nonlinear material behaviors.

Figure B.21 in Appendix B displays stress-strain curves for confined and unconfined concrete. These curves are derived from the Mander model. Figure B.22 in Appendix B shows stress-strain curves for reinforcement steel.

2.7.2.2 Defined Fiber Hinges M3-M2-P

Within the software, the analysis and behavior of fiber hinges M3-M2-P are examined and simulated.

Fiber hinges were utilized for both columns and beams, dividing the sections into smaller elements for analysis, with each element examined based on its specific properties through analysis.

2.7.2.3 Time History Analysis

Three earthquake records, as described Section 2.4.3, are employed for this analysis. Seismomatch and SAP 2000 software are utilized to meticulously align these earthquake records with the desired response spectrum, guaranteeing an accurate modeling of structural response under different seismic scenarios

Figure No. 3 explain Time-history before and after matched with response spectrum by Seismomatch and SAP2000.

Figure 3

Time-history before and after matched with response spectrum for Z=0.3 by Seismomatch and SAP 2000

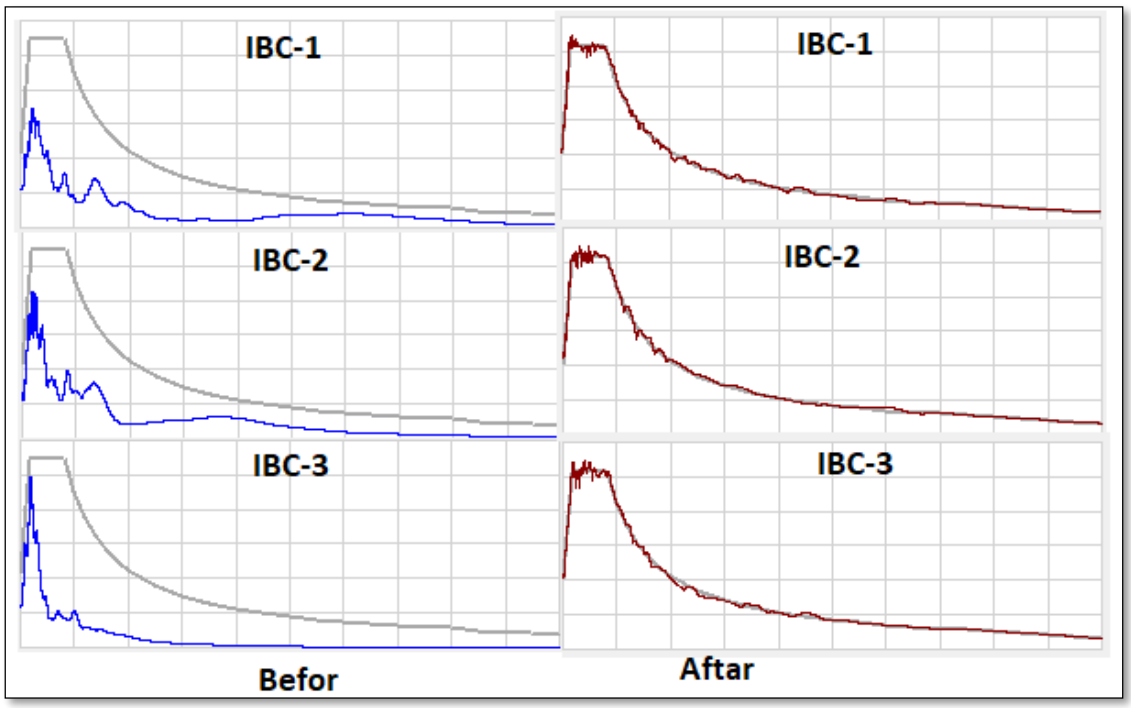

2.8 Analyze result and Calculating the Deflection Amplification Factor (C_d)

Using SAP2000 for linear and nonlinear time history analysis,which can determin the maximum elastic and maximum inelastic displacement response for each record. To calculate C_d value, the maximum value of inelastic displacement (δi_{max}) obtained from nonlinear time-history analysis records is divided by the maximum value of elastic displacement (δe_{max}) from the three linear time-history analysis records.

The maximum elastic displacement on the roof (δe_{max}), used to calculate the C_d, is divided by the response reduction factor (R).

Figure B.23 in Appendix B illustrates the sequential formation of plastic hinges in two case studies.

The results of this analysis provide valuable insights into the role and efficacy of fiber hinges within reinforced concrete structures.

Through nonlinear and linear time history analysis, the elastic and inelastic displacements can be obtained to calculate the C_d value. Table 4 illustrates this process.

Table 4

Computation of the C_d value for parametric study

Earthqueck record	elastic displacement (δe) (cm)	inelastic displacement (δi) (cm)	Cd=(δi)/ (δe)
IBC-1	4.40	15.03	
IBC-2	4.10	17.80	4.05
IBC-3	3.95	17.40	

Table A .11 through Table A .47 in Appendix A Shows C_d calculation details for 36 study cases.

Hysteresiloop for column hing have fuiler is visually represented in figure 4.

Figure 4

Hysteresis Loop and Hinge Performance

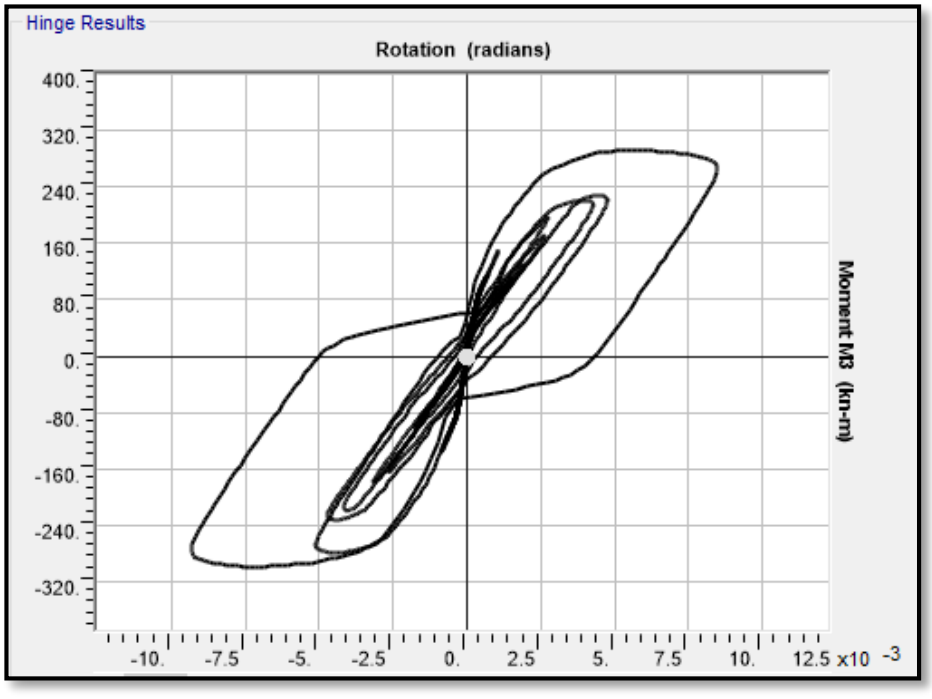

Figure No. 5 shows the elastic and inelastic displacements at each floor for three ground records analyzed using linear and nonlinear time history analysis.

Figure 5

Elastic and inelastic displacement for each floor by linear and nonlinear analysis for three-time history records

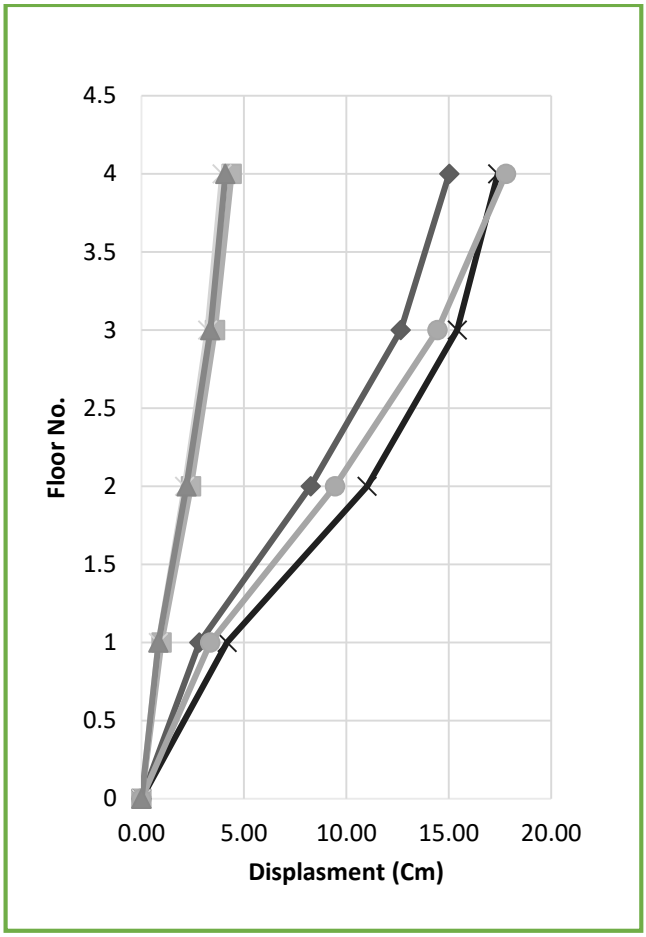

In the Appendix Figure B.29 through Figure B.65 Show 36 case study elastic and inelastic displacement Vs. Floor Number.

Chapter Three

Result Analysis and C_d -Factor Evaluation

3.1 Overview

In this chapter will examines the outcomes of analyzing the 40 case studies. Each case study presents building characteristics alongside the C_d value obtained from the analysis. Excel and SPSS were utilized to illustrate the correlation between each parameters and the C_d value , and providing an explanation for this relationship.

Following that, the factors affecting the C_d value are identified. Then, a relationship will devlope linking these parameters to the C_d value based on the building's characteristics.

3.2 Parametric Study

The following table provides propeties of the models employed in the 40 case studies, outlining the specific configurations, dimensions, and reinforcement components applied to the columns and beams in each case. All details regarding columns and beams in the table have been extracted from ETABS software, ensuring compliance with the design requirements outlined in the ASCE7-16 Code and the ACI-318 Code in design structure as special momant-risiting frams (SMRFs). Table E.8 in Appendix A shows models specifications reinforcement employed in this research

3.3 Analysis Results

The analysis was carried out using SAP2000 software, as described earlier. Table No. 5 demonstrates the relationship between the C_d factor and the time period (T_n) , linking these factors with the number of stories, story height, span length, and the number of bays.

Table 5

Analysis results for 36 case studies

#	# Floors	# bays	Span Length	Floor Height	T_n (0.1N)	T_n Empirical	T_n	C_d
Case-1	4.00	3.00	5.00	3.00	0.40	0.44	4.36	4.05
Case-2	4.00	3.00	7.00	3.00	0.40	0.44	3.92	3.79
Case-3	4.00	4.00	5.00	3.50	0.40	0.50	4.10	3.74
Case-4	4.00	4.00	7.00	3.50	0.40	0.50	3.73	3.57
Case-5	4.00	5.00	6.00	4.00	0.40	0.57	3.87	3.45
Case-6	4.00	5.00	5.00	3.00	0.40	0.44	3.41	3.92
Case-7	4.00	3.00	5.00	3.50	0.40	0.50	4.09	3.94
Case-8	4.00	3.00	7.00	3.50	0.40	0.50	3.76	3.72
Case-9	4.00	3.00	6.00	4.00	0.40	0.57	3.91	3.69
Case-10	8.00	3.00	5.00	3.00	0.80	0.81	3.70	3.86
Case-11	8.00	3.00	7.00	3.00	0.80	0.81	3.65	3.77
Case-12	8.00	4.00	5.00	3.50	0.80	0.94	3.72	3.57
Case-13	8.00	4.00	7.00	3.50	0.80	0.94	3.44	3.44
Case-14	8.00	5.00	6.00	4.00	0.80	1.05	2.93	3.21
Case-15	8.00	5.00	5.00	3.00	0.80	0.81	3.49	3.73
Case-16	8.00	3.00	5.00	3.50	0.80	0.94	3.77	3.74
Case-17	8.00	3.00	7.00	3.50	0.80	0.94	3.60	3.59
Case-18	8.00	3.00	6.00	4.00	0.80	1.05	3.33	3.29
Case-19	12.00	3.00	5.00	3.00	1.20	1.17	2.97	3.30
Case-20	12.00	3.00	7.00	3.00	1.20	1.17	3.03	3.25
Case-21	12.00	4.00	5.00	3.50	1.20	1.35	3.24	3.19
Case-22	12.00	4.00	7.00	3.50	1.20	1.35	3.09	3.09
Case-23	12.00	5.00	6.00	4.00	1.20	1.52	3.08	3.06
Case-24	12.00	5.00	5.00	3.00	1.20	1.17	2.89	3.10
Case-25	12.00	3.00	5.00	3.50	1.20	1.35	2.81	3.22
Case-26	12.00	3.00	7.00	3.50	1.20	1.35	2.97	3.15
Case-27	12.00	3.00	6.00	4.00	1.20	1.52	3.13	3.12
Case-28	16.00	3.00	5.00	3.00	1.60	1.52	3.35	3.22
Case-29	16.00	3.00	7.00	3.00	1.60	1.52	3.24	2.99
Case-30	16.00	4.00	5.00	3.50	1.60	1.74	3.04	3.20
Case-31	16.00	4.00	7.00	3.50	1.60	1.74	2.97	2.94
Case-32	16.00	5.00	6.00	4.00	1.60	1.97	2.73	2.77
Case-33	16.00	5.00	5.00	3.00	1.60	1.52	2.90	3.07
Case-34	16.00	3.00	5.00	3.50	1.60	1.74	3.07	3.13
Case-35	16.00	3.00	7.00	3.50	1.60	1.74	2.53	2.97
Case-36	16.00	3.00	6.00	4.00	1.60	1.97	2.42	2.82

3.4 Results and Discussion

After collecting all the analysis results, C_d values were obtained for 36 buildings. Each building had distinct characteristics, including floor heights, span lengths, number of floors, and bays, with different frequencies. This variety of properties enabled us to study the influence of each characteristic on C_d and understand how strongly each one is associated with C_d, as well as the reasons for this association. These analysis results also helped in developing a relationship that allows us to determine the value of C_d based on it is characteristics.

3.4.1 Correlation B C_d and Building Characteristics

The relationship between building characteristics and the C_d factor was investigated using Excel and SPSS programs, based on the analysis results presented in the previous Table No. 5. Table No. 6 and Figure B.25 in the appendix B illustrate the relationship between different parameters represented by building characteristics and C_d.

Table 6

A correlation table was generated using Excel

	No. Floors	**No. bays**	**Span Length**	**Floor Height**	T_n	C_d
No. Floors	1.00					
No. bays	0.00	1.00				
Span Length	0.00	-0.21	1.00			
Floor Height	0.00	0.12	0.15	1.00		
T_n	0.93	-0.01	0.18	0.19	1.00	
C_d	-0.85	-0.17	-0.25	-0.32	-0.86	1.00

The table in the image shows the values of four variables: floors, number of bays, span length, floor height , Time-period (T_n), and deflection amplification factor (C_d) .The correlation coefficient measures how closely two variables are related, and ranges from -1 (perfect negative correlation) to 1 (perfect positive correlation).

The correlation analysis highlights several significant relationships between different parameters:

There is a highly positive correlation (0.93) between the number of floors and the building's period of time (T_n). This outcome was anticipated, and there are mathematical relationships that validate it. Hence, when establishing a relationship to calculate the C_d valuev , it is adequate to utilize the time-period parameter (T_n).

Conversely, there is a very strong negative correlation (-0.86) between the coefficient C_d and the building's time-period (T_n), indicating that C_d decreases with longer time periods (T_n).

A moderate negative correlation (-0.32) is observed between the coefficient C_d and floor height, although weaker compared to correlations with the number of floors or the periodic time.

A weak negative correlation (-0.25) is noted between the coefficient C_d and span length, with the Cd coefficient decreasing slightly as the span length increases.

Additionally, there is a weak negative correlation (-0.17) between the coefficient C_d and the number of bays, and thus this relationship is not significant compared to others.

3.4.2 The Effect of Time Period on C_d

The correlation analysis reveals a strong association between the periodic time (T_n), the number of floors, and the coefficient C_d. The Figure No. 6 shows the relationship between the time-period and the C_d coefficient.

Figure 6

The relationship between the periodic time and C_d factor

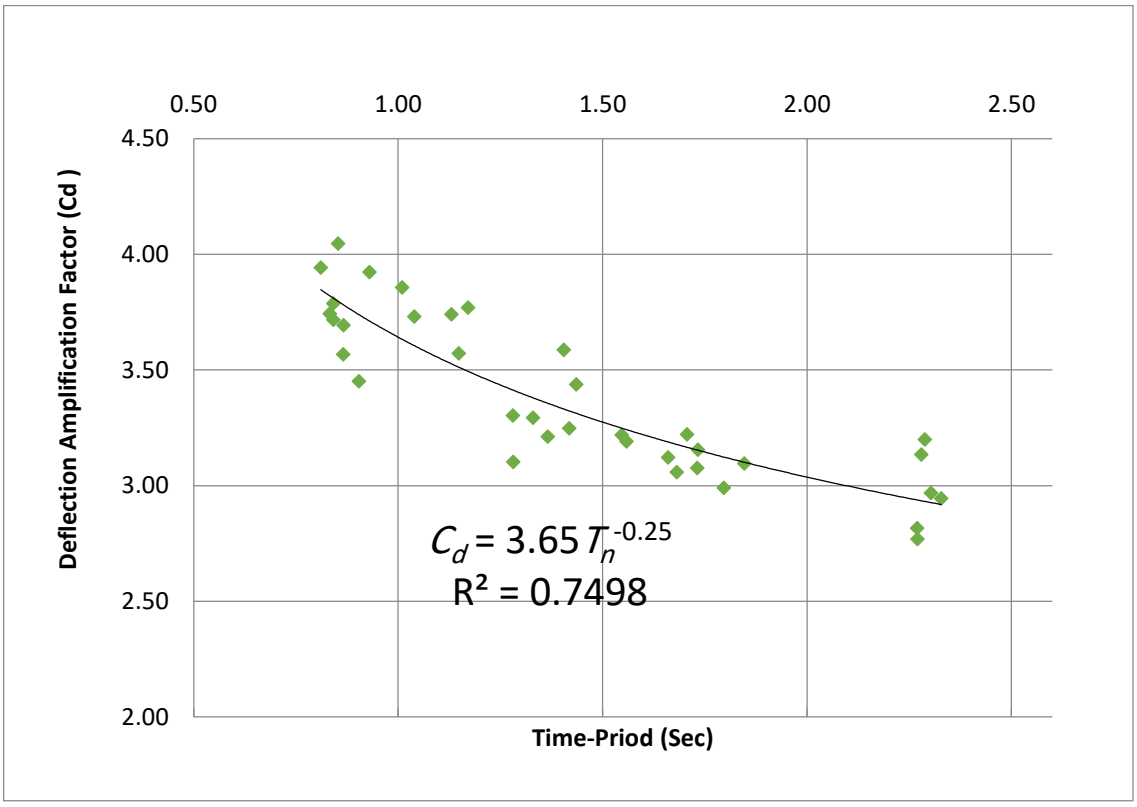

Figure No. 6 shows that as the height of the building increases, C_d decreases. This is in contrast with the codes ASCE7-16 which set a conctant value for the same structural system type regardless of the building period of 5.5. To explain the inverse relationship between C_d with time period associated with the number of floors, create a graph which linking C_d to the number of floors shown in Figure B.28 in the Appendix B , where

buildings that are fixed in span length, number of bays, and floor height and variable in number of floors were chosen and it was called a system.

From Figure B.28 in the Appendix B, it is observed that C_d decreases with increasing time periods (T_n). The reason for this is that buildings respond differently to seismic vibrations based on their time periods (T_n). In buildings with short periods (T_n), seismic vibrations have a faster impact. This rapid response leads to a significant decrease in seismic force impact and an increase in non-elastic deformations. On the other hand, buildings with long natural periods respond more slowly to seismic vibrations. Consequently, they experience a slight decrease in seismic force impact and fewer non-elastic deformations.

Figure No. 7 illustrates how the time period (T_n) of a structure influences the seismic force it experiences as it transitions from elastic to inelastic behavior. This is determined by analyzing the modal response spectrum and the force-displacement relationship of both the inelastic system and its linear counterpart.

Figure 7

Influence of Structure Time Period on Seismic Force and Inelastic displacement when Transition from Elastic to Inelastic Behavior through Modal Response Spectrum Analysis

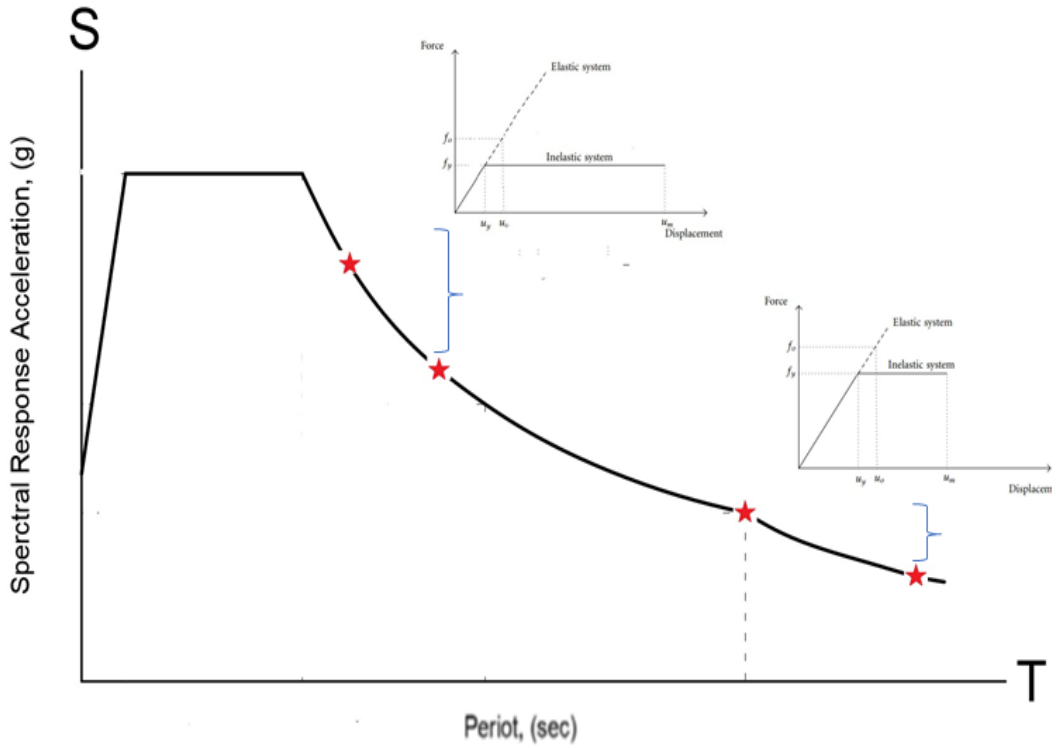

3.4.3 The Effect of Span Length on C_d

To understand the relationship between span length and C_d, refer to the graph depicted in Figure 8. This graph illustrates how the value of C_d changes as the span length increases. The results show that as the span length increases, C_d value decreases.

Figure 8

Variation of the C_d concerning the span length (5m and 7m) while altering the number of floors

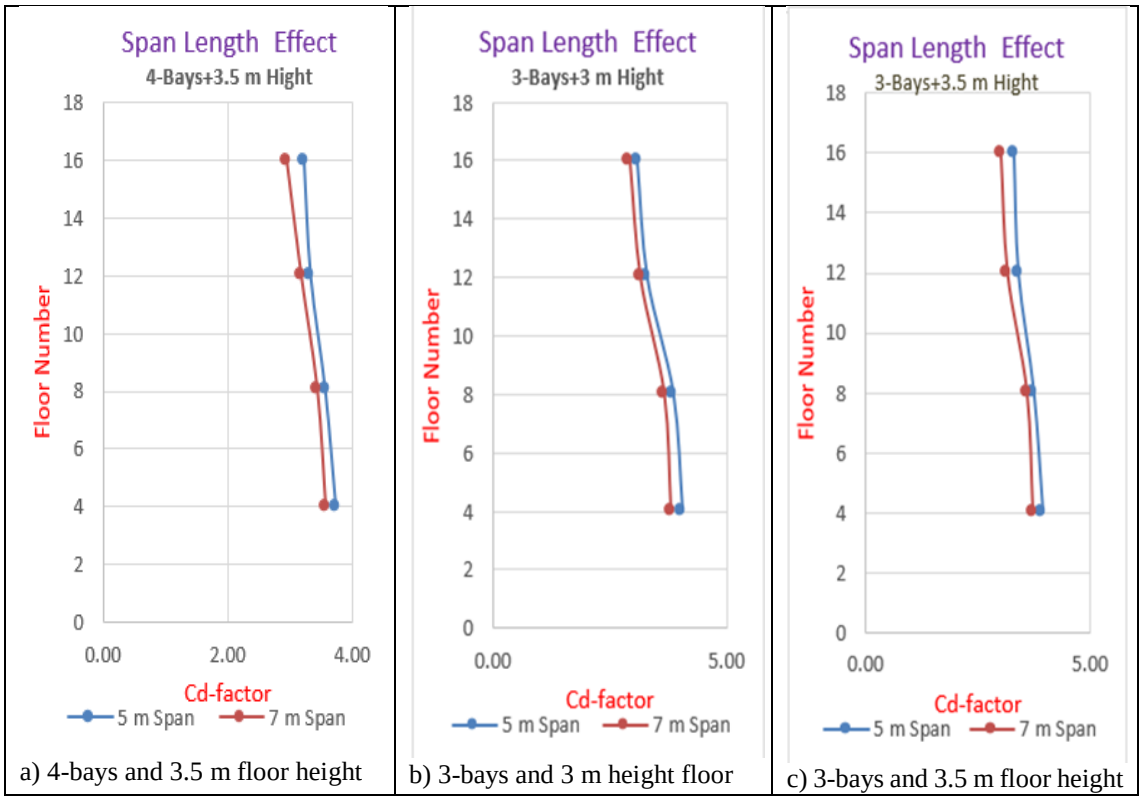

a) 4-bays and 3.5 m floor height

b) 3-bays and 3 m height floor

c) 3-bays and 3.5 m floor height

This observation is because the building's time period (T_n) affects the value of C_d, as discussed earlier in the section titled "The Effect of Time Period on C_d. The results presented in Table No. 5 indicate that buildings with longer spans have a longer time period (T_n) compared to those with shorter spans. This is because longer spans typically have a larger surface area and, consequently, more mass. Moreover, longer spans require larger dimensions and additional columns, adding to the mass. Mass, along with stiffness, is a key factor in determining the time period (T_n) of a building. Therefore, buildings with longer spans have a lower C_d value compared to those with shorter spans. This is due to the decrease in inelastic displacement as the span length increases, leading to decrease C_d.

3.4.4 The Effect of Floor Height on C_d

To investigate the effect of floor height on C_d, graphs were created shown in Figure 9, which shows how C_d values change with increasing floor height when the value of the rest of the parameters such as span length, number of bays, and number of floors are fixed.

The story height of a building affects the dynamic response of the structure. As the story height increases, it affects various dynamic properties such as time period , and overall structural behavior under dynamic loads.

Variations in floor height affect a building's time period (T_n) This happens because the positions of the building's mass centers change . Through the results obtained and shown in Table No. 5 , revealed that increasing floor height resulted in a higher time period (T_n) value. And accordingly, raising the height of the stories increase the flexibility of the structure and reduce inelastic displacement, leading to a decrease in the C_d value, as explained earlier on discussion effect of time period (T_n) on C_d. Conversely, decreasing floor height tends to increase the C_d value.

The relationship between story height and C_d value is shown in Figure No. 9. The results show that when floor height increases, C_d value decreases.

Figure 9

Variation of the C_d Factor concerning the Floor height (3m, and 3.5m) while altering the number of floors

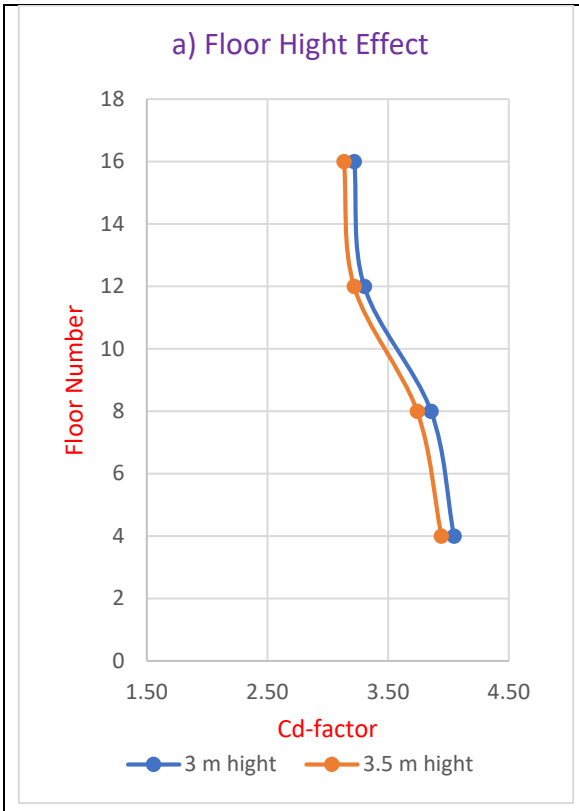

a) 3-bays and 7 m Span length

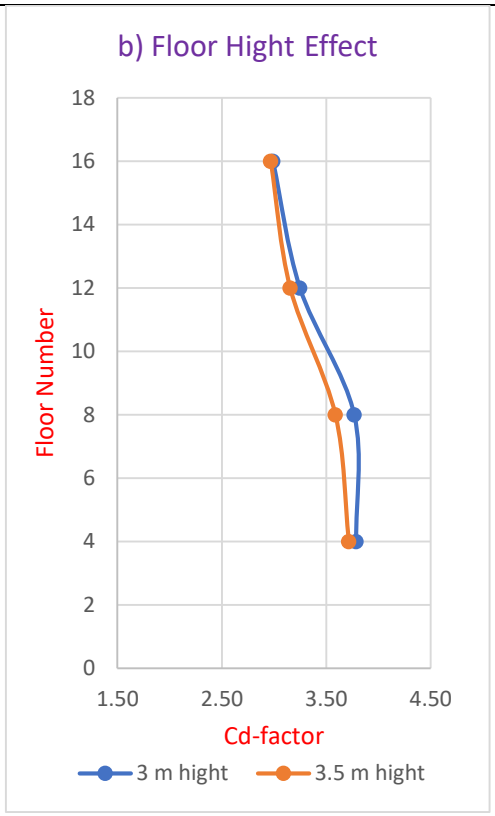

b) 3-bays and 7 m Span length

3.4.5 The Effect of Number of Bays on C_d

To understand the connection between the number of bays and C_d, we referred to figure No. 10 , depicting the relationship's nature. It is clear from the graph that there is an inverse relationship between the number of bays and the C_d value. When a building is subjected to dynamic loads, its stiffness affects how much it deflects or moves under the applied force. Buildings with more bays tend to resist deformation better. As a result, the Cd decreases compared to buildings with fewer bays. On the other hand, when the number of bays decreases, fewer plastic hinges will be needed for the structure to fail.

Figure 10

Variation of the Cd Factor concerning the number of bays (3,4, and5) while altering the number of floors

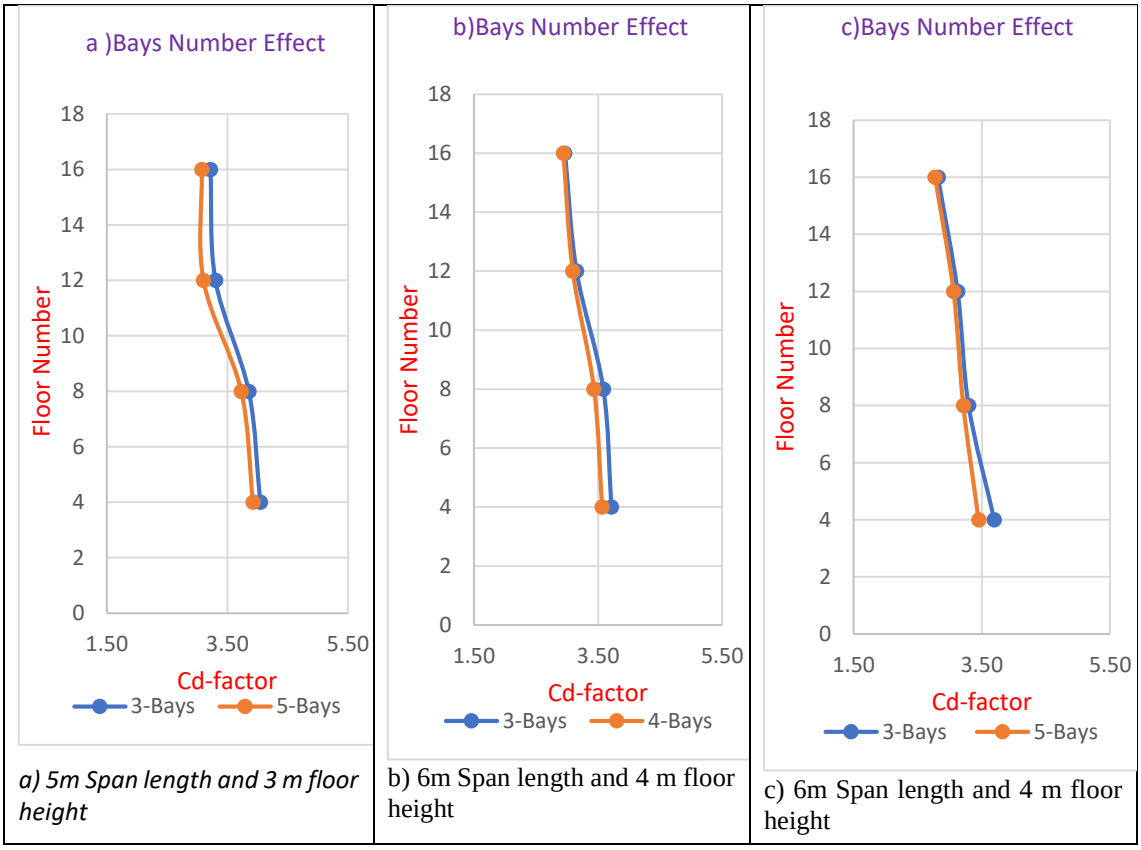

a) 5m Span length and 3 m floor height

b) 6m Span length and 4 m floor height

c) 6m Span length and 4 m floor height

3.5 Proposed Equation for C_d

In order to devlope an equation for calculating C_d value for each building, considering dimensions and height, we will utilize the SPSS program. This software will conduct regression analysis to establish connections among various parameters influencing C_d value.

To derive a reliable equation, we must follow specific steps after analyzing data obtained from linear and non-linear Time history analyses to compute C_d. First, conduct regression analysis. Second, assess the error rate generated by the equation. Finally, validate the equation using four analyzed cases and get their corresponding C_d values.

3.5.1 Regression Analysis

In order to perform the regression, we resorted to multiple linear regression, and Equation No. 16 represents the formula of the equation.

$$Y = \beta 0 + \Sigma j = 1..p\beta jXj + \varepsilon \quad (16)$$

In this equation:

Y :is the dependent variable, the one we're trying to predict or understand.
$\beta 0$: is the intercept, indicating the value of Y when all explanatory variables are zero.
Xj :represents the jth explanatory variable in the model, where j ranges from 1 to p.
βj :is the coefficient associated with the jth explanatory variable, showing how much Y changes when Xj changes by one unit, keeping all other variables constant.
ε :is the random error term, accounting for the difference between the observed Y value and the predicted value by the model. It has an average value of 0 and a variance of σ^2.

In essence, this equation illustrates how the dependent variable Y is affected by several explanatory variables $X1, X2, \ldots, Xp$, each with its own coefficient βj, alongside an intercept and a random error term.

According to the statistical analysis depicted in Table No. 7, the Adjusted R-Square indicates a strong and satisfactory correlation, standing at 0.792. Moreover, most variables exhibit acceptable statistical significance, except for the span length variable, which displays a slightly elevated value. However, given its relevance to the equation, it will be retained for further analysis.

Table 7

Regression Statistics for equation to compute C_d value.

Regression Statistics	C_d value
Multiple R	0.903
R Square	0.815
Adjusted R Square	0.791
Standard Error	0.028
Observations	36

The equation's No. 17 and. 18 formula will be as follows in light of the earlier data in Table No. 8.

Table 8

Coefficients of equation to compute C_d value.

	Coefficients	Standard Error	t Stat	P-value
Intercept	0.93	0.057	16.34	8.69E-17
numbre of Bays	-0.014	0.006	-2.21	0.03413
Span Length	-0.0045	0.0058	-0.77	0.442365
Floor Height	-0.027	0.014	-1.97	0.047651
T_n	-0.101	0.0097	-10.42	1.18E-11

It appears from the results obtained from the regression analysis that both span length have a high P-value and therefore will be neglected in the proposed equation. When the P-value is high (usually greater than 0.05), the coefficients in the equation can be neglected because they do not add. Statistical significance to the model. (Moore, David S., al, 1989).

$$Cd_{new} = (B_0 + B_1 * Tn + B_2 * No.Bays + B_3 * \text{Floor Height}) * Cd_{code}$$

$$Cd_{new} = \eta * Cd_{code} \quad (17)$$

$$\eta = 0.93 - 0.101\,Tn - 0.014B - 0.027\text{H} \quad (18)$$

Where:

Tn: Fundamental period of the structure, in (sec).

B: Number of Bays.

H: Floor Heights.

3.5.2 Residual

In order to assess regression models, it's important to establish certain metrics. These metrics typically revolve around the concepts of residuals and errors, which measure how accurately a model predicts individual data points (Onyutha, Charles, et al.2015). In some cases, a residual error below 10% of the range of the dependent variable may be considered acceptable, while in others, a smaller or larger error may be warranted based on the requirements of the analysis and the precision needed for the predictions (Roy, Banerjee, & Pal, 2016).

Figure B.1 in Appendix B displays the residual as a fuction of time-period, floor height, span length and No. of bays. The figure hows good destribution of residuals around the zero

Table No. 9 indicates that the equation is statistically valid, and the error rate is below 10%, specifically at 2.7%, which is considered highly favorable.

Table 9

ANOVA table by SPSS software for C_d equation.

	df	SS	MS	F	Significance F
Regression	4	0.114	0.028	34.309	5.61E-11
Residual	31	0.025	0.000		
Total	35	0.140			

3.5.3 Validate the Equation

To validate the equation, four case studies (which are different from those used in the parametric study) were analyzed using the SAP 2000 program, as detailed in table No. 10, to obtain the C_d values.

Table 10

Root Mean Squared Error of the fitted model

CASES	INPUT					OUTPUT		
#	#Floors	# bays	Span Length	Floor Height	T_n	C_d- analysis	C_d - Equation	Sum of squares
Case-1	4	4	5	3.5	0.89	3.68	3.8	0.01
Case-2	8	5	6	3	0.93	3.76	3.75	0
Case-3	12	3	7	4	1.19	3.59	3.62	0
Case-4	16	4	6	3	1.73	3.27	3.4	0.01

Table No. 10 presents the C_d values obtained through analysis alongside those derived computed from the equation. The sum of squared errors, calculated without incorporating the error rate from equation, was found to be 2% lower than the permissible threshold for exceedance 10% . This allows the equation to be adopted and its results trusted.

Chapter Four
Conclusion and Recommendation

4.1 Overview

In this thesis, the deflection amplification factor (C_d) was studied in moment-resisting reinforced concrete frames (RC-MRFs) with a special sway configuration. It aims to determine the accurate C_d value for each building by developing a simplified predictive equation to calculate the C_d value. Thus, it helps in solving the problem of seismic separations between two adjacent buildings .

4.2 Conclusions

Based on the study, the following conclusions can be drawn:

1. C_d value was found to be between 4.05 and 2.77 after design and analysis. This suggests that the ASCE 7-16 code, which suggests a value of 5.5 for the same structural system, is is considered conservative.
2. The number of floors significantly impacts the C_d which is closely linked to the building's time period. Moderate effects are observed for floor height, while negligible effects were noticed for the number of bays and span length.
3. Increasing the building's time period (T_n) was found to decrease the C_d value. This reduction happens because taller structures require longer time periods, which reduce of dynamic forces less than building with short time periods (Short hight bulding). Thus , buildings with long time period have inelastic defromation less than buildings have short time period during earthquakes.
4. C_d decreases with increasing span length and floor height. An increase in span length leads to a longer time period (T_n) due to the heightened mass resulting from expanded floor area and enlarged dimensions of the concrete sections in structural elements such as columns and beams. On the other hand, when the floor height increases, the center of mass of the floor changes vertically, causing the time period (T_n) to increase also . As mentioned above longer time period (T_n) correlate with reduced inelastic deformation, the C_d value decreases.
5. Increasing the number of bays decreases C_d value. This is because fewer plastic hinges are needed for the structure to fail when there are decreases bays.

6. An equation (mathematical expression) had been proposed to calculate C_d that takes into account the building characteristics.

4.3 Proposed Equations

The simplified equation (Equation No. 19) can be used for predicting the value of the defliction amplification factor *(C_d)*. These equation were developed using statistical regression from data obtained from analysis using SAP 2000.

These equation are subjected to some limitations are illustrated below:

$$Cd_{new} = \eta * Cd_{code} \quad (19)$$

Where:

$$\eta = 0.93 - 0.101\,Tn - 0.014B - 0.027\mathrm{H} \quad (20)$$

Where:

Tn: Fundamental period of the structure, in (sec).

B: Number of Bays.

H: Floor Heights.

limitations of equation No. 19:

1. This equation is applicable to buildings with sway special moment-resisting reinforced concrete frames (RC-SMRFs) .
2. The equation is generated for buildings with square plan .
3. Characteristics of the materials for which the equation was created: B350 concrete and A615Gr60 reinforcement.
4. The equation is applied for columns with square cross section
5. The column cross section area falls within the ranges ($0.09\ m^2 < AC < 1.2\ m^2$).
6. The range for the number of bays (B) used in the equation is ($3 < B < 5$)
7. The range for the Floor Height (H) used in the equation is ($3 < H < 4$)
8. Applicable t0o seismicity hazerd with Z=0.3

4.4 Recommendations and Future Studies

To enhance the understanding garnered from this study, there are various avenues for future research that could be pursued. These include:

1. Performing a similar analysis using non-linear time history analysis, encompassing a wider array of earthquakes and diverse seismic zones.
2. Investigating alternative building formations, including the incorporation of rectangular shapes, to evaluate their influence on C_d factor.
3. Exploring additional parameters such as damping, material efficiency, and other factors that may impact C_d.
4. Examining different structural systems, such as bearing wall systems, to expand the breadth of insights into seismic design considerations.

References

Alwahsh, E., Sader, S., & Juhari, A. H. ((n.d)). *ACADEMIC HUBS: Using applied research and community services to build resilience of nations and communities to disasters.*

American Society of Civil Engineers. (2022). Minimum design loads and associated criteria for buildings and other structures. *ASCE/SEI 7-22*.

Bhowmik, T. (2011). *FRP-confined capsule-shaped columns under axial and lateral loadings.* (PhD thesis). National University of Singapore.

Chopra, A. K. (2017). *Dynamics of structures (4th ed.).* Prentice Hall International Series in Civil Engineering and Engineering Mechanics.

Chopra, A. K. (2017). *Dynamics of structures: Theory and applications to earthquake engineering (5th ed.).* Berkeley: University of California.

El-Hussain, I., Sader, S., & Juhari, A. H. (2018). Developing a seismic source model for the Arabian Plate. *Arabian Journal of Geosciences, 11*, pp. 1-29. Retrieved from https://doi.org/10.1007/s12517-018-3686-3

Erlangga, W., Teguh, M., & Saputro, I. T. (2020). Development of time histories based on shallow crustal earthquake sources considering the new version of the Indonesian earthquake map. *International Conference on Sustainable Civil Engineering Structures and Construction Materials* (pp. 1-10). Singapore: Springer Nature Singapore.

Filippou, C. A. (2013). *Seismic capacity assessment and retrofitting of reinforced concrete building.* (Master's thesis).

Ghosh, S. K. (2014). Significant changes from ASCE 7-05 to ASCE 7-10, part 1: Seismic design provisions. *PCI Journal, 59(1).*

Harris, K. D., & Robinson, N. D. (2013). *Practical solutions.* STRUCTURE, 18.

Huang, Y., Wang, L., Yang, Z., & Wei, H. (2023). A simplified method for evaluating the diaphragm flexibility for frame-shear wall structure under earthquake load. *Buildings, 13(2),* p. 376. Retrieved from https://doi.org/10.3390/buildings13020376

International Code Council. (1997). *Uniform building code, Volume 2, Structure engineering design provision.* Falls Church, VA: International Code Council, Inc.

Konstantinidis, D. K., Kappos, A. J., & Izzuddin, B. A. (2007). Analytical stress–strain model for high-strength concrete members under cyclic loading. *Journal of Structural Engineering, 133(4).* Retrieved from https://doi.org/10.1061/(ASCE)0733-9445(2007)133:4(484)

Kumar, C. M., & Sahoo, D. (2014). *Moment curvature characteristics for structural elements of RC buildings.*

Lallotra, B., & Singhal, D. (2017). State of the art report: A comparative study of structural analysis and design software—STAAD Pro, SAP-2000 & ETABS software. *International Journal of Engineering and Technology, 9(2),* pp. 1030-1043.

Mahmoudi, M., & Sadr Abad, M. J. (2022). Assessment on the deflection amplification factor of steel buckling-restrained bracing frames. *Advances in Structural Engineering, 25(2),* pp. 231-246. Retrieved from https://doi.org/10.1177/13694332211069255

Mander, J. B., Priestley, M. J., & Park, R. (1988). Theoretical stress-strain model for confined concrete. *Journal of Structural Engineering, 114(8),* pp. 1804-1826.

Meghraoui, M. (2015). *Paleoseismic history of the Dead Sea fault zone. In Encyclopedia of Earthquake Engineering*. Retrieved from https://doi.org/10.1007/978-3-642-36197-5_40-1

Merter, O., & Ucar, T. (2013). A comparative study on nonlinear static and dynamic analysis of RC frame structures. *Journal of Civil Engineering and Science, 2(3),* pp. 155-162.

Monteiro, R., Dursun, B., & Andrade, J. (2016). Towards integrated seismic risk assessment in Palestine—application to the city of Nablus. *Proceedings of the VII European Congress on Computational Methods in Applied Sciences and Engineering (ECCOMAS Congress 2016)*.

Onyutha, C., & Willems, P. (2015). Empirical statistical characterization and regionalization of amplitude–duration–frequency curves for extreme peak flows in the Lake Victoria Basin, East Africa. *Hydrological Sciences Journal, 60(6)*, pp. 997-1012. Retrieved from https://doi.org/10.1080/02626667.2015.1051375

Pozo, F., Martínez, M., & Martínez, E. (2009). Nonlinear modeling of hysteretic systems with double hysteretic loops using position and acceleration information. *Nonlinear Dynamics, 57*, pp. 1-12. Retrieved from https://doi.org/10.1007/s11071-009-9512-8

Qafeshah, L., & Radwan, D. (2023). *he seismic design of Bethlehem General Hospital*. Retrieved from http://localhost:8080/xmlui/handle/123456789/8918

Razvi, S., & Saatcioglu, M. (1999). Confinement model for high-strength concrete. *Journal of Structural Engineering, 125(3)*, pp. 281-289.

Rizwan, M., & Shah, S. A. (2021). Seismic damage assessment of deficient reinforced concrete frame structures. *Civil and Environmental Engineering, 17(1)*, pp. 31-44.

Roy, K., Banerjee, D., & Pal, S. (2016). Be aware of error measures: Further studies on validation of predictive QSAR models. *Chemometrics and Intelligent Laboratory Systems, 152*, pp. 18-33. Retrieved from https://doi.org/10.1016/j.cemlabs.2016.02.008

Sabah, R., Öztorun, N. K., & Sayin, B. (2022). Development of an FEA program with full-size stiffness and mass matrices for dynamic analysis of high-rise buildings: A comparison with SAP2000. *Case Studies in Construction Materials, 17*, p. e01490. Retrieved from https://doi.org/10.1016/j.cscm.2022.e01490

Scott, B. D. (1980). *Stress: strain relationships for confined concrete: Rectangular sections.*

Sengupta, P., & Li, B. (2017). Hysteresis modeling of reinforced concrete structures: State of the art. *ACI Structural Journal, 114(1)*, pp. 25-38.

Simiu, E. (2011). *Design of buildings for wind: A guide for ASCE 7-10 standard users and designers of special structures.* John Wiley & Sons.

Solomos, G., Pinto, A., & Dimova, S. (2008). A review of the seismic hazard zonation in national building codes in the context of Eurocode 8. *JRC Scientific and Technical Reports*.

Spacone, E., & Filippou, F. C. (1991). *A fiber beam-column element for seismic response analysis of reinforced concrete structures.* Report No. UCB/EERC-91/17. Earthquake Engineering Research Center.

Taghinezhad, R., Ghasemi, H., & Mohammadi, S. (2017). Numerical investigation of deflection amplification factor in moment resisting frames using nonlinear pushover analysis. *International Journal of Innovations in Engineering and Science, 2(12)*, pp. 1-7.

Vecchio, F. J., & Emara, M. B. (1992). Shear deformations in reinforced concrete frames. *ACI Structural Journal, 89(1)*, pp. 46-56.

List of Abbreviations

Abbreviations	Meaning
ACI	American Concrete Institute
ASCE	American Society of Civil Engineers- Structural Engineering Institute
UBC	Uniform Building Code
NEHRP	National Earthquake Hazards Reduction Program
RC	Reinforced Concrete
NLTHA	Nonlinear time-history analysis
LTHA	linear time-history analysis
SMRF	Special Moment Resisting Frame System
OMRF	Ordinary moment-resisting frame
EBF	Eccentrically braced frame
CBF	Concentrically braced frame.
PGA	Peak ground acceleration
IBC	The International Building Code
BRB	Buckling restrained brace
SDOF	Single Degree of Freedom
DAF	Deflection Amplification Factor
RS	response spectrum
Ss	0.2 Sec Spectral Accel
S1	1 Sec Spectral Accel
Fv	Short-Period Site Coefficient
Fa	Long -Period Site Coefficient
SDS	Design Spectral Response acceleration parameter at short period
SD1	Design Spectral Response acceleration parameter at 1-s period
EuroCode8	European code 8
ASCE-7-16	American Society of Civil Engineers
C_d	Deflection Amplification Factor
δe	Maximum elastic displacement
δi	Maximum inelastic displacement
Δ_m	Maximum inelastic displacement According UBS 97
Δ_s	Maximum elastic displacement According UBS 97
β	Constant =0.7
R_μ	Coefficient of ductility behavior
R	Deflection amplification factor According National Building Code of Canada

Q	Deflection amplification factor According México Building Code
q	Deflection amplification factor According Eurocode No. 8
S_d	design response spectrum acceleration at the structure's period T
S_a	The design ground acceleration.
T	The fundamental natural period of the structure
T_o	The reference period, usually taken as 1 second
T_n	Time Period for the Structure
E	Modulus Of Elasticity
F_y	Minimum Yield Stress
fc	Specified Concrete Compressive Strength
A	Coefficient Of Thermal Expansion,
G	Shear Modulus
N	Number of stories
h	Structural height
C_t	Coefficient with a fixed value of 0.0466 for MRF-RC
ϵ	the random error term
B	Number of Bays
L	Span length, in(m)
H	Story heights, in (m)
μ	Ductility Reduction Factor

Appendices

Appendix A

Tables

Table A. 1

Cd value According of in NEHRP Recommended Provisions for the structure systems [20]

Framing system	C_d
SMRF	5.5
OMRF	4
Dual System EBF + SMRF	4
CBF + SMRF	5
Building Frame System EBF	4
CBF	4.5

Note: SMRF = special moment-resisting frame; OMRF = ordinary moment-resisting frame; EBF = eccentrically braced frame; CBF = concentrically braced frame.

Table A. 2

Deflection amplification factor in different building codes [20]

Building code	Deflection amplification factor
Uniform Building Code (1991)	$3Rw\ /8$
NEHRP Seismic Provisions (1991)	C_d
National Building Code of Canada (1990)	R
`México Building Code (1987)	Q
Eurocode No. 8 (1988)	q
Less than Q in short period range	

Table A. 3

Time-History record properties

earthquake record mane	Date	Magnitude:	(PGA)
Hachinohe (IBC1)	1968	7.2	0.229 g
Kobe (IBC2)	1995	6.8	0.833 g
Imperial Valley (IBC3)	1940	6.9	0.350 g

Table A. 4

Comparison of models for confined and unconfined concrete (Razvi and Saa ,Mander, and Kent and Park)

model	Long. steel	spacing	Lateral steel size	Lateral steel config.	Effective area	Section geometry	Lateral pressure	Lateral steel stress
Razvi and Saa.	*	*	*	*	*	*	*	*
Mander	*	*	*	*	*	*	*	*
Kent and Park			*			*	*	

Table A. 5

Geometric and design layout of prototype RC frame

Members /material	Prototype geometry	1/3rd scaled model geometry
Bay length	5487 mm (18 feet)	1828.8 mm (6 feet)
Story height	3658 mm (12 feet)	1219.2 mm (4 feet)
Beams	304 mm x 459 mm (12 in x 18 in)	102 mm x 153 mm (4 in x 6 in)
Columns	304 mm x 304 mm (12 in x 12 in)	102 mm x 102 mm (4 in x 4 in)
Slab	153 mm (6 in)	51 mm (2 in)
Reinforcement rebar	414 MPa (60000 psi)	414 MPa (60000 psi)
Concrete	21 MPa (3000 psi)	21 MPa (3000 psi)

Table A. 6

General properties of the RC framed structure used in macro modeling

Parameters	Details
Number of Stories	4 floors.
Floor Height	3 meters.
Span Lengths	5 meters.
Number of Structural Bays	3 Bays
Area of Building Floor	225m^2

Table A. 7

SIDL account details

material	Density (KN/m3)	thickness	SID
Tiles	18	1	0.18
Fill materials (fine aggregate)	16	10	1.6
Mortars	21	2	0.42
Plastering	21	1.5	0.31
partitions	-	-	0.5
Sum			3.0

Table A. 8

models Specifications reinforcement employed in the Research.

Cases	Story-Bay-Span-Height	Beam	Base Column	Column
Case-1	4-3-5-3	(0.45*0.25) (T5 ϕ16mm) (B 4 ϕ16mm)	(0.45*0.45) (8 ϕ20mm)	(0.45*0.45) (8 ϕ16mm)
Case-2	4-3-7-3	(0.60*0.30) (T9 ϕ20mm) (B4 ϕ16mm)	(0.60*0.60) (20 ϕ25mm)	(0.60*0.60) (16 ϕ20mm)
Case-3	4-4-5-3.5	(0.55*0.25) (T4 ϕ20mm) (B4 ϕ16mm)	(0.55*.55) (16ϕ20mm)	(0.55*0.55) (16 ϕ16mm)
Case-4	4-4-7-3.5	(0.70*0.30) (T6ϕ20mm) (B4 ϕ20mm)	(0.70*.70) (20ϕ25mm)	(0.70*.70) (16ϕ20mm)
Case-5	4-5-6-4	(0.65*0.30) (T7ϕ20mm) (B4 ϕ20mm)	(0.70*.70) (20ϕ25mm)	(0.70*.70) (16ϕ20mm)
Case-6	4-5-5-3	(0.45*0.25) (T5 ϕ16mm) (B 4 ϕ16mm)	(0.45*0.45) (8 ϕ20mm)	(0.45*0.45) (8 ϕ16mm)
Case-7	4-3-5-3.5	(0.75*0.30) (T5 ϕ20mm) (B 4 ϕ20mm)	(0.75*0.75) (24 ϕ20mm)	(0.75*0.75) (24 ϕ20mm)
Case-8	4-3-7-3.5	(0.85*0.30) (T6 ϕ20mm) (B 5 ϕ20mm)	(0.85*0.85) (28 ϕ20mm)	(0.85*0.85) (24 ϕ20mm)

Case-9	4-3-6-4	(0.75*0.30) (T5 ϕ20mm) (B 4 ϕ20mm)	(0.75*0.75) (24 ϕ25mm)	(0.75*0.75) (24ϕ20mm)
**Case-10	4-4-5-3	(0.45*0.25) (T5 ϕ16mm) (B 4 ϕ16mm)	(0.45*0.45) (8 ϕ20mm)	(0.45*0.45) (8 ϕ16mm)
Case-11	8-3-5-3	(0.75*0.30) (T5 ϕ20mm) (B 4 ϕ20mm)	(0.75*0.75) (24 ϕ20mm)	(0.75*0.75) (24 ϕ20mm)
Case-12	8-3-7-3	(0.85*0.30) (T6 ϕ20mm) (B 5 ϕ20mm)	(0.85*0.85) (28 ϕ20mm)	(0.85*0.85) (24 ϕ20mm)
Case-13	8-4-5-3.5	(0.75*0.30) (T5 ϕ20mm) (B 4 ϕ20mm)	(0.75*0.75) (24 ϕ25mm)	(0.75*0.75) (24ϕ20mm)
Case-14	8-4-7-3.5	(0.90*0.35) (T6 ϕ25mm) (B 4 ϕ25mm)	(0.80*0.80) (24 ϕ25mm)	(0.80*0.80) (20ϕ20mm)
Case-15	8-5-6-4	(0.90*0.30) (T6 ϕ25mm) (B4 ϕ25mm)	(0.85*0.85) (28 ϕ25mm)	(0.85*0.85) (28 ϕ20mm)
Case-16	8-5-5-3	(0.75*0.30) (T5 ϕ20mm) (B 4 ϕ20mm)	(0.75*0.75) (24 ϕ20mm)	(0.75*0.75) (24 ϕ20mm)
Case-17	8-3-5-3.5	(0.75*0.30) (T5 ϕ20mm) (B 4 ϕ20mm)	(0.75*0.75) (24 ϕ25mm)	(0.75*0.75) (24ϕ20mm)
Case-18	8-3-7-3.5	(0.90*0.35) (T6 ϕ25mm) (B 4 ϕ25mm)	(0.80*0.80) (24 ϕ25mm)	(0.80*0.80) (20ϕ20mm)
Case-19	8-3-6-4	(0.90*0.30) (T6 ϕ25mm) (B4 ϕ25mm)	(0.85*0.85) (28 ϕ25mm)	(0.85*0.85) (28 ϕ20mm)
**Case-20	8-4-5-3	(0.75*0.30) (T5 ϕ20mm) (B 4 ϕ20mm)	(0.75*0.75) (24 ϕ20mm)	(0.75*0.75) (24 ϕ20mm)
Case-21	12-3-5-3	(0.85*0.30) (T8 ϕ20mm) (B7 ϕ20mm)	(0.80*0.80) (24 ϕ25mm)	(0.80*0.80) (20ϕ20mm)
Case-22	12-3-7-3	(1.00*0.40) (T8 ϕ25mm) (B7 ϕ25mm)	(0.90*0.90) (36 ϕ25mm)	(0.90*0.90) (28ϕ20mm)
Case-23	12-4-5-3.5	(0.85*0.30) (T6 ϕ20mm) (B 5 ϕ20mm)	(0.85*0.85) (28 ϕ20mm)	(0.85*0.85) (24 ϕ20mm)
Case-24	12-4-7-3.5	(1.00*0.40) (T7ϕ25mm) (B6 ϕ25mm)	(0.85*0.85) (30 ϕ28mm)	(0.85*0.85) (24 ϕ20mm)
Case-25	12-5-6-4	(1.10*0.40) (T7ϕ25mm) (B6 ϕ25mm)	(0.90*0.90) (36 ϕ28mm)	(0.90*0.90) (24 ϕ20mm)
Case-26	12-5-5-3	(0.85*0.30) (T8 ϕ20mm) (B7 ϕ20mm)	(0.80*0.80) (24 ϕ25mm)	(0.80*0.80) (20ϕ20mm)
Case-27	12-3-5-3.5	(0.85*0.30) (T6 ϕ20mm) (B 5 ϕ20mm)	(0.85*0.85) (28 ϕ20mm)	(0.85*0.85) (24 ϕ20mm)
Case-28	12-3-7-3.5	(1.00*0.40) (T7ϕ25mm) (B6 ϕ25mm)	(0.85*0.85) (30 ϕ28mm)	(0.85*0.85) (24 ϕ20mm)
Case-29	12-3-6-4	(1.10*0.40) (T7ϕ25mm) (B6 ϕ25mm)	(0.90*0.90) (36 ϕ28mm)	(0.90*0.90) (24 ϕ20mm)
**Case-30	12-4-5-3	(0.85*0.30) (T8 ϕ20mm) (B7 ϕ20mm)	(0.80*0.80) (24 ϕ25mm)	(0.80*0.80) (20ϕ20mm)
Case-31	16-3-5-3	(0.85*0.30) (T8 ϕ20mm) (B7 ϕ20mm)	(0.90*0.90) (30 ϕ28mm)	(0.90*0.90) (30ϕ28mm)
Case-32	16-3-7-3	(1.00*0.45) (T8 ϕ25mm) (B7 ϕ25mm)	(1.10*1.10) (42ϕ28mm)	(1.10*1.10) (24ϕ28mm)
Case-33	16-4-5-3.5	(1.00*0.35) (T8 ϕ20mm) (B7 ϕ20mm)	(1.00*1.00) (36ϕ25mm)	(1.00*1.00) (32ϕ25mm)
Case-34	16-4-7-3.5	(1.00*0.35) (T8 ϕ20mm) (B7 ϕ20mm)	(1.00*1.00) (42ϕ28mm)	(1.00*1.00) (32ϕ20mm)
Case-35	16-5-6-4	(1.00*0.35) (T7 ϕ25mm) (B6 ϕ25mm)	(1.10*1.10) (42ϕ25mm)	(1.10*1.10) (20ϕ28mm)

Case-36	16-5-5-3	(1.00*0.40) (T8 ϕ25mm) (B7 ϕ25mm)	(0.90*0.90) (30 ϕ28mm)	(0.90*0.90) (30ϕ28mm)
Case-37	16-3-5-3.5	(1.00*0.35) (T8 ϕ20mm) (B7 ϕ20mm)	(1.00*1.00) (36ϕ25mm)	(1.00*1.00) (32ϕ25mm)
Case-38	16-3-7-3.5	(1.00*0.35) (T8 ϕ20mm) (B7 ϕ20mm)	(1.00*1.00) (42ϕ28mm)	(1.00*1.00) (32ϕ20mm)
Case-39	16-3-6-4	(1.00*0.35) (T7 ϕ25mm) (B6 ϕ25mm)	(1.10*1.10) (42ϕ25mm)	(1.10*1.10) (20ϕ28mm)
**Case-40	16-4-5-3	(0.85*0.30) (T8 ϕ20mm) (B7 ϕ20mm)	(0.90*0.90) (30 ϕ28mm)	(0.90*0.90) (30ϕ28mm)
		*** this cases for equation validation		

Table A. 9

Model Summary (Regression Statistics) for Time-period Equation

Regression Statistics	
Multiple R	0.966
R Square	0.932
Adjusted R Square	.930
Standard Error	0.31699

Table A. 10

ANOVA for Time-period

	Sum of squares	**Df`**	**MS**	**F**	**Significance F**
Regression	8.144	1	8.114	467.781	0.000
Residual	0.590	34	0.017		
Total	8.703	35			

Table A. 11

Coefficients for Time-period Equation

	Coefficients	**Standard Error**	**t Stat**	**P-value**
(Constant)	0.411	0.052	7.862	0.00
H	0.031	0.001	21.628	0.00

Table A. 12

C_d calculation details for case1

Case-1	**Tn**	**0.85334**	**4.05**	**Cd**		
Floor	**ELASTIC**			**INELASTIC**		
	IBC-1	**IBC-2**	**IBC-3**	**IBC-1**	**IBC-2**	**IBC-3**
4	4.40	4.10	3.95	15.03	17.80	17.40
3	3.59	3.36	3.23	12.66	14.46	15.42
2	2.42	2.20	2.11	8.26	9.45	11.02
1	0.98	0.83	0.83	2.83	3.36	4.18
0	0.00	0.00	0.00	0.00	0.00	0.00

Table A. 13

Cd calculation details for case2

Case-2		Tn	0.84136	3.79	Cd	
Floor	ELASTIC			INELASTIC		
	IBC-1	IBC-2	IBC-3	IBC-1	IBC-2	IBC-3
4	4.48	4.80	4.56	15.86	18.18	16.64
3	3.48	3.86	3.59	13.07	14.85	14.20
2	2.13	2.48	2.29	8.70	9.69	10.05
1	0.76	0.93	0.82	3.61	3.92	4.55
0	0.00	0.00	0.00	0.00	0.00	0.00

Table A. 14

C_d calculation details for case3

Case-3		Tn	0.83293	3.74	Cd	
Floor	ELASTIC			INELASTIC		
	IBC-1	IBC-2	IBC-3	IBC-1	IBC-2	IBC-3
4	4.36	4.19	4.56	14.47	17.07	16.91
3	3.56	3.41	3.67	12.31	14.40	15.08
2	2.38	2.22	2.35	8.66	9.91	11.41
1	0.94	0.85	0.90	3.98	4.37	5.69
0	0.00	0.00	0.00	0.00	0.00	0.00

Table A. 15

C_d calculation details for case 4

Case-4		Tn	0.86563	3.57	Cd	
Floor	ELASTIC			INELASTIC		
	IBC-1	IBC-2	IBC-3	IBC-1	IBC-2	IBC-3
4	4.26	5.10	4.11	15.20	18.19	17.87
3	3.33	3.92	3.15	13.35	16.03	15.75
2	2.25	2.49	2.02	8.75	11.63	11.43
1	0.86	0.88	0.74	3.45	5.17	5.08
0	0.00	0.00	0.00	0.00	0.00	0.00

Table A. 16

C_d calculation details for case 5

Case-5		Tn	0.90459	3.45	Cd	
Floor	ELASTIC			INELASTIC		
	IBC-1	IBC-2	IBC-3	IBC-1	IBC-2	IBC-3
4	4.10	4.25	5.50	16.22	17.56	18.98
3	3.23	3.65	4.88	13.45	15.10	16.42
2	1.74	1.78	2.46	9.53	9.74	11.74
1	0.65	0.63	0.89	3.86	3.87	5.35
0	0.00	0.00	0.00	0.00	0.00	0.00

Table A. 17

C_d calculation details for case 6

Case-6		Tn	0.930383	3.92	Cd	
Floor	ELASTIC			INELASTIC		
	IBC-1	IBC-2	IBC-3	IBC-1	IBC-2	IBC-3
4	4.83	4.18	4.53	14.75	17.06	18.95
3	3.89	3.58	3.95	12.55	14.35	17.07
2	2.47	2.47	2.63	8.90	9.77	13.21
1	1.72	1.00	0.83	4.10	4.24	6.78
0	0.00	0.00	0.00	0.00	0.00	0.00

Table A. 18

C_d calculation details for case 7

Case-7		Tn	0.81101	3.94	Cd	
Floor	ELASTIC			INELASTIC		
	IBC-1	IBC-2	IBC-3	IBC-1	IBC-2	IBC-3
4	4.22	4.10	4.30	14.40	16.95	16.15
3	3.35	3.28	3.44	12.22	14.27	14.33
2	2.31	2.08	2.15	8.57	9.83	10.77
1	0.89	0.76	0.84	3.92	4.50	5.36
0	0.00	0.00	0.00	0.00	0.00	0.00

Table A. 19

C_d calculation details for case 8

Case-8		Tn	0.84163	3.72	Cd	
Floor	ELASTIC			INELASTIC		
	IBC-1	IBC-2	IBC-3	IBC-1	IBC-2	IBC-3
4	4.49	4.90	4.77	15.89	18.21	17.11
3	3.49	3.95	3.72	13.22	15.15	14.88
2	2.15	2.92	2.62	8.66	9.83	10.68
1	0.78	0.92	0.84	3.45	3.90	4.72
0	0.00	0.00	0.00	0.00	0.00	0.00

Table A. 20

Cd calculation details for case 9

Case-9		Tn	0.86709	3.69	Cd	
Floor	ELASTIC			INELASTIC		
	IBC-1	IBC-2	IBC-3	IBC-1	IBC-2	IBC-3
4	4.92	5.04	4.16	16.20	18.61	17.70
3	3.82	3.96	3.23	13.32	15.04	15.19
2	2.54	2.48	1.96	8.89	9.72	10.78
1	0.97	0.91	0.69	3.17	3.89	4.90
0	0.00	0.00	0.00	0.00	0.00	0.00
			average			

Table A. 21

C_d calculation details for case 10

Case-10		Tn	1.01	3.86	Cd	
Floor	ELASTIC			INELASTIC		
	IBC-1	IBC-2	IBC-3	IBC-1	IBC-2	IBC-3
8	4.36	4.10	4.85	17.98	18.70	18.50
7	4.07	3.88	4.50	17.06	17.60	17.40
6	3.64	3.52	3.97	15.22	15.69	15.52
5	3.18	2.95	3.28	13.50	13.85	13.70
4	2.52	2.39	2.46	10.84	11.43	11.31
3	1.89	1.73	1.82	7.75	8.48	8.39
2	1.11	0.95	1.29	4.56	5.22	5.16
1	0.38	0.36	0.52	1.67	2.08	2.06
0	0.00	0.00	0.00	0.00	0.00	0.00

Table A. 22

Cd calculation details for case 11

Case-11		Tn	1.1712	3.77	Cd	
Floor	ELASTIC			INELASTIC		
	IBC-1	IBC-2	IBC-3	IBC-1	IBC-2	IBC-3
8	4.84	5.66	5.94	20.69	21.11	22.40
7	4.50	4.96	5.39	19.34	19.81	20.72
6	4.06	4.47	4.76	17.34	18.09	18.71
5	3.45	3.94	3.99	14.60	15.69	15.92
4	2.73	3.24	3.35	11.25	12.60	12.44
3	1.97	2.36	2.42	7.77	8.93	8.53
2	1.14	1.36	1.40	4.31	5.04	4.66
1	0.38	0.45	0.43	1.38	1.65	1.47
0	0.00	0.00	0.00	0.00	0.00	0.00

Table A. 23

Cd calculation details for case 12

Case-12		Tn	1.1482	3.57	Cd	
Floor	ELASTIC			INELASTIC		
	IBC-1	IBC-2	IBC-3	IBC-1	IBC-2	IBC-3
8	5.26	6.14	5.60	19.67	21.94	21.80
7	5.03	5.76	5.10	18.44	20.20	20.72
6	4.65	5.20	4.63	17.13	18.71	18.95
5	4.08	4.69	3.99	14.99	16.65	16.41
4	3.33	3.95	3.38	12.03	13.80	13.12
3	2.44	2.96	2.58	8.63	10.16	8.64
2	1.46	1.79	1.62	5.01	6.02	5.28
1	0.53	0.63	0.56	1.71	2.11	1.78
0	0.00	0.00	0.00	0.00	0.00	0.00

Table A. 24

Cd calculation details for case13

Case-13	Tn	1.4361	3.44	Cd		
Floor	ELASTIC			INELASTIC		
	IBC-1	IBC-2	IBC-3	IBC-1	IBC-2	IBC-3
8	6.25	7.10	6.70	21.70	19.54	24.40
7	5.91	6.64	6.23	20.60	18.29	23.21
6	5.39	6.04	5.59	18.80	16.37	21.25
5	4.66	5.31	4.97	16.24	14.08	18.95
4	3.70	4.31	4.10	12.80	11.64	15.07
3	2.68	3.08	3.04	9.20	8.75	11.16
2	1.62	1.86	1.88	5.36	5.32	7.34
1	0.58	0.65	0.65	1.94	1.90	2.90
0	0.00	0.00	0.00	0.00	0.00	0.00

Table A. 25

Cd calculation details for case 14

Case-14	Tn	1.3663	3.21	Cd		
Floor	ELASTIC			INELASTIC		
	IBC-1	IBC-2	IBC-3	IBC-1	IBC-2	IBC-3
8	7.84	7.12	8.55	26.26	27.45	23.54
7	7.39	6.74	7.99	24.99	26.76	22.58
6	6.74	6.13	7.10	22.93	24.70	20.71
5	5.91	5.28	6.33	19.98	21.73	18.30
4	4.61	4.26	5.25	16.20	17.81	15.31
3	3.49	3.08	3.85	11.72	13.03	11.41
2	2.81	1.82	2.19	6.87	7.75	7.19
1	0.72	0.60	0.82	2.40	2.77	2.32
0	0.00	0.00	0.00	0.00	0.00	0.00

Table A. 26

Cd calculation details for case15

Case-15	Tn	1.04	3.73	Cd		
Floor	ELASTIC			INELASTIC		
	IBC-1	IBC-2	IBC-3	IBC-1	IBC-2	IBC-3
8	5.93	5.21	6.60	24.62	23.34	22.15
7	5.48	4.92	6.05	23.55	22.25	21.26
6	5.02	4.44	5.56	21.79	20.51	19.75
5	4.47	3.80	4.84	19.46	18.00	17.51
4	3.72	3.08	4.00	16.27	14.72	14.45
3	2.75	2.27	3.22	12.28	10.95	10.66
2	1.69	1.38	1.68	7.69	6.76	6.48
1	0.69	0.50	1.02	2.68	2.86	2.55
0	0.00	0.00	0.00	0.00	0.00	0.00

Table A. 27

Cd calculation details for case 16

Case-16		Tn	1.1307	3.74	Cd	
Floor	ELASTIC			INELASTIC		
	IBC-1	IBC-2	IBC-3	IBC-1	IBC-2	IBC-3
8	5.37	5.89	4.94	21.07	20.65	22.02
7	5.14	5.48	4.56	19.93	19.85	20.92
6	4.77	4.88	4.03	18.09	18.85	19.13
5	4.27	4.35	3.47	15.48	16.38	16.56
4	3.57	3.60	2.90	12.17	13.56	13.23
3	2.68	2.66	2.17	8.43	9.95	9.34
2	1.62	1.59	1.31	4.85	5.87	5.29
1	0.57	0.57	0.46	1.65	2.04	1.77
0	0.00	0.00	0.00	0.00	0.00	0.00

Table A. 28

Cd calculation details for case 17

Case-17		Tn	1.4056	3.59	Cd	
Floor	ELASTIC			INELASTIC		
	IBC-1	IBC-2	IBC-3	IBC-1	IBC-2	IBC-3
8	7.30	6.58	7.99	26.90	27.91	28.66
7	6.88	6.10	7.42	25.59	26.70	28.02
6	6.28	5.46	6.82	23.47	24.75	25.88
5	5.44	4.83	5.96	20.47	21.96	22.57
4	4.39	4.00	4.85	16.55	18.24	18.25
3	3.17	2.95	3.36	11.88	13.48	13.10
2	1.85	1.76	2.06	6.89	8.02	7.60
1	0.63	0.61	0.72	2.43	2.85	2.68
0	0.00	0.00	0.00	0.00	0.00	0.00

Table A. 29

Cd calculation details for case 18

Case-18		Tn	1.3302	3.29		
Floor	ELASTIC			INELASTIC		
	IBC-1	IBC-2	IBC-3	IBC-1	IBC-2	IBC-3
8	8.22	7.98	7.66	26.07	27.07	25.44
7	8.89	7.78	8.07	24.78	25.79	24.18
6	8.08	7.11	7.32	22.73	23.72	22.15
5	6.98	6.15	6.43	19.87	20.79	19.28
4	5.65	4.91	5.24	16.06	16.97	15.60
3	4.12	3.49	3.78	11.65	12.33	11.21
2	2.44	2.01	2.25	6.76	7.26	6.51
1	0.77	0.69	0.78	2.33	2.54	2.24
0	0.00	0.00	0.00	0.00	0.00	0.00

Table A. 30

Cd calculation details for case19

Case-19		Tn	1.28072	3.30	Cd	
Floor	ELASTIC			INELASTIC		
	IBC-1	**IBC-2**	**IBC-3**	**IBC-1**	**IBC-2**	**IBC-3**
12	7.14	6.10	7.16	22.95	23.22	23.65
11	6.87	5.87	6.90	22.30	22.74	22.99
10	6.51	5.58	6.45	21.37	21.66	22.04
9	6.05	5.16	6.11	20.15	20.43	20.78
8	5.55	4.74	5.71	18.62	18.91	19.19
7	4.92	4.20	5.19	16.78	17.09	17.28
6	4.26	3.63	4.57	14.65	14.95	15.04
5	3.53	3.02	3.67	12.23	12.51	12.50
4	2.76	2.35	2.88	9.53	9.77	9.70
3	1.96	1.64	2.47	6.67	6.86	6.74
2	1.11	0.94	1.42	3.80	3.93	3.82
1	0.37	0.32	0.48	1.31	1.37	1.31
0	0.00	0.00	0.00	0.00	0.00	0.00

Table A. 31

C_d calculation details for case20

Case-20		**Tn**	**1.4189**	**3.25**	**Cd**	
Floor	ELASTIC			INELASTIC		
	IBC-1	**IBC-2**	**IBC-3**	**IBC-1**	**IBC-2**	**IBC-3**
12	8.16	8.52	7.19	27.16	27.62	27.67
11	6.92	8.22	6.69	26.64	27.90	26.93
10	6.59	7.85	6.19	25.32	26.80	25.85
9	6.19	7.34	5.46	23.82	25.31	24.37
8	5.67	6.72	4.82	21.92	23.42	22.49
7	5.02	6.07	4.41	19.67	21.14	20.24
6	4.23	5.32	3.71	17.24	18.47	17.27
5	3.38	4.47	3.31	14.49	15.43	14.63
4	2.64	3.52	2.62	11.38	12.05	11.35
3	1.89	2.48	1.86	8.01	8.45	7.88
2	1.13	1.43	1.08	4.60	4.83	4.46
1	0.37	0.49	0.37	1.56	1.65	1.54
0	0.00	0.00	0.00		0.00	0.00

Table A. 32:

C_d calculation details for case 21

Case-21		**Tn**	**1.55882**	**3.19**	**Cd**	
Floor	ELASTIC			INELASTIC		
	IBC-1	**IBC-2**	**IBC-3**	**IBC-1**	**IBC-2**	**IBC-3**
12	8.20	7.42	9.49	28.95	26.60	30.28
11	7.89	7.14	8.76	28.12	26.06	29.58
10	7.47	6.74	8.20	26.88	25.25	28.53
9	6.94	6.19	7.77	25.15	24.41	27.05
8	6.38	5.61	7.25	22.95	22.66	25.10
7	5.65	5.25	6.59	20.31	20.78	22.65
6	4.89	4.72	5.81	17.62	18.46	19.71
5	4.06	4.05	4.66	14.58	15.67	16.32

4	3.16	3.27	3.66	11.22	12.42	12.49
3	2.22	2.38	3.14	7.71	8.80	8.45
2	1.27	1.41	1.80	4.35	5.10	4.63
1	0.43	0.49	0.61	1.57	1.86	1.56
0	0.00	0.00	0.00	0.00	0.00	0.00

Table A. 33

C_d calculation details for case 22

Case-22	**Tn**	**1.8466**		**3.09**	**Cd**	
Floor	ELASTIC			INELASTIC		
	IBC-1	**IBC-2**	**IBC-3**	**IBC-1**	**IBC-2**	**IBC-3**
12	11.73	9.76	8.87	33.25	33.16	36.30
11	11.00	9.43	8.58	32.72	32.50	35.65
10	10.42	8.95	8.13	31.38	31.46	34.01
9	9.68	8.32	7.50	29.52	30.00	31.79
8	8.89	7.60	6.73	27.17	28.11	29.10
7	7.88	6.83	6.03	24.36	25.78	26.04
6	6.82	6.11	5.42	21.15	22.97	22.27
5	5.66	5.24	4.71	17.58	19.63	19.12
4	4.41	4.22	3.81	13.78	15.73	15.12
3	3.09	3.06	2.84	9.89	11.34	10.74
2	1.77	1.83	1.65	5.57	6.67	6.21
1	0.60	0.66	0.58	2.04	2.33	2.11
0	0.00	0.00	0.00	0.00	0.00	0.00

Table A. 34:

C_d calculation details for case23.

Case-23	**Tn**	**1.68176**		**3.06**	**Cd**	
Floor	ELASTIC			INELASTIC		
	IBC-1	**IBC-2**	**IBC-3**	**IBC-1**	**IBC-2**	**IBC-3**
12	9.30	11.74	10.63	34.56	34.11	35.90
11	9.09	10.98	10.22	33.51	33.27	34.87
10	8.77	10.39	9.68	31.85	31.97	33.26
9	8.32	9.66	8.98	29.60	30.15	31.10
8	7.73	8.88	8.27	26.85	27.85	28.51
7	7.02	7.86	7.32	23.67	25.07	25.59
6	6.16	6.80	6.32	20.18	21.84	22.38
5	5.16	5.66	5.26	16.50	18.20	18.84
4	4.06	4.40	4.09	12.74	14.30	14.91
3	2.92	3.08	2.86	8.95	10.01	10.64
2	1.78	1.77	1.64	5.22	5.75	6.20
1	0.66	0.60	0.55	1.84	1.93	2.14
0	0.00	0.00	0.00	0.00	0.00	0.00

Table A. 35

C_d calculation details for case24

Case-24		Tn	1.28174	3.10	Cd	
Floor	ELASTIC			INELASTIC		
	IBC-1	**IBC-2**	**IBC-3**	**IBC-1**	**IBC-2**	**IBC-3**
12	7.80	7.06	7.50	21.65	24.20	23.47
11	7.62	6.87	7.24	21.50	23.87	22.92
10	7.34	6.58	6.90	20.75	23.03	22.08
9	7.28	6.19	6.43	19.32	21.87	20.92
8	6.46	5.60	5.96	17.78	20.39	19.43
7	5.83	5.11	5.39	16.01	18.57	17.59
6	5.09	4.45	4.73	14.03	16.39	15.40
5	4.24	3.71	3.96	11.80	13.82	12.89
4	3.31	2.91	3.10	9.29	10.90	10.08
3	2.34	2.05	2.19	6.69	7.74	7.06
2	1.35	1.18	1.38	3.81	4.52	4.05
1	0.46	0.40	0.43	1.34	1.64	1.47
0	0.00	0.00	0.00	0.00	0.00	0.00

Table A. 36

C_d calculation details for case 25

Case-25		Tn	1.54679	3.22	Cd	
Floor	ELASTIC			INELASTIC		
	IBC-1	**IBC-2**	**IBC-3**	**IBC-1**	**IBC-2**	**IBC-3**
12	8.79	9.81	9.20	29.02	31.57	30.10
11	8.33	9.77	9.61	28.14	30.87	29.35
10	7.90	9.11	9.19	26.86	29.86	28.28
9	7.12	8.28	8.93	25.11	28.50	26.79
8	6.33	7.71	7.94	22.89	26.72	24.83
7	5.51	7.23	7.19	20.25	24.48	22.20
6	4.94	6.55	6.38	17.27	21.71	19.41
5	4.24	5.72	5.45	14.20	18.41	16.02
4	3.38	4.64	5.46	10.93	14.47	12.26
3	2.40	3.35	4.35	7.52	10.07	8.32
2	1.37	1.92	1.79	4.24	5.71	4.57
1	0.46	0.69	0.61	1.47	2.45	1.53
0	0.00	0.00	0.00	0.00	0.00	0.00

Table A. 37

C_d calculation details for case26

Case-26		Tn	1.7332	3.15	Cd	
Floor	ELASTIC			INELASTIC		
	IBC-1	**IBC-2**	**IBC-3**	**IBC-1**	**IBC-2**	**IBC-3**
12	11.55	10.90	9.56	32.78	31.65	36.43
11	11.08	10.22	9.17	31.88	30.99	35.33
10	10.62	9.68	8.95	30.51	29.97	33.65
9	9.85	8.95	8.15	28.64	28.58	31.43
8	8.90	8.06	7.37	26.28	26.79	28.73
7	8.00	7.21	6.62	23.47	24.59	25.67
6	6.97	6.42	5.77	20.28	21.95	22.33
5	5.95	5.47	4.92	16.75	18.79	18.69

4	4.72	4.39	3.91	13.25	15.08	14.70
3	3.41	3.16	2.82	9.35	10.87	10.38
2	2.01	1.86	1.66	5.43	6.38	5.97
1	0.70	0.66	0.58	1.88	2.20	2.01
0	0.00	0.00	0.00	0.00	0.00	0.00

Table A. 38

C_d calculation details for case27

Case-27		**Tn**	**1.66059**	**3.12**	**Cd**	
Floor	ELASTIC			INELASTIC		
	IBC-1	**IBC-2**	**IBC-3**	**IBC-1**	**IBC-2**	**IBC-3**
12	11.34	10.55	9.43	35.41	34.31	35.40
11	11.02	9.87	9.27	34.18	33.32	34.24
10	10.64	9.39	9.07	32.40	31.90	32.54
9	10.15	8.87	8.75	30.05	30.01	30.34
8	9.42	8.25	8.23	27.23	27.66	27.73
7	8.48	7.49	7.70	24.01	24.87	24.80
6	7.35	6.50	6.94	20.49	21.63	21.59
5	6.17	5.49	6.01	16.77	17.98	18.07
4	4.91	4.32	4.87	12.95	13.99	14.22
3	3.52	3.07	3.57	9.08	9.76	10.06
2	2.06	1.82	2.13	5.26	5.36	5.80
1	0.75	0.65	0.76	1.81	1.85	1.95
0	0.0	0.0	0.0	0.0	0.0	0.0

Table A. 39

C_d calculation details for case28

Case-28		**Tn**	**1.7066**	**3.22**	**Cd**	
Floor	ELASTIC			INELASTIC		
	IBC-1	**IBC-2**	**IBC-3**	**IBC-1**	**IBC-2**	**IBC-3**
16	9.9	10.2	9.1	31.5	32.8	30.1
15	9.6	10.2	9.2	30.8	32.1	29.5
14	9.3	9.9	9.0	30.0	31.1	28.6
13	8.9	9.6	8.8	28.8	30.0	27.5
12	8.5	9.2	8.5	27.5	28.6	26.2
11	8.1	8.7	8.0	25.9	26.9	24.7
10	7.6	8.2	7.5	24.1	25.0	23.0
9	7.0	7.3	6.9	21.2	22.3	20.6
8	6.5	6.7	6.2	19.3	20.1	18.4
7	5.8	5.9	5.3	17.1	17.8	16.4
6	5.0	5.0	4.4	14.8	15.4	14.1
5	4.1	4.0	3.6	12.1	12.6	11.6
4	3.2	3.1	2.7	9.2	9.6	8.8
3	2.2	2.1	1.9	6.3	6.5	6.0
2	1.2	1.7	1.0	3.4	3.6	3.3
1	0.4	1.2	0.3	1.1	1.1	1.0
0	0.0	0.0	0.0	0.0	0.0	0.0

Table A. 40

C_d calculation details for case29

Case29		Tn	1.7968	2.99	Cd	
Floor	ELASTIC			INELASTIC		
	IBC-1	IBC-2	IBC-3	IBC-1	IBC-2	IBC-3
16	15.1	13.5	14.4	45.1	43.3	44.4
15	15.2	13.3	13.9	44.4	42.6	43.4
14	14.9	13.0	13.3	43.4	41.6	41.9
13	14.6	12.8	13.0	42.1	40.2	40.0
12	14.0	12.4	12.6	40.6	38.5	37.5
11	13.3	11.9	12.1	38.8	36.4	34.6
10	12.3	11.3	11.5	36.7	34.0	31.4
9	11.4	10.5	10.8	34.3	31.3	28.1
8	10.2	9.6	9.9	31.5	27.9	25.0
7	8.8	8.5	8.9	27.5	24.3	21.8
6	7.4	7.3	7.8	24.4	20.2	18.3
5	5.9	5.9	6.5	20.0	15.9	14.5
4	4.5	4.5	5.0	15.1	11.5	11.1
3	3.1	3.0	3.4	10.1	7.3	7.6
2	1.7	1.6	1.9	5.3	3.4	4.1
1	0.5	0.5	0.6	1.6	1.0	1.3
0	0.0	0.0	0.0	0.0	0.0	0.0

Table A. 41

C_d calculation details for case30

Case-30		Tn	2.2885	3.20	Cd	
Floor	ELASTIC			INELASTIC		
	IBC-1	IBC-2	IBC-3	IBC-1	IBC-2	IBC-3
16	15.96	14.35	13.85	41.75	51.06	49.61
15	15.44	13.73	13.21	40.96	50.21	48.53
14	14.90	13.42	13.12	39.59	49.01	46.98
13	14.26	12.89	12.48	38.39	47.43	44.91
12	13.58	12.72	12.29	36.96	45.44	42.33
11	12.81	12.22	11.16	35.25	43.30	39.29
10	11.90	11.61	11.04	33.38	40.20	35.85
9	9.73	10.44	10.54	31.22	36.94	32.13
8	9.21	9.25	9.60	28.76	33.30	28.25
7	8.56	8.06	8.91	25.94	29.30	24.31
6	7.36	6.86	7.84	22.72	24.93	21.51
5	6.10	5.66	6.85	19.07	20.18	17.20
4	4.81	3.91	5.18	15.01	15.17	13.71
3	3.44	3.12	3.66	10.65	10.17	9.81
2	2.02	1.82	2.14	6.15	5.59	5.69
1	0.59	0.63	0.76	2.15	1.85	1.94
0	0.00	0.00	0.00	0.00	0.00	0.00

Table A. 42

C_d calculation details for case31

Case31		Tn	2.3285	2.94	Cd	
Floor	ELASTIC			INELASTIC		
	IBC-1	IBC-2	IBC-3	IBC-1	IBC-2	IBC-3
16	16.4	16.8	15.9	42.6	43.8	49.3
15	16.3	16.4	15.6	41.4	43.0	48.3
14	16.1	16.1	15.2	40.8	41.7	46.8
13	15.8	15.7	14.7	39.3	40.2	44.9
12	15.3	15.2	14.1	37.5	38.3	42.4
11	14.6	14.5	13.5	35.3	36.2	39.5
10	13.6	13.1	13.0	32.8	33.8	36.2
9	12.5	12.6	12.3	30.0	31.3	32.6
8	11.2	11.4	11.5	27.7	28.4	28.7
7	9.9	10.2	10.4	25.0	25.3	24.8
6	8.6	8.8	9.1	21.9	21.9	20.7
5	7.1	7.3	7.7	18.3	18.3	16.7
4	5.6	5.7	6.1	14.3	14.5	13.0
3	4.7	3.9	4.3	9.9	10.2	8.8
2	2.2	2.2	2.4	5.4	5.6	4.9
1	0.6	0.7	0.8	1.7	1.8	1.5
0	0		0	0	0	0

Table A. 43

C_d calculation details for case32

Case-32		Tn	2.2705	2.77	Cd	
Floor	ELASTIC			INELASTIC		
	IBC-1	IBC-2	IBC-3	IBC-1	IBC-2	IBC-3
16	16.4	16.8	17.8	41.6	49.3	47.3
15	16.4	15.7	17.5	41.0	48.2	46.8
14	15.8	15.3	17.0	40.1	47.1	45.2
13	15.1	14.6	16.2	39.0	45.7	43.1
12	14.2	13.8	15.3	37.6	43.9	40.5
11	13.2	12.8	14.2	36.0	41.6	37.4
10	12.1	11.7	13.0	34.2	39.0	34.0
9	11.0	10.9	12.1	32.1	35.9	30.4
8	9.8	10.0	11.1	29.8	32.4	26.3
7	8.5	8.6	9.6	27.0	28.5	22.3
6	8.0	7.7	8.5	23.8	24.2	19.1
5	5.8	6.3	7.0	20.0	19.6	15.9
4	4.4	4.9	5.5	15.8	14.8	12.3
3	3.1	3.5	3.8	11.1	10.0	8.5
2	1.7	2.0	2.2	6.4	5.4	4.8
1	1.7	0.7	0.7	2.2	1.8	1.6
0	0	0	0	0	0	0

Table A. 44

C_d calculation details for case33

Case-33		Tn	1.7319	3.07	Cd	
Floor	ELASTIC			INELASTIC		
	IBC-1	IBC-2	IBC-3	IBC-1	IBC-2	IBC-3
16	11.0	10.6	11.4	31.3	31.3	34.9
15	10.6	10.4	10.8	30.8	30.9	34.2
14	10.3	10.0	10.5	30.1	30.3	33.3
13	10.0	9.6	10.1	29.1	29.6	32.0
12	9.6	9.0	9.6	27.8	28.4	30.3
11	8.9	8.4	9.0	26.3	27.2	28.5
10	8.5	7.7	8.3	24.6	25.7	26.3
9	7.9	7.2	7.7	22.5	24.0	24.0
8	7.2	6.5	7.0	20.3	22.0	21.5
7	6.4	5.7	6.2	17.8	20.0	18.8
6	5.5	4.9	5.3	15.1	16.9	16.0
5	4.5	4.0	4.3	12.2	13.9	12.9
4	3.5	3.1	3.3	9.3	10.2	9.7
3	2.4	2.1	2.3	6.2	7.2	6.5
2	1.4	1.2	1.3	3.4	3.9	3.5
1	0.4	0.4	0.4	1.1	1.3	1.1
0	0	0	0	0	0	0

Table A. 45

C_d calculation details for case34

Case-34		Tn	2.28	3.13	Cd	
Floor	ELASTIC			INELASTIC		
	IBC-1	IBC-2	IBC-3	IBC-1	IBC-2	IBC-3
16	15.2	15.9	16.7	48.5	40.2	52.3
15	14.6	12.6	13.1	47.7	39.5	51.3
14	14.0	12.2	12.6	46.6	38.5	49.9
13	13.6	11.8	12.1	45.2	37.2	48.2
12	12.5	11.1	11.6	43.5	35.6	46.1
11	11.9	10.4	10.9	41.4	33.8	43.5
10	11.5	9.6	10.4	39.0	31.7	40.5
9	11.1	8.7	9.7	36.2	29.2	37.1
8	10.3	7.8	8.0	33.0	26.5	33.5
7	9.3	6.8	7.0	29.3	23.3	28.9
6	8.1	5.8	5.8	25.3	19.9	24.2
5	6.7	4.7	4.5	20.8	16.1	19.4
4	5.2	3.7	4.5	15.9	12.3	14.2
3	3.8	2.7	3.2	10.9	8.3	9.7
2	2.1	1.6	1.8	6.0	4.7	5.3
1	0.7	0.7	0.6	0.2	1.6	1.8
0	0	0	0	0	0	0

Table A. 46

C_d calculation details for case35

Case-35		Tn	2.3034	2.97	Cd	
Floor	ELASTIC			INELASTIC		
	IBC-1	IBC-2	IBC-3	IBC-1	IBC-2	IBC-3
16	17.1	17.9	17.4	53.2	41.4	43.2
15	17.0	17.8	17.2	52.2	40.6	42.5
14	16.4	17.2	16.6	50.8	39.6	41.5
13	15.7	16.4	15.9	49.0	38.2	40.1
12	14.8	15.5	15.0	46.7	36.5	38.5
11	13.2	13.9	13.4	44.0	34.4	36.6
10	12.6	13.2	12.7	40.9	32.0	34.3
9	11.4	12.0	11.6	37.4	29.3	31.7
8	10.4	10.9	10.6	33.3	26.5	28.7
7	9.4	9.9	9.6	29.0	24.0	25.3
6	8.2	8.7	8.4	24.2	21.1	21.1
5	7.0	7.3	7.1	19.2	17.6	17.6
4	5.4	5.7	5.5	14.2	13.6	13.7
3	3.8	4.0	3.9	9.2	9.4	9.4
2	2.1	2.2	2.1	4.8	5.1	5.1
1	0.7	0.7	0.7	1.4	1.6	1.6
0	0	0	0	0	0	0

Table A. 47

C_d calculation details for case36

Case36		Tn	2.27	2.82	Cd	
Floor	ELASTIC			INELASTIC		
	IBC-1	IBC-2	IBC-3	IBC-1	IBC-2	IBC-3
16	15.9	18.2	16.8	42.5	41.9	51.3
15	15.5	17.7	16.3	41.7	41.1	50.3
14	15.0	17.1	15.5	40.6	40.0	48.9
13	14.3	16.4	14.7	39.3	38.6	47.2
12	13.5	15.5	14.0	37.6	36.9	45.1
11	12.4	14.1	13.4	35.6	34.9	42.7
10	11.8	13.5	12.8	33.3	32.6	39.9
9	10.9	12.5	12.0	30.6	30.0	36.6
8	9.9	11.3	11.1	27.7	27.2	32.9
7	8.7	10.0	10.0	24.3	24.0	28.8
6	7.5	8.6	8.7	20.7	20.6	24.3
5	6.1	7.0	7.2	16.7	16.8	19.5
4	4.7	5.4	5.6	12.6	12.8	14.5
3	3.3	3.7	4.0	8.9	8.7	9.6
2	1.8	2.1	2.0	4.6	4.8	5.2
1	0.6	0.7	0.7	1.5	1.6	1.6
0	0	0	0	0	0	0

Appendix B

Figures

Figure B. 2

Seismic Hazard Map and Seismic Zone Factor (Source ESSEU, Earth Sciences and Seismic Engineering Unit at NNU)

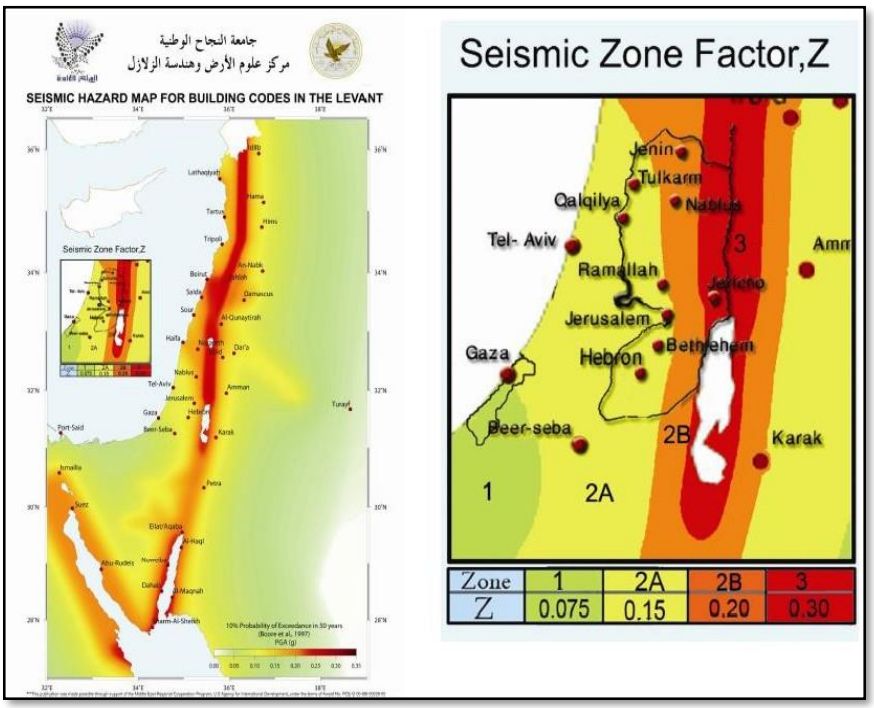

Figure B. 3

Design response spectrum

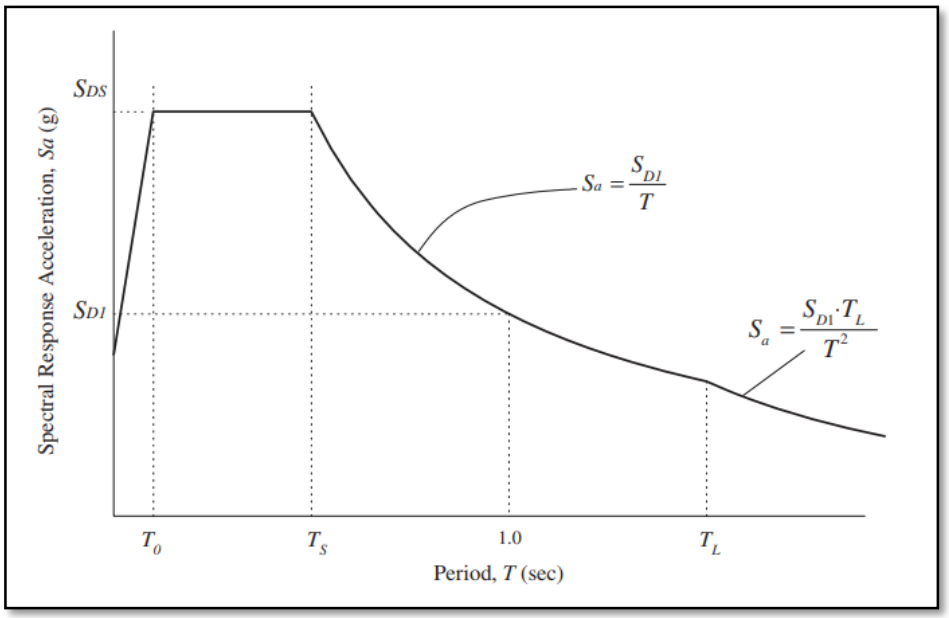

Figure B. 4

Recordings adopted by the International Building Code (IBC)

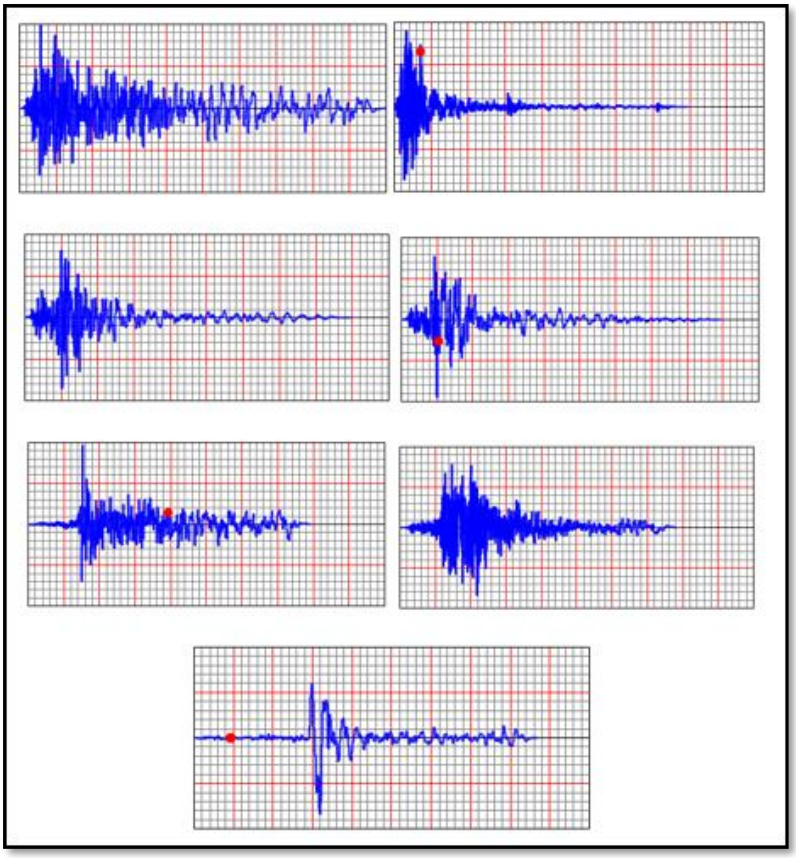

Figure B. 5

Time history matching to response spectrum by Sap 2000 which matched before by Seisomatch software

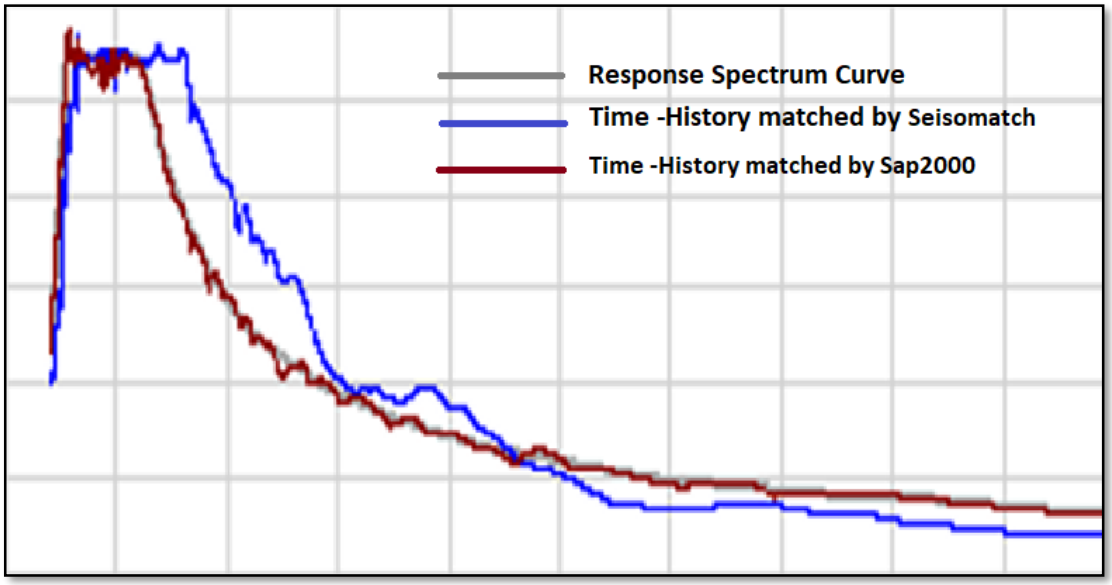

Figure B. 6

Fiber hinge [21, 22]

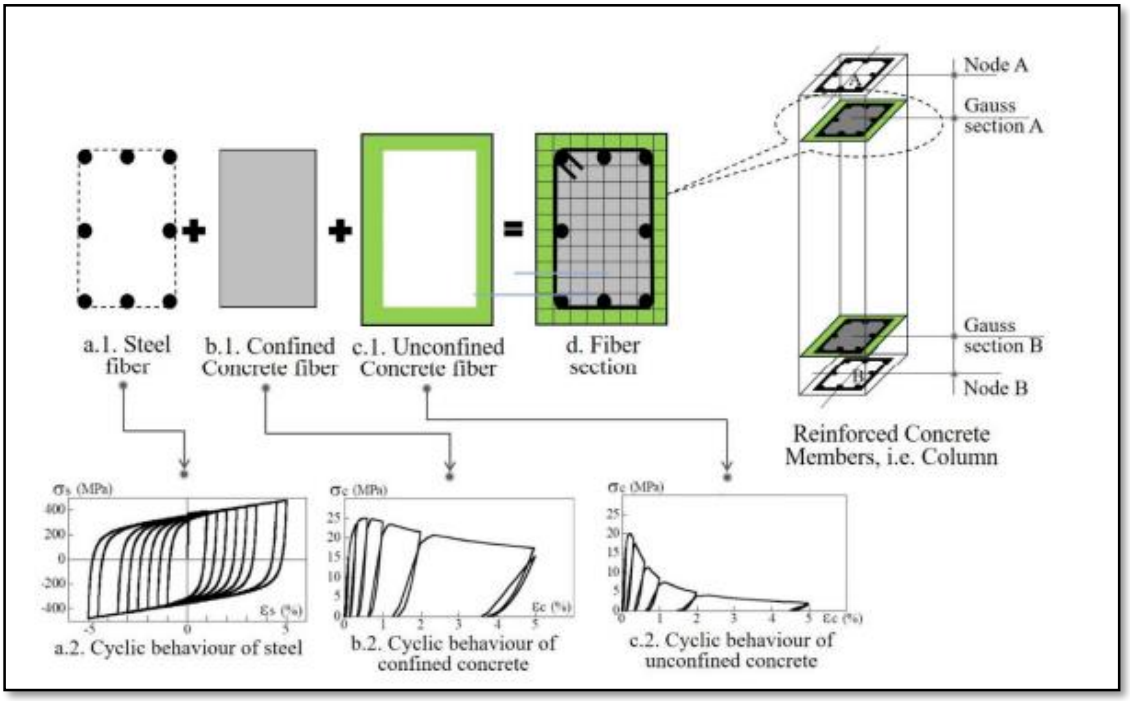

Figure B. 7

Concrete area with effective confinement [23]

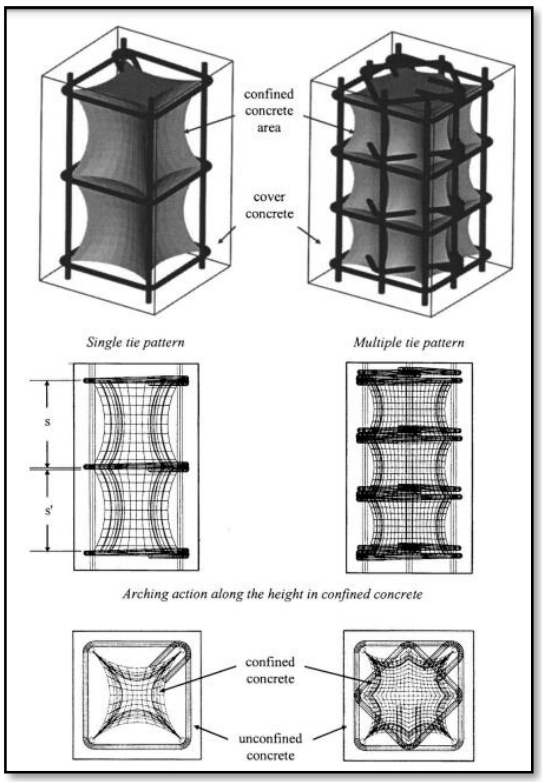

Figure B. 8

Stress-Strain curve by Kent and Park (1971). [14]

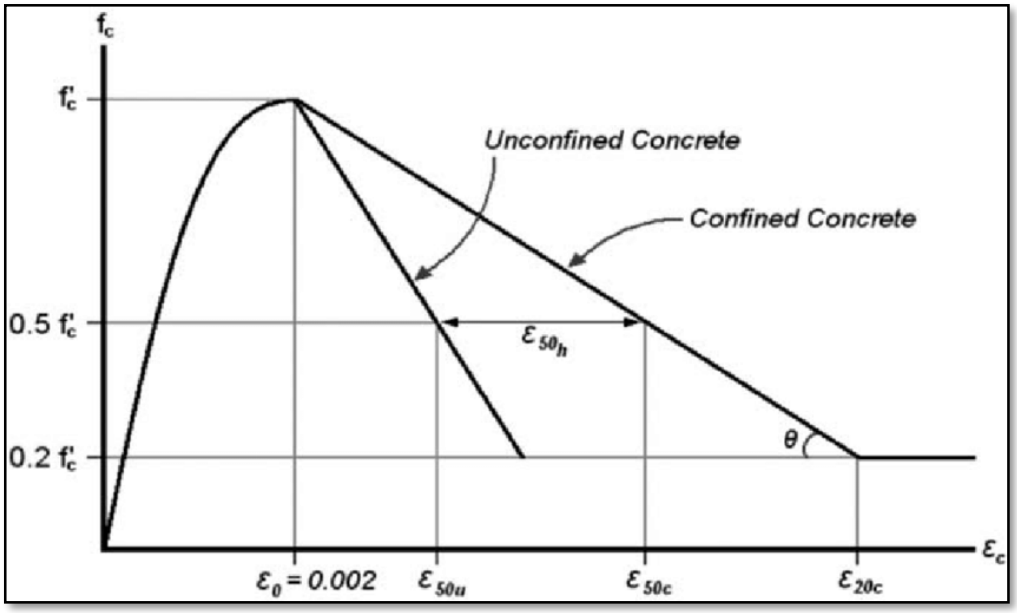

Figure B. 9

Stress- Strain Model proposed by Mander et al (1988)

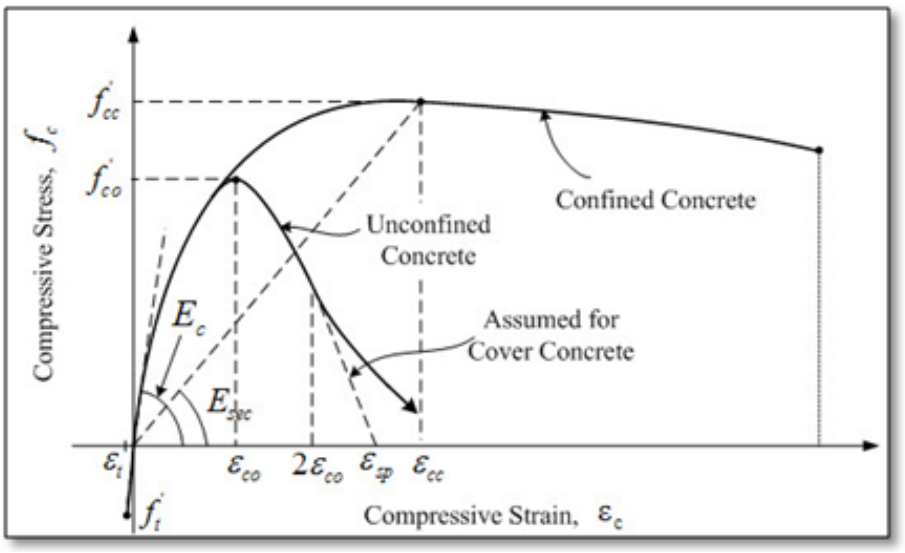

A) comprissive behavior

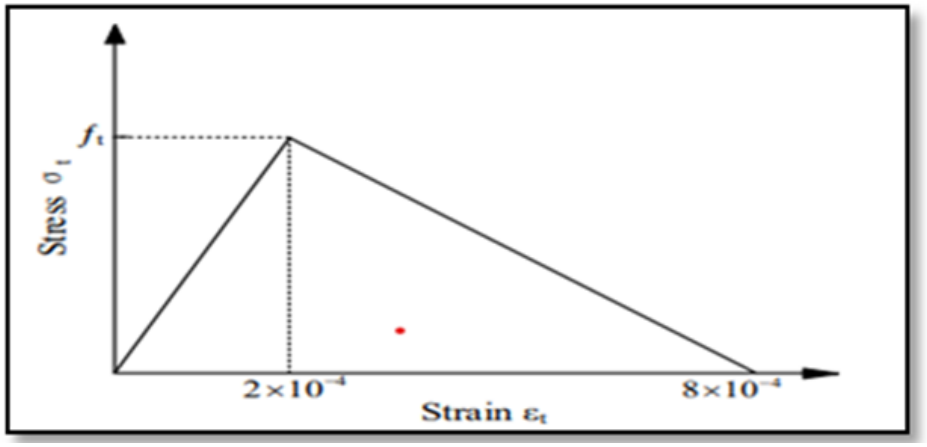

b) Tension behavior

Figure B. 10

Proposed Stress-Strain curve by Saatcioglu and Razvi

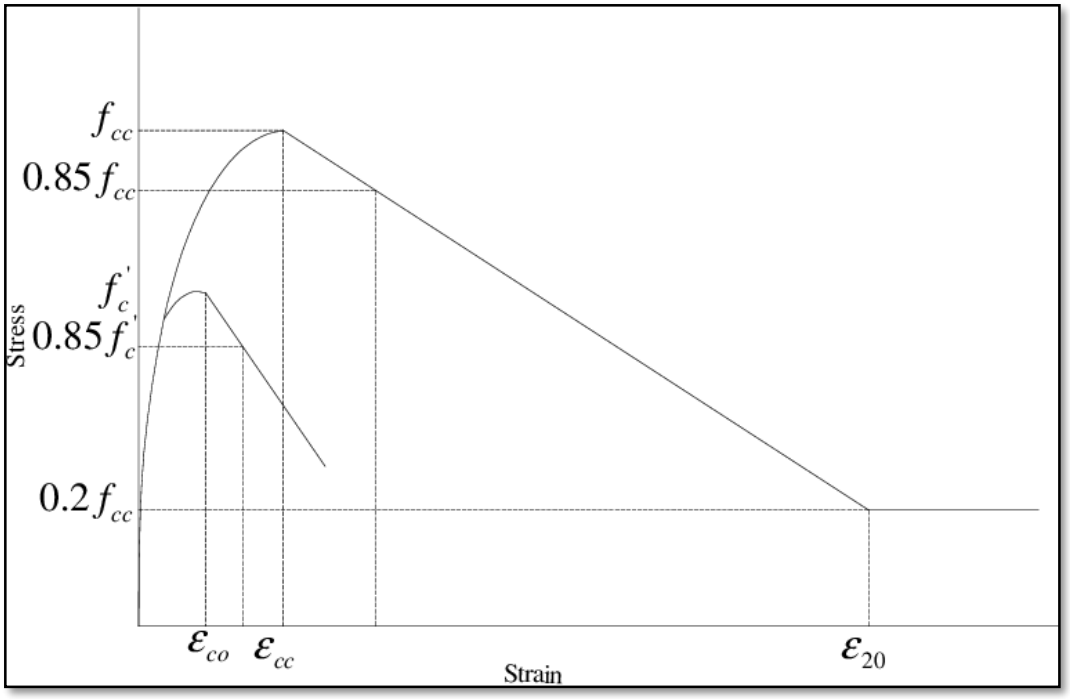

Figure B. 11

Stress-strain Curve for steel reinforcement [24]

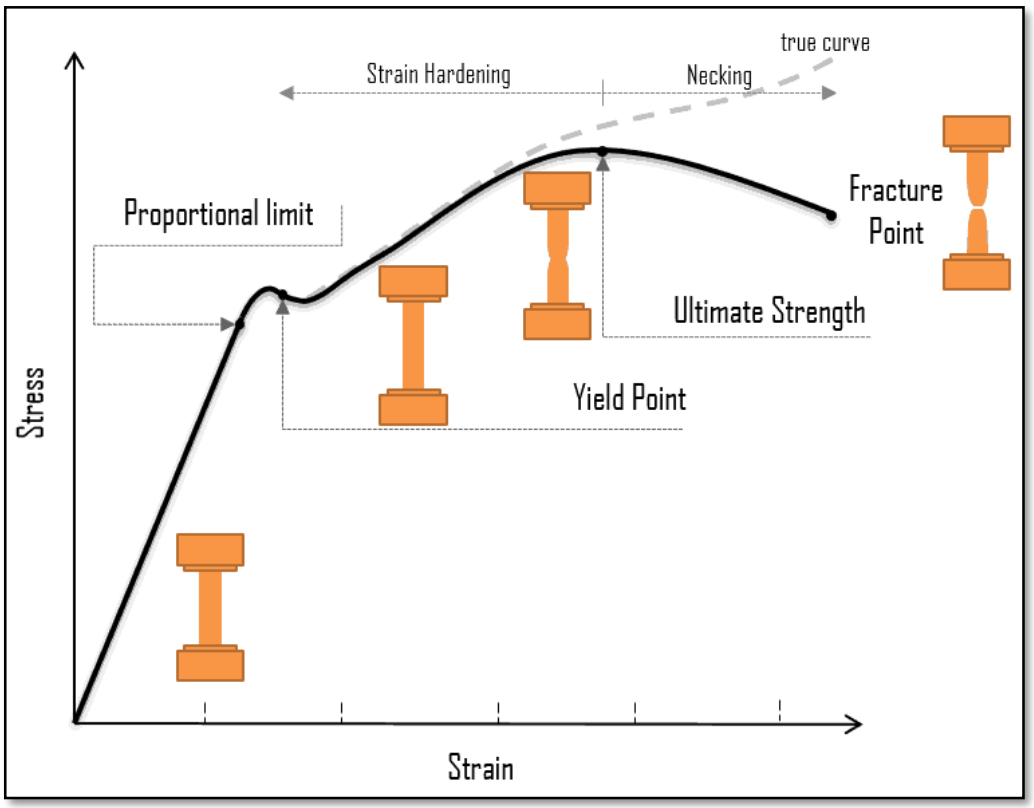

Figure B. 12

Takeda Hysteresis Mode

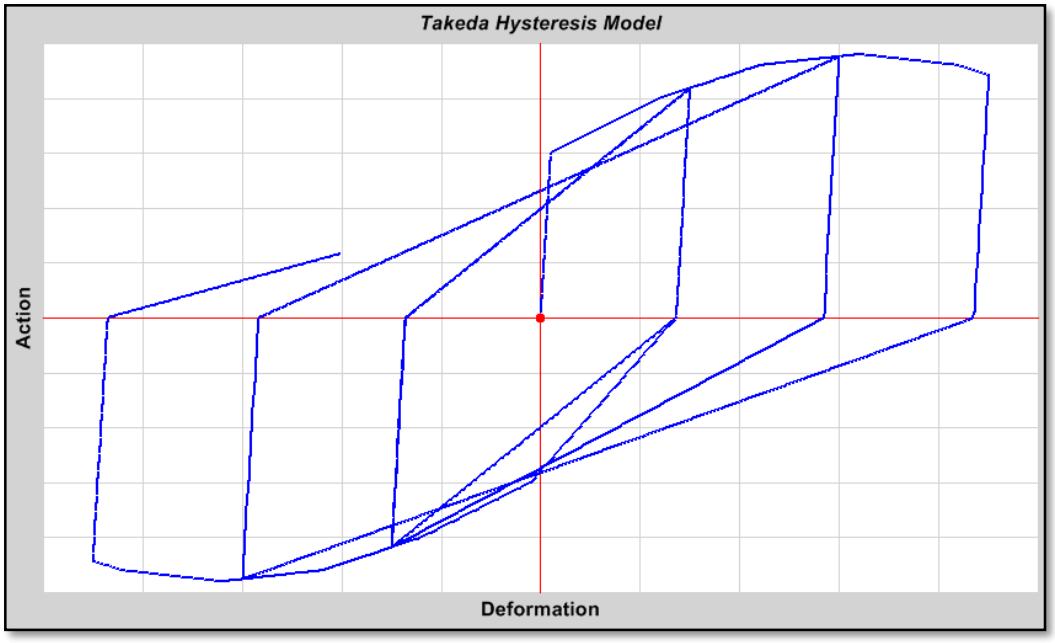

Figure B. 13

Kinematic Hardening hysteresis model

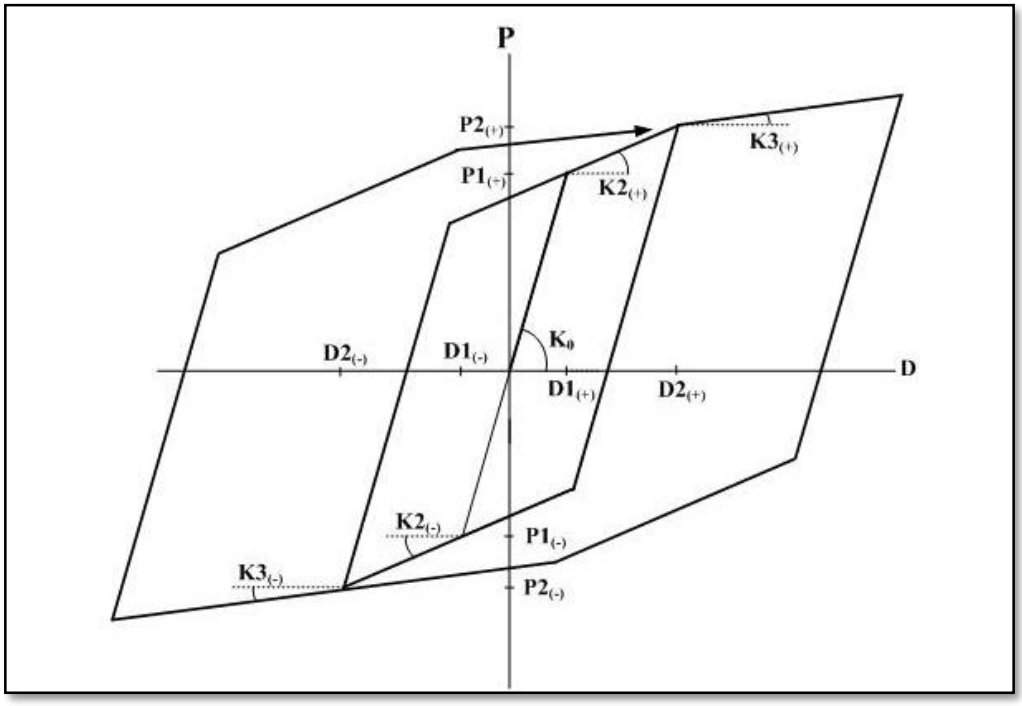

Figure B. 14

Deflection amplification factor for different story levels in ordinary and special MRF

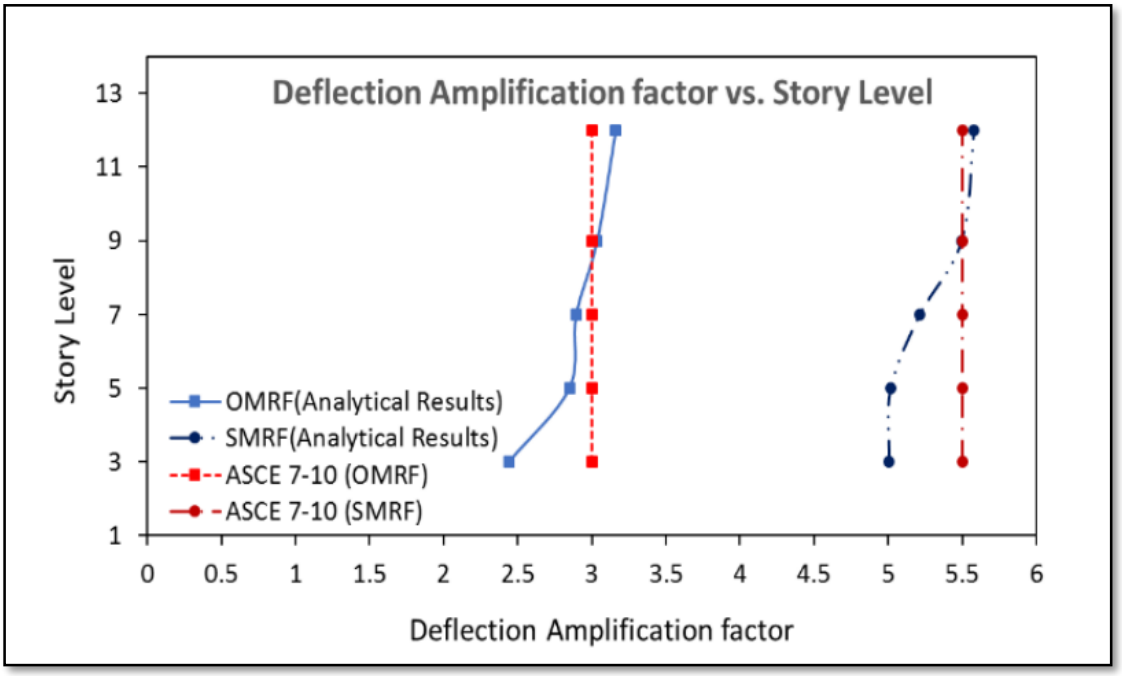

Figure B. 15

Variation of Fundamental Period with Structural Height [5]

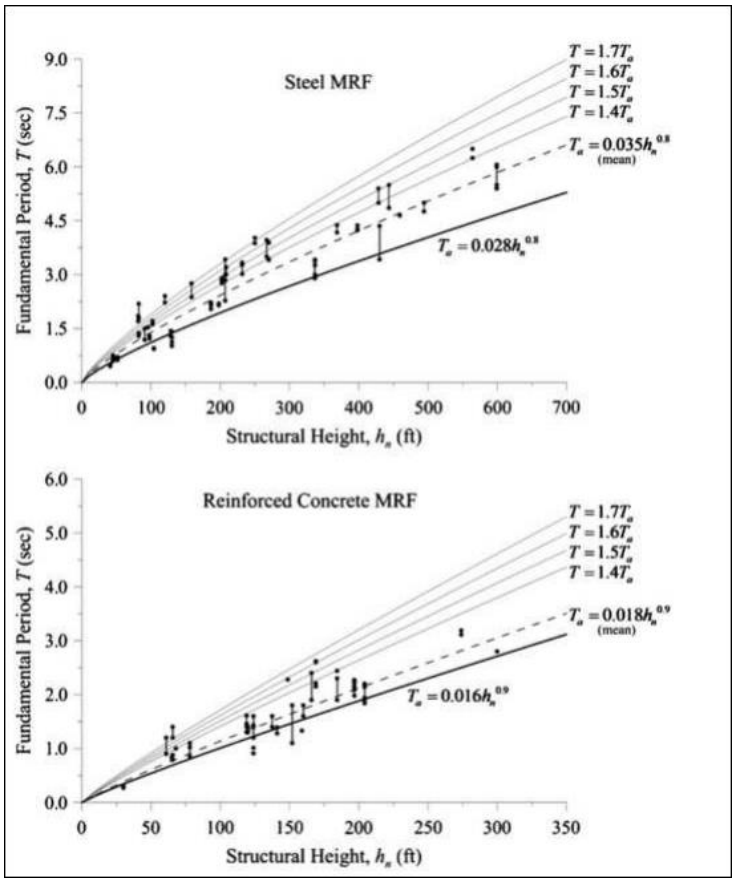

Figure B. 16

Validation through a Single Degree of Freedom (SDOF) Approach

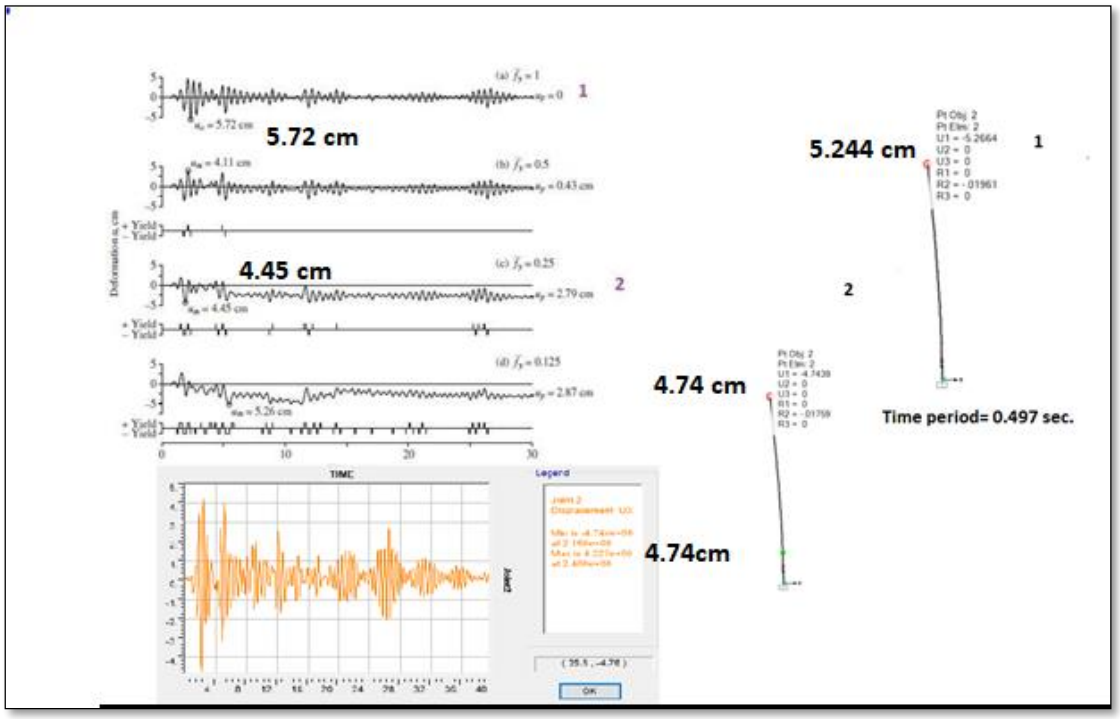

Figure B. 17

Validation via Analysis of a Concrete Frame

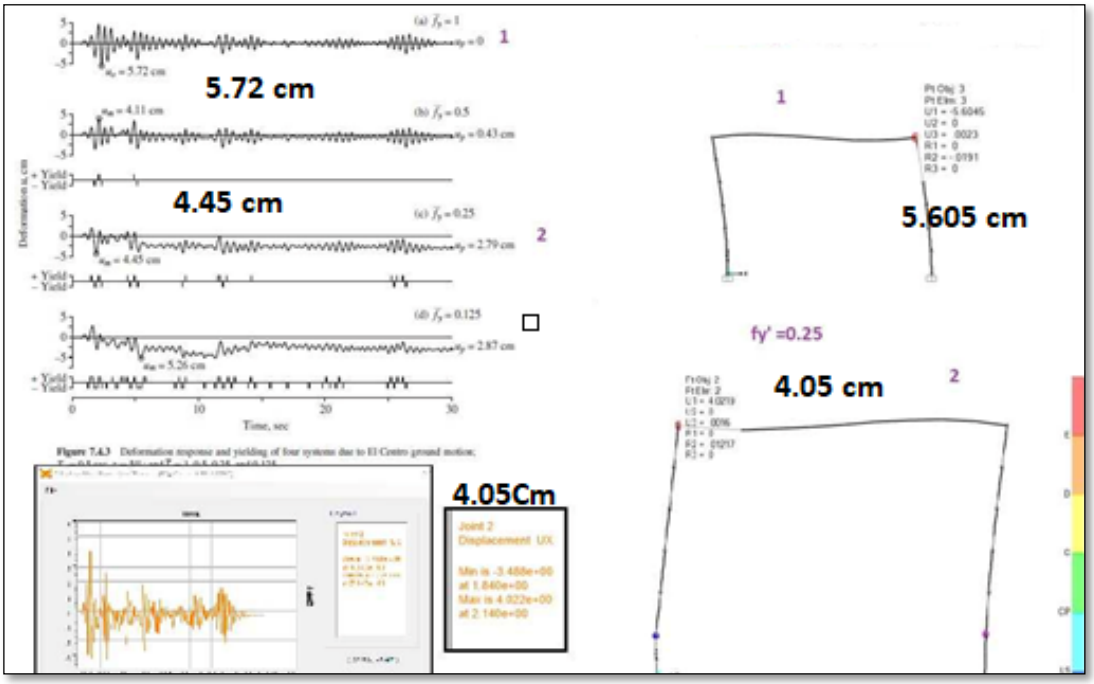

Figure B. 18

Geometric and design layout of prototype RC frame

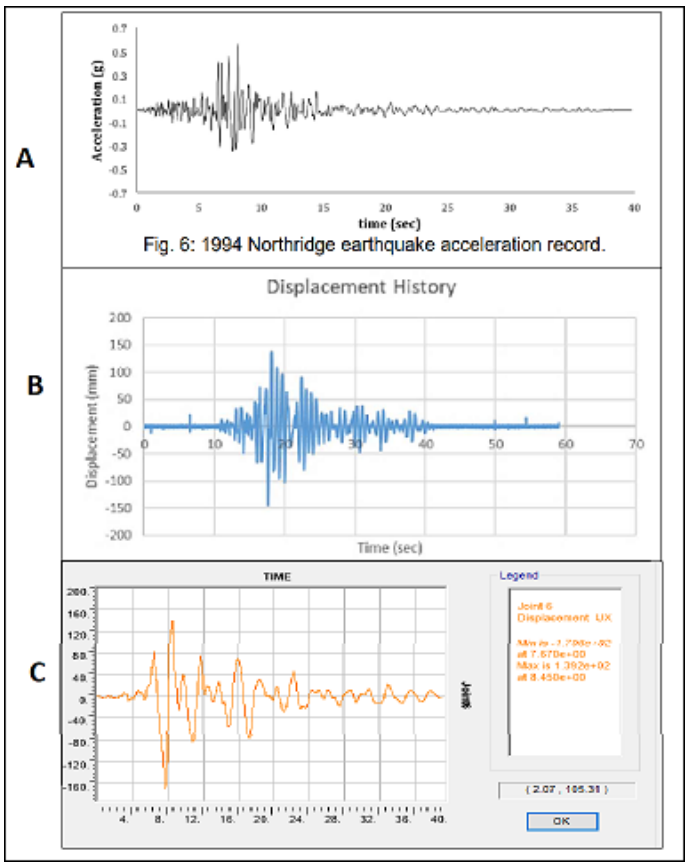

Figure B. 19

Column Axis plan

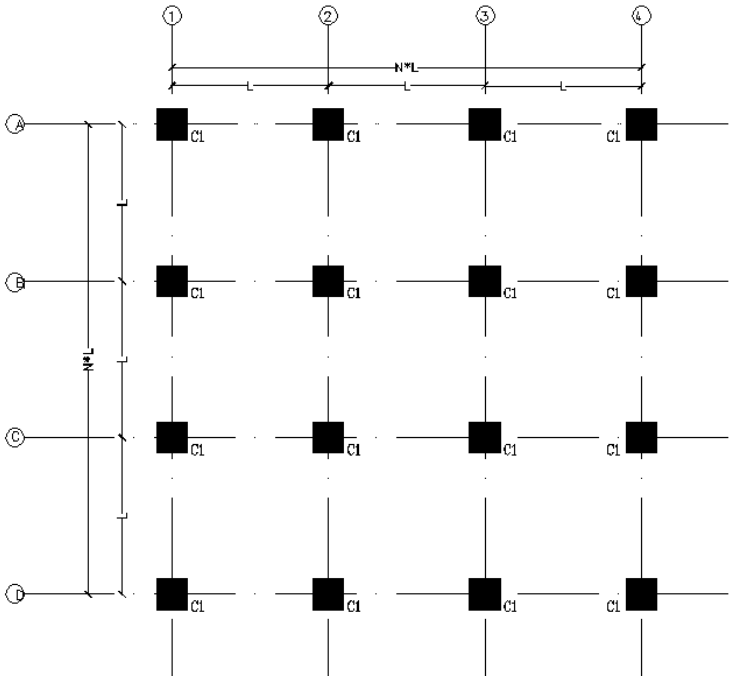

Figure B. 20

3D ETABS model

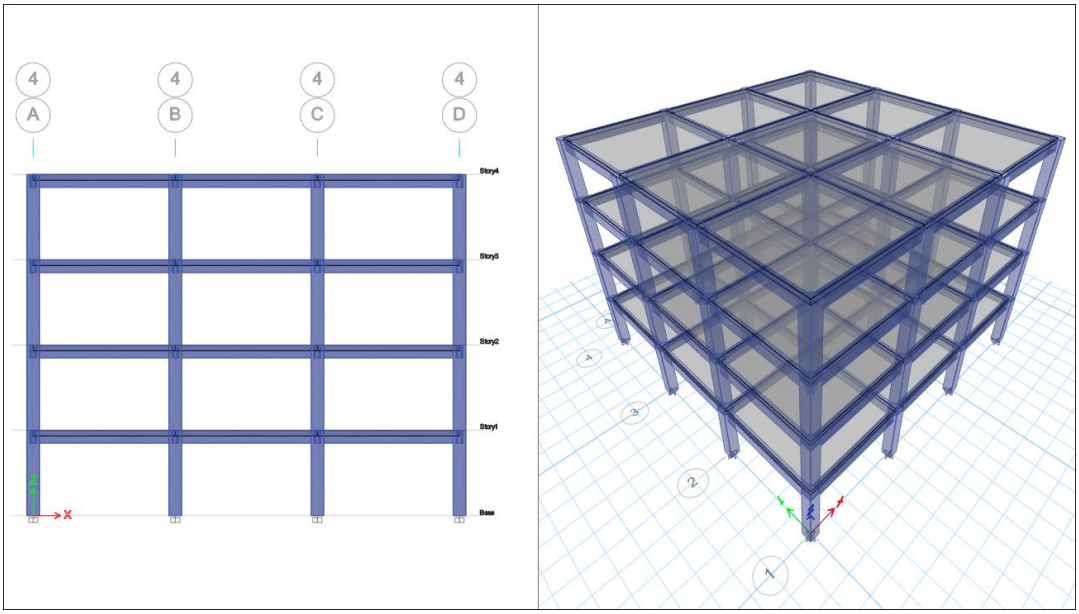

Figure B. 21

Three time histories record using for analysis

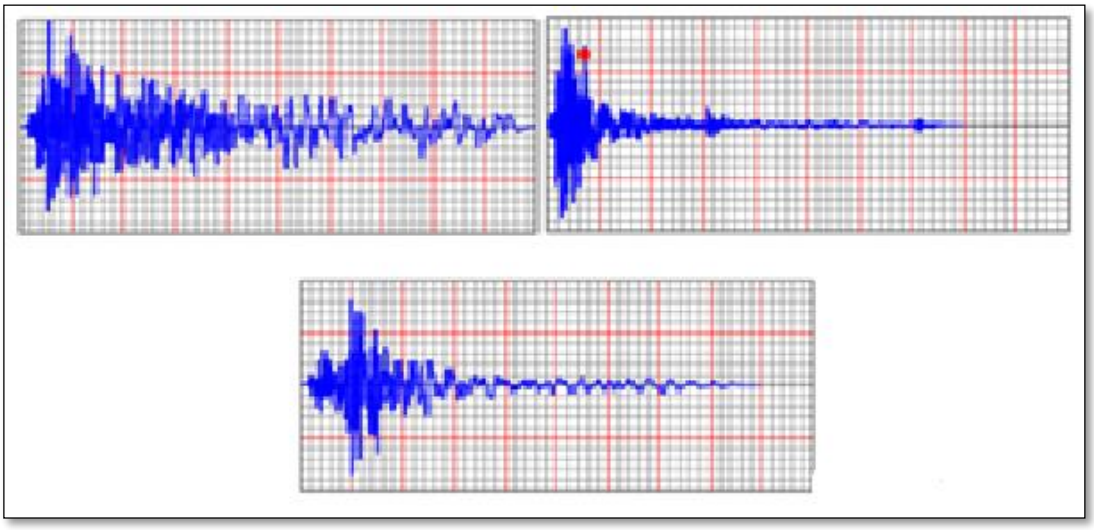

Figure B. 22

Mander Confined and unconfined Concrete model for concrete B350 by the SAP2000 Software.

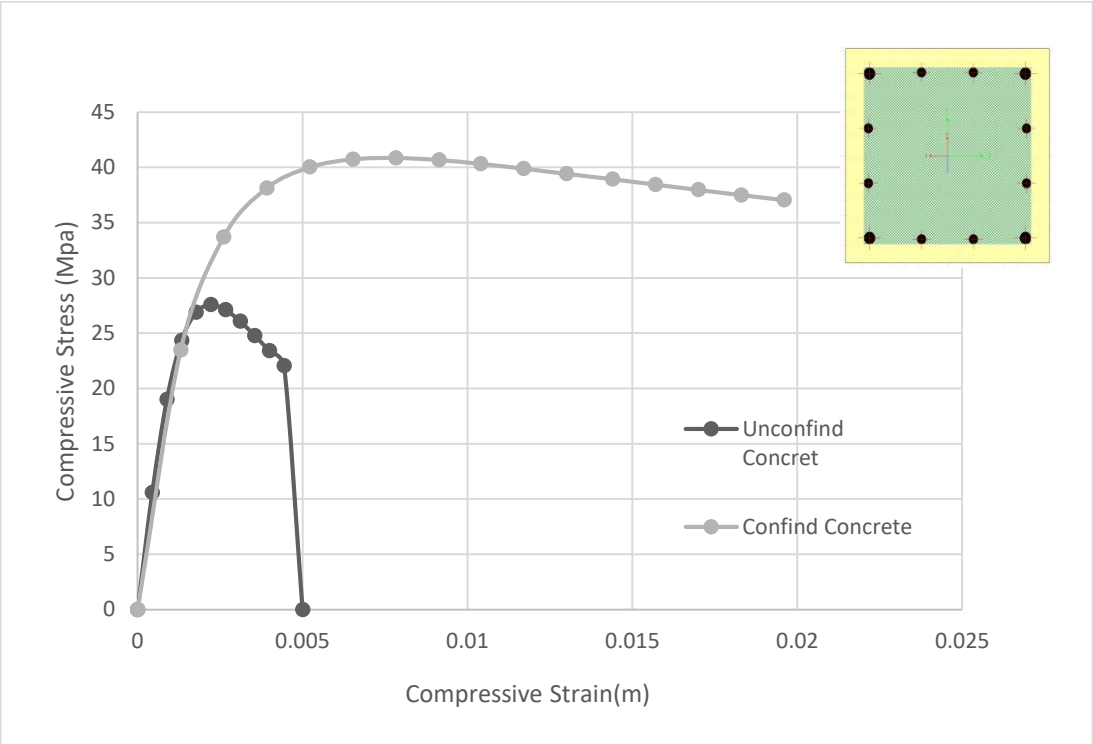

Figure B. 23

Stress - strain curve for reinforcements steel by the SAP2000 Software

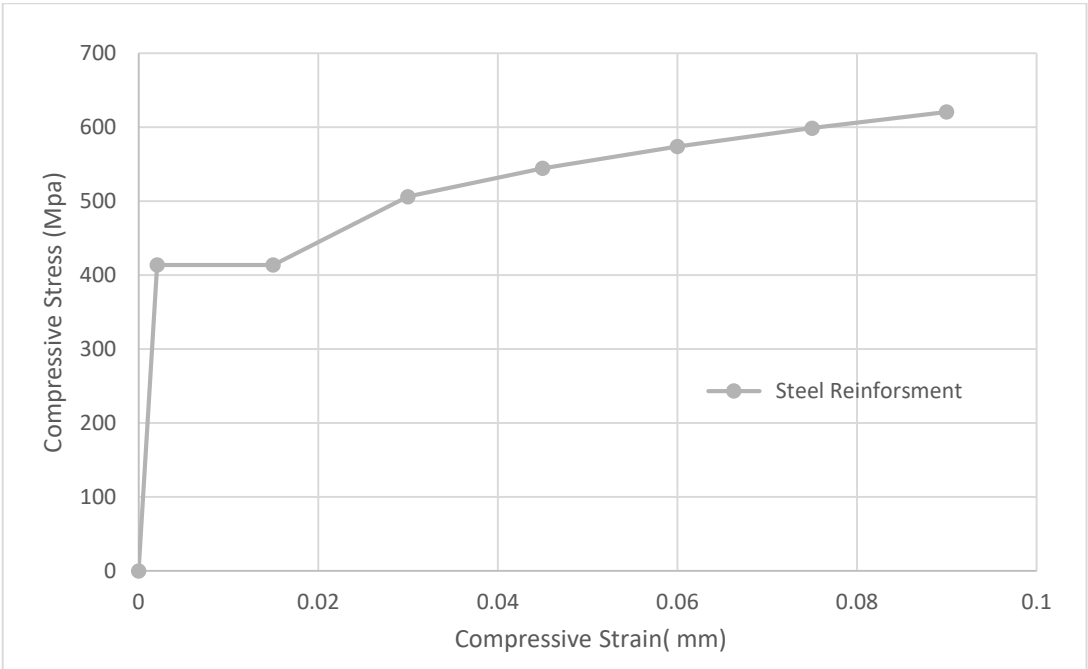

Figure B. 24

The sequential formation of plastic hinges

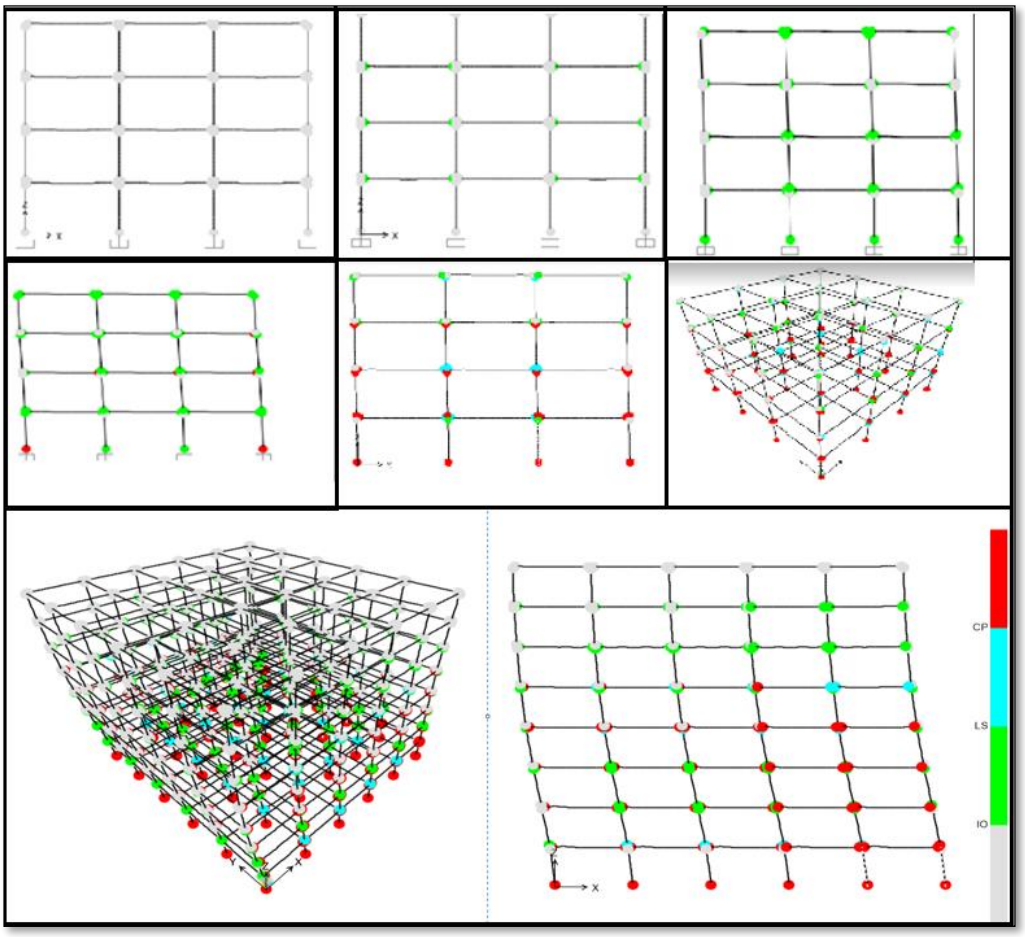

Figure B. 25

Single –deree freedom system .using by Anil K. Chopra

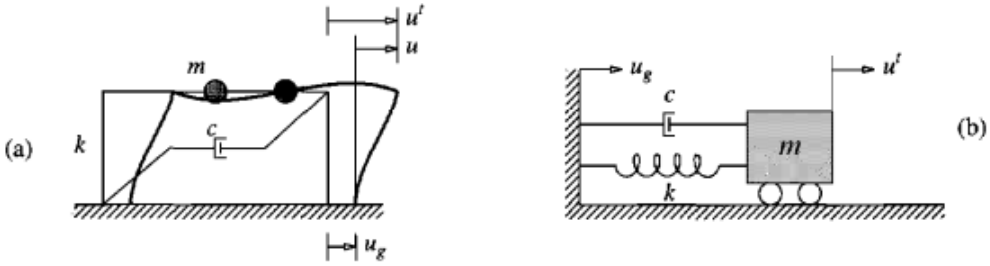

Figure 6.2.1 Single-degree-of-freedom systems.

Figure B. 26

Ductility demand for elastoplastic system due to El Centro ground motion

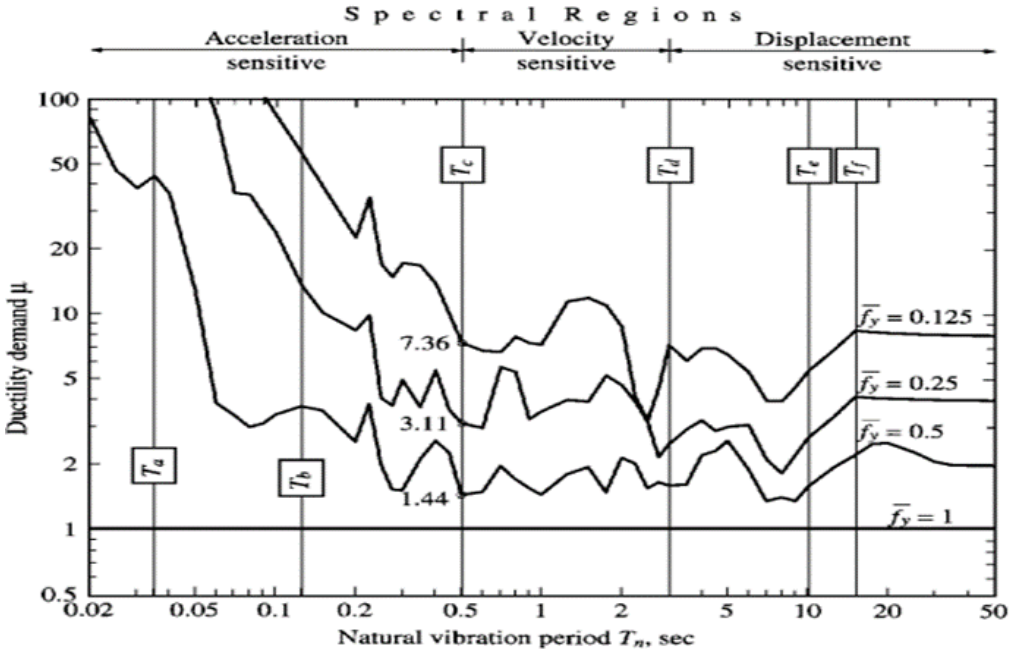

Figure B. 27

A correlation was generated using SPSS

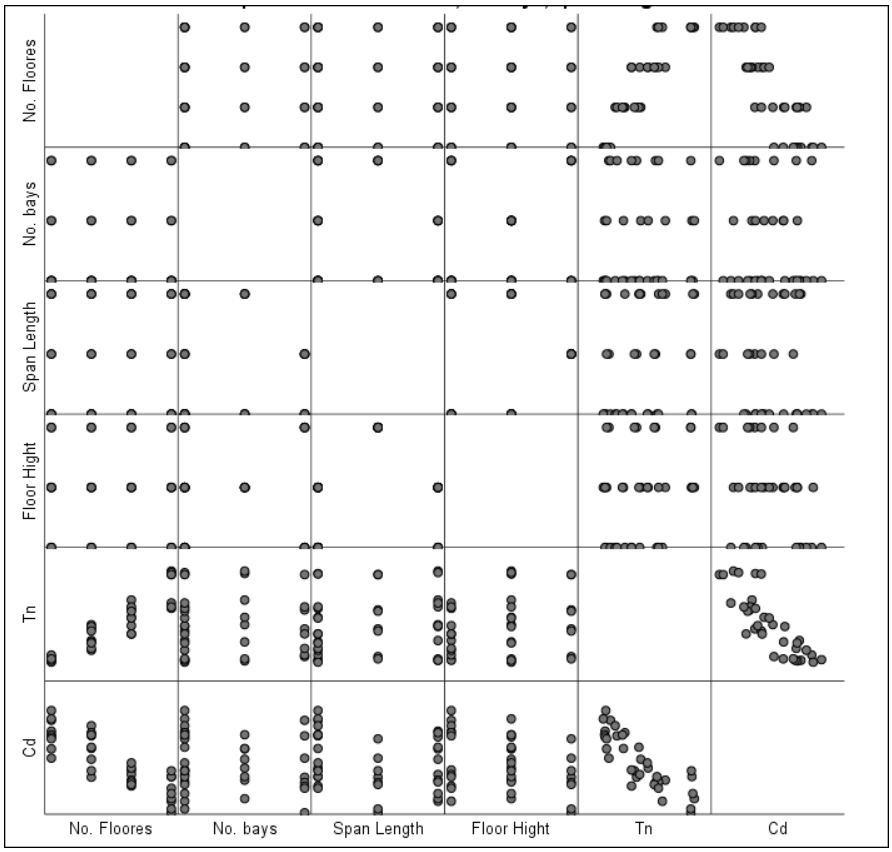

Figure B. 28

The residual errors for Cd equation devloped by regression analysis

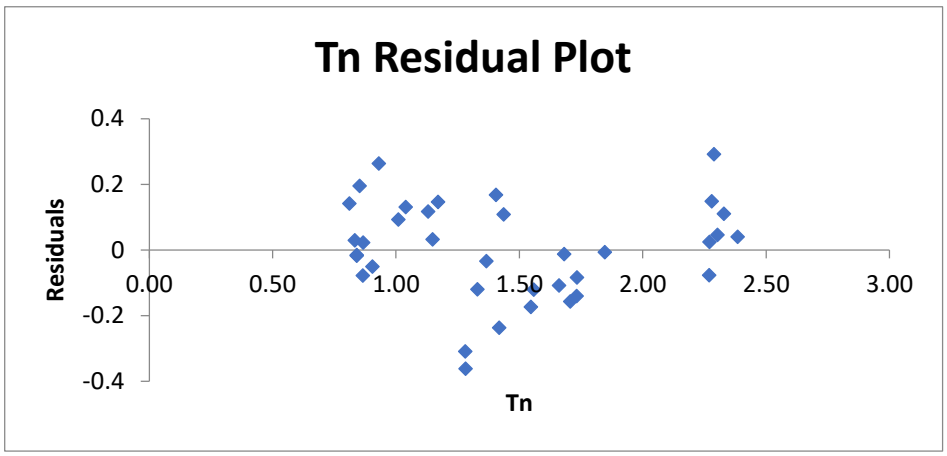

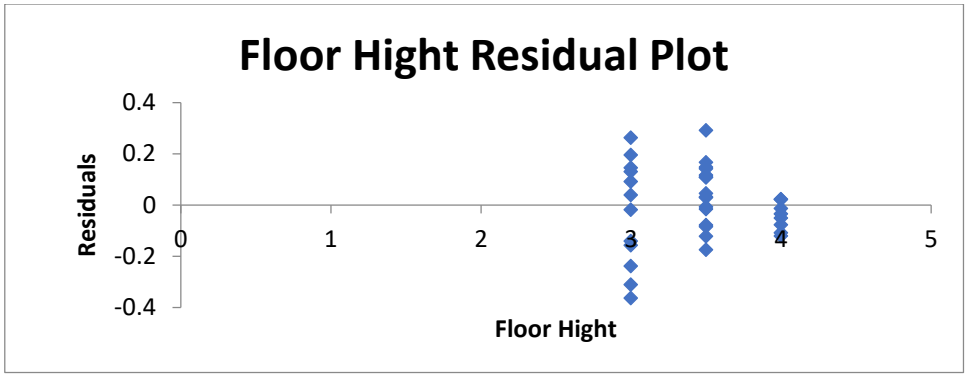

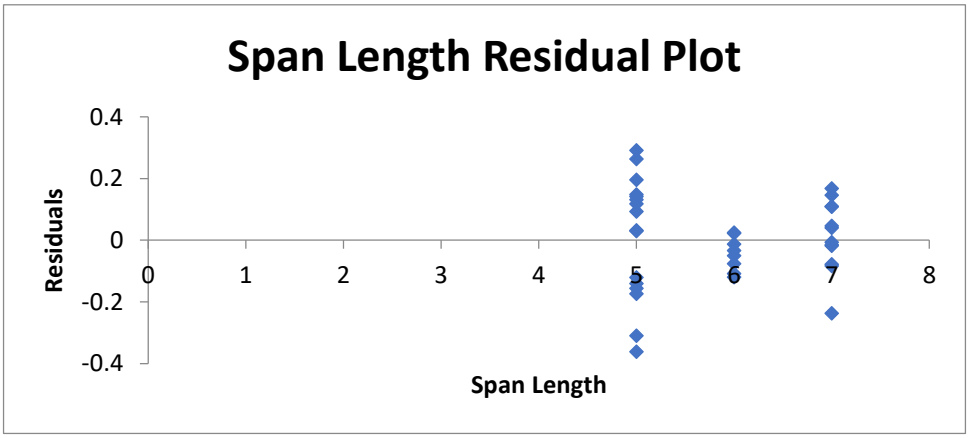

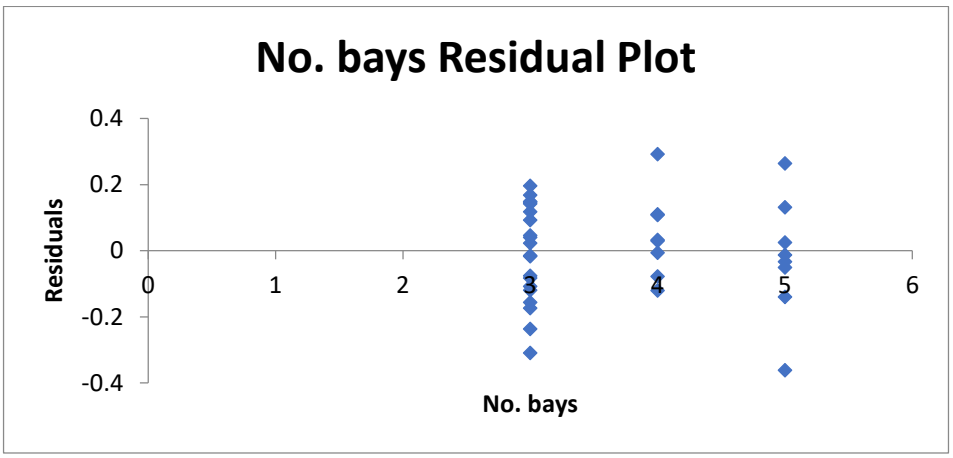

Figure B. 29

C_d normalization through dividing the coefficient (C_d) for each system by the minimum C_d value versus the floor number

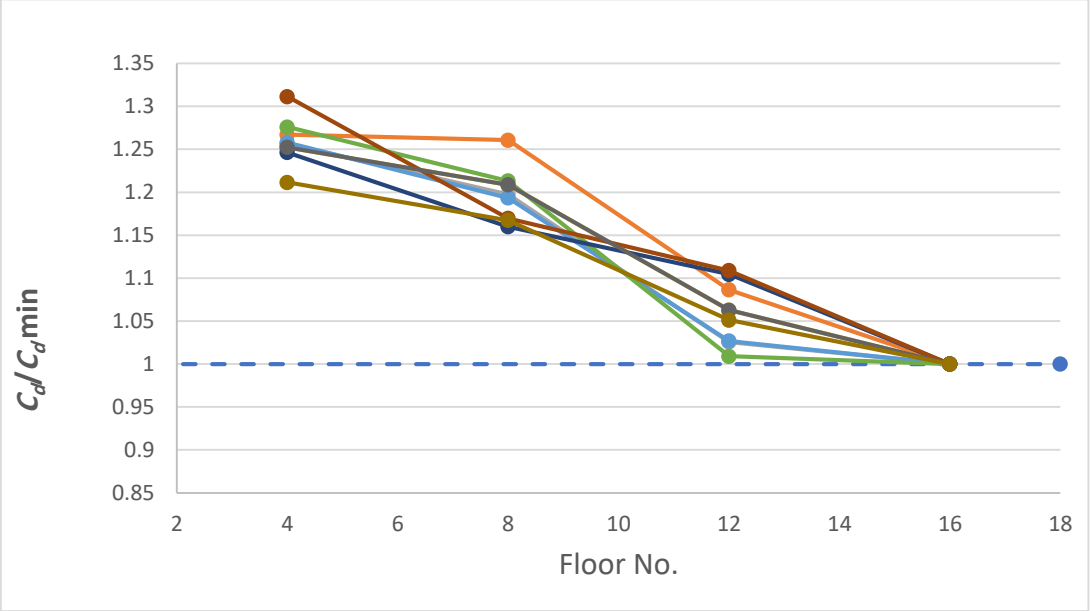

Figure B. 30

General Structural Response

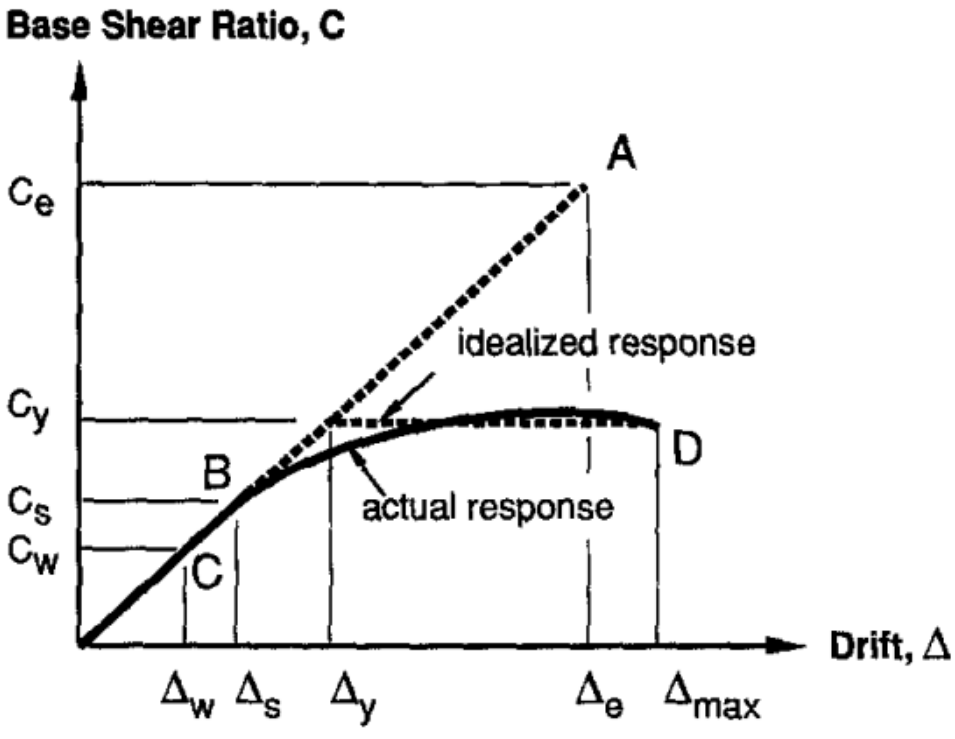

Figure B. 31

Elastic and inelastic displacement through each floor by linear and nonlinear time history analysis for three records

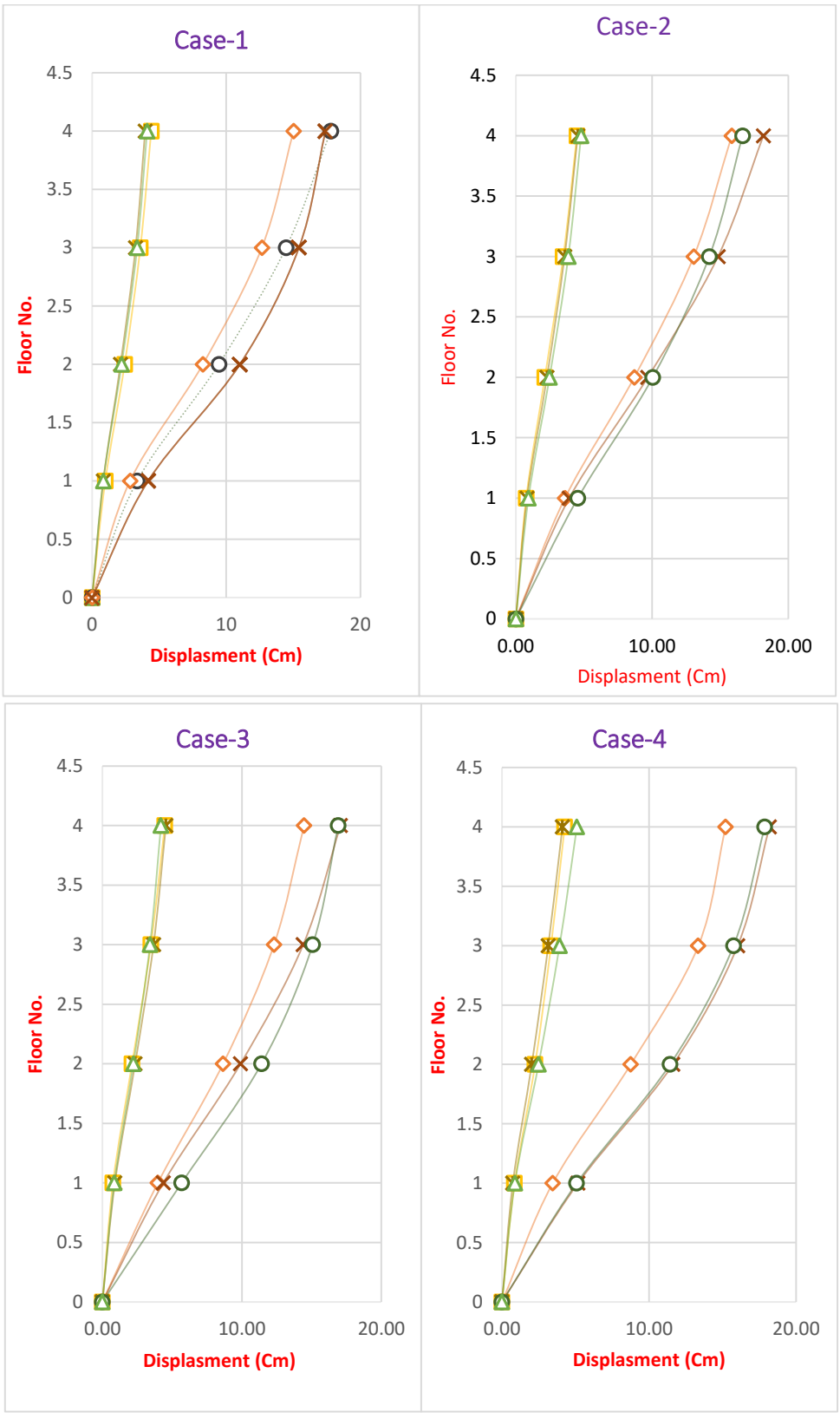

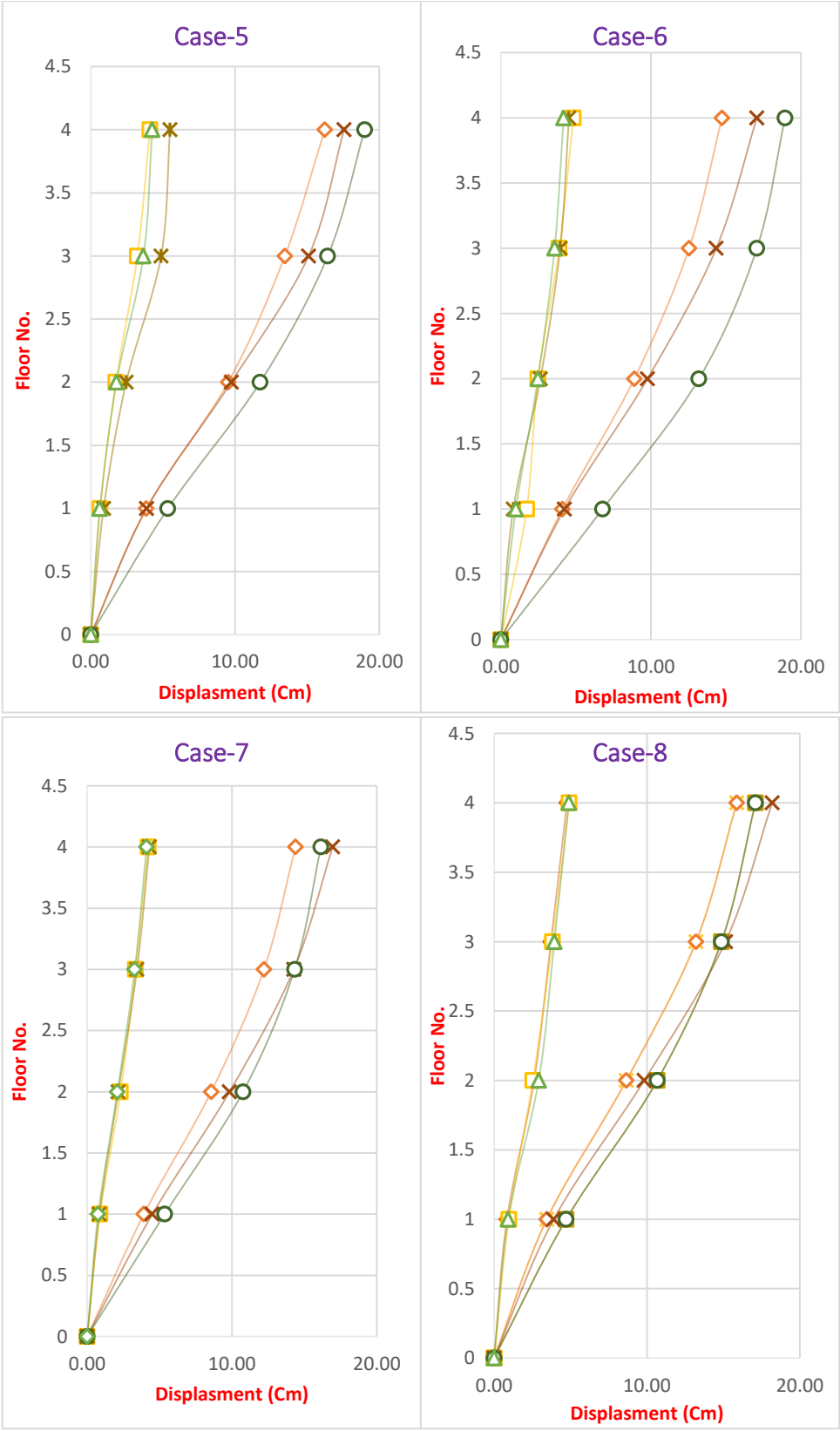
Case-5
Floor No.
Displasment (Cm)
0
0.5
1
1.5
2
2.5
3
3.5
4
4.5
0.00
10.00
20.00
Case-6
Floor No.
Displasment (Cm)
Case-7
Floor No.
Displasment (Cm)
Case-8
Floor No.
Displasment (Cm)

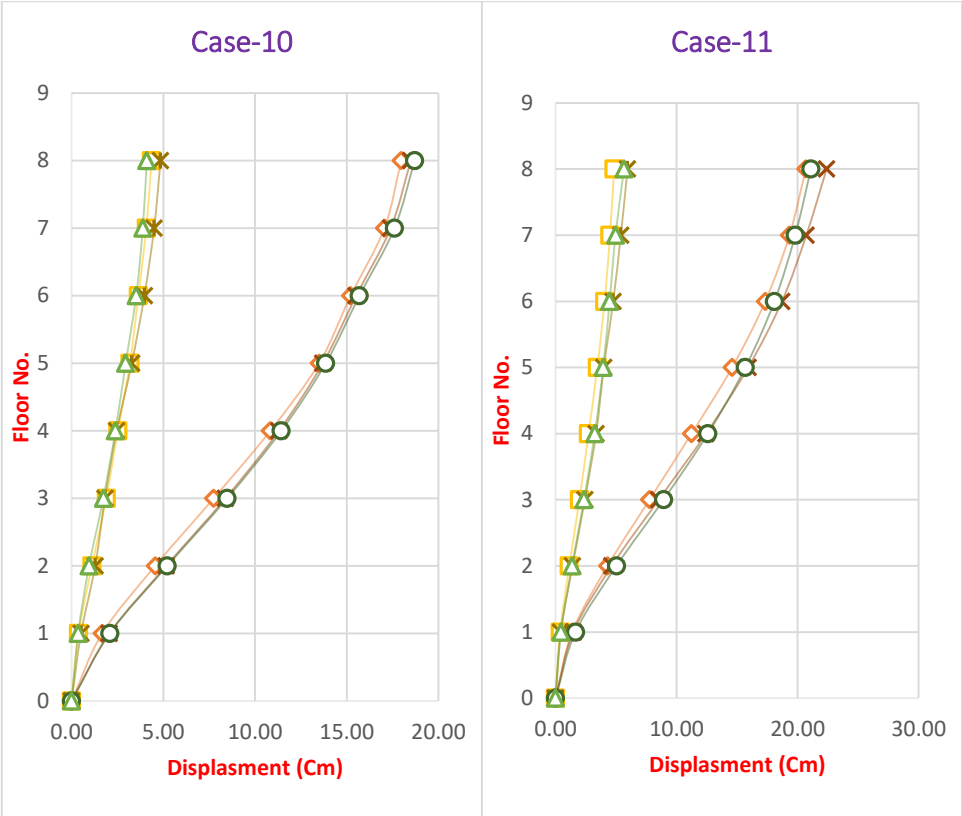
Case-10
Floor No.
Displasment (Cm)
0
1
2
3
4
5
6
7
8
9
0.00
5.00
10.00
15.00
20.00

Case-11
Floor No.
Displasment (Cm)
0
1
2
3
4
5
6
7
8
9
0.00
10.00
20.00
30.00

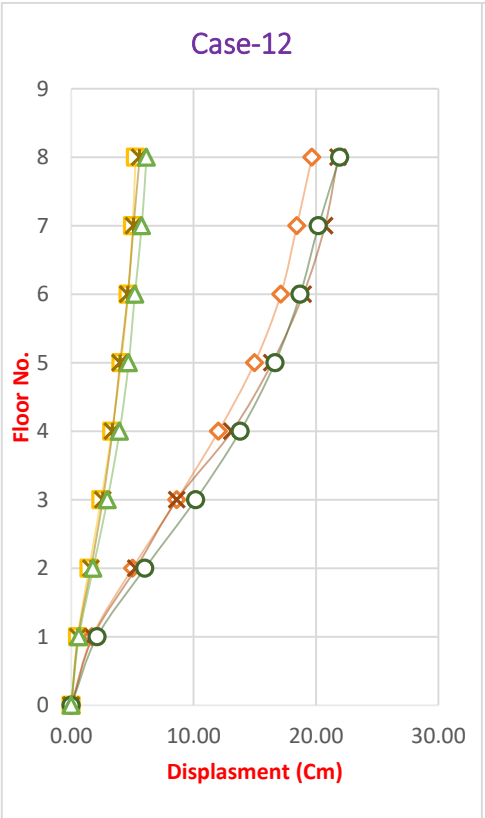
Case-12
Floor No.
Displasment (Cm)
0
1
2
3
4
5
6
7
8
9
0.00
10.00
20.00
30.00

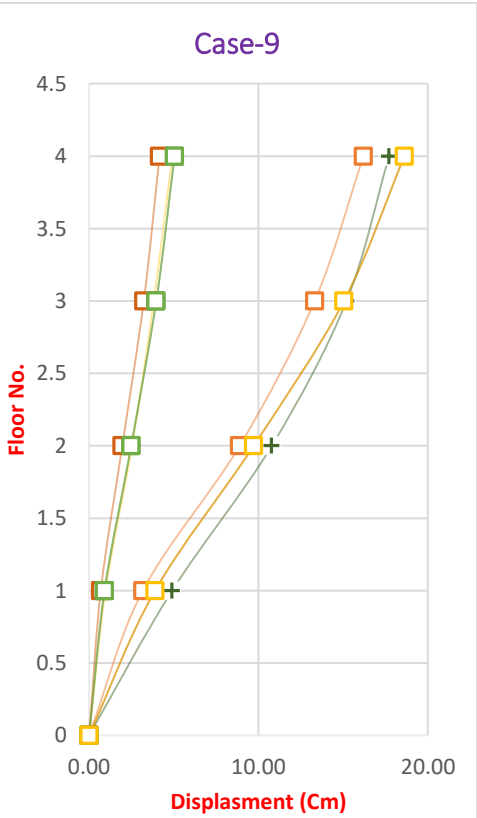
Case-9
Floor No.
Displasment (Cm)
0
0.5
1
1.5
2
2.5
3
3.5
4
4.5
0.00
10.00
20.00

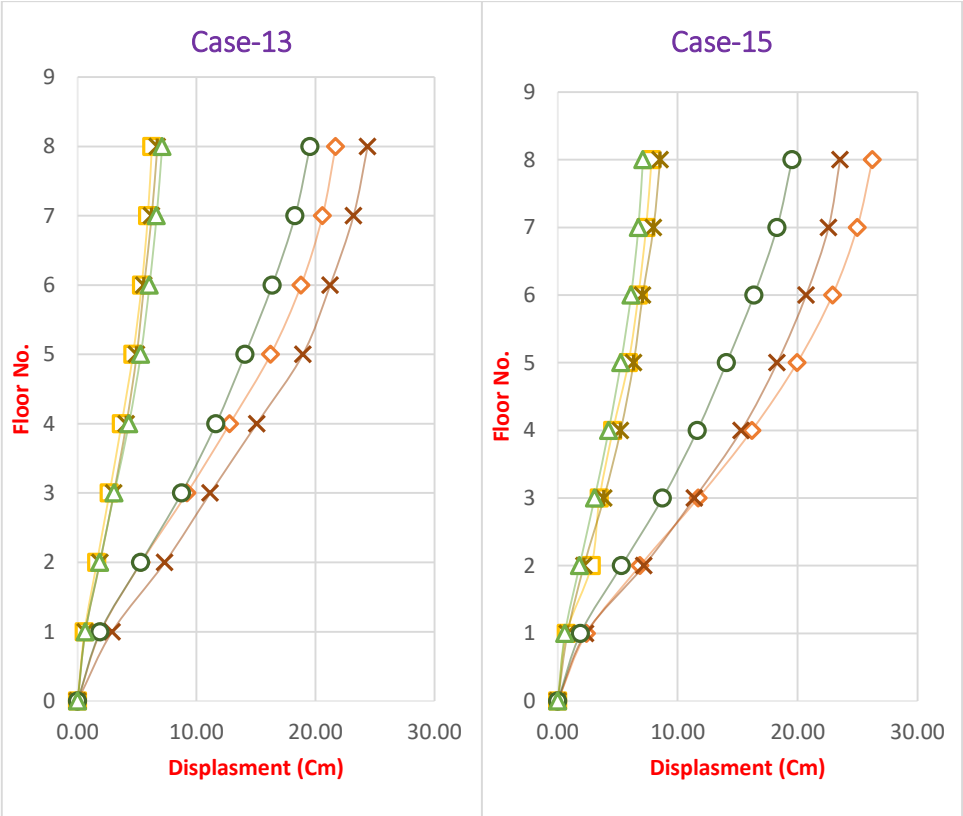
Case-13
Floor No.
Displasment (Cm)
0
1
2
3
4
5
6
7
8
9
0.00
10.00
20.00
30.00

Case-15
Floor No.
Displasment (Cm)
0
1
2
3
4
5
6
7
8
9
0.00
10.00
20.00
30.00

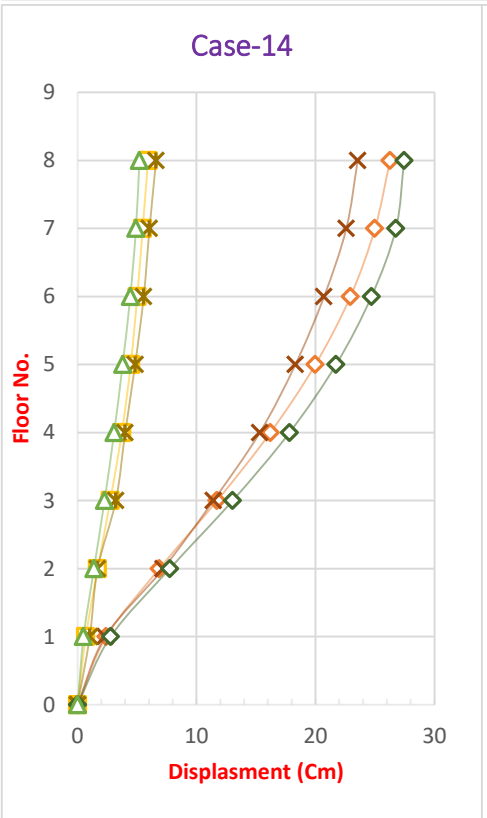
Case-14
Floor No.
Displasment (Cm)
0
1
2
3
4
5
6
7
8
9
0
10
20
30

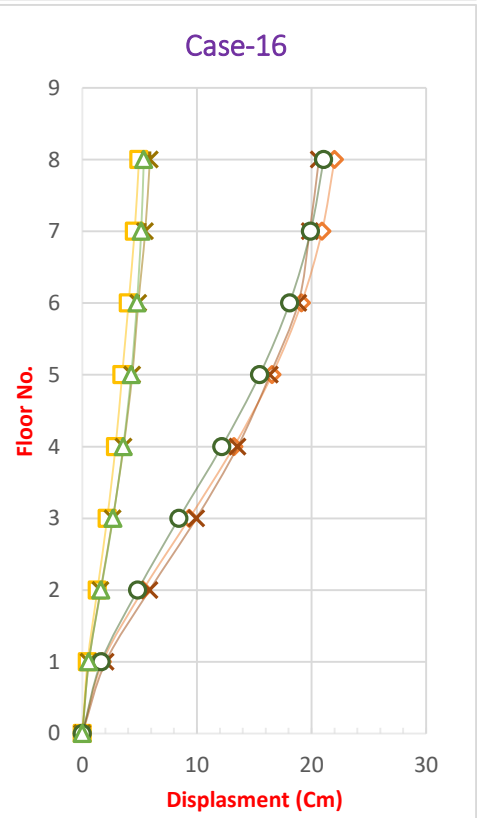
Case-16
Floor No.
Displasment (Cm)
0
1
2
3
4
5
6
7
8
9
0
10
20
30

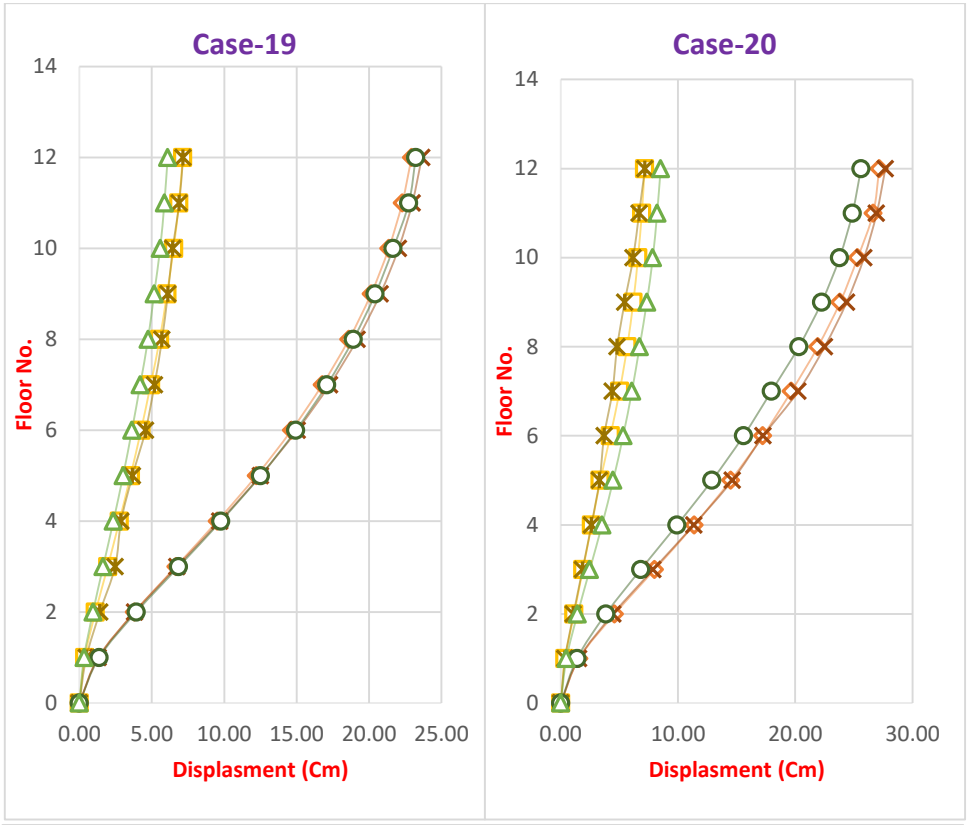
Case-19
Floor No.
Displasment (Cm)
0.00
5.00
10.00
15.00
20.00
25.00
Case-20
Floor No.
Displasment (Cm)
0.00
10.00
20.00
30.00

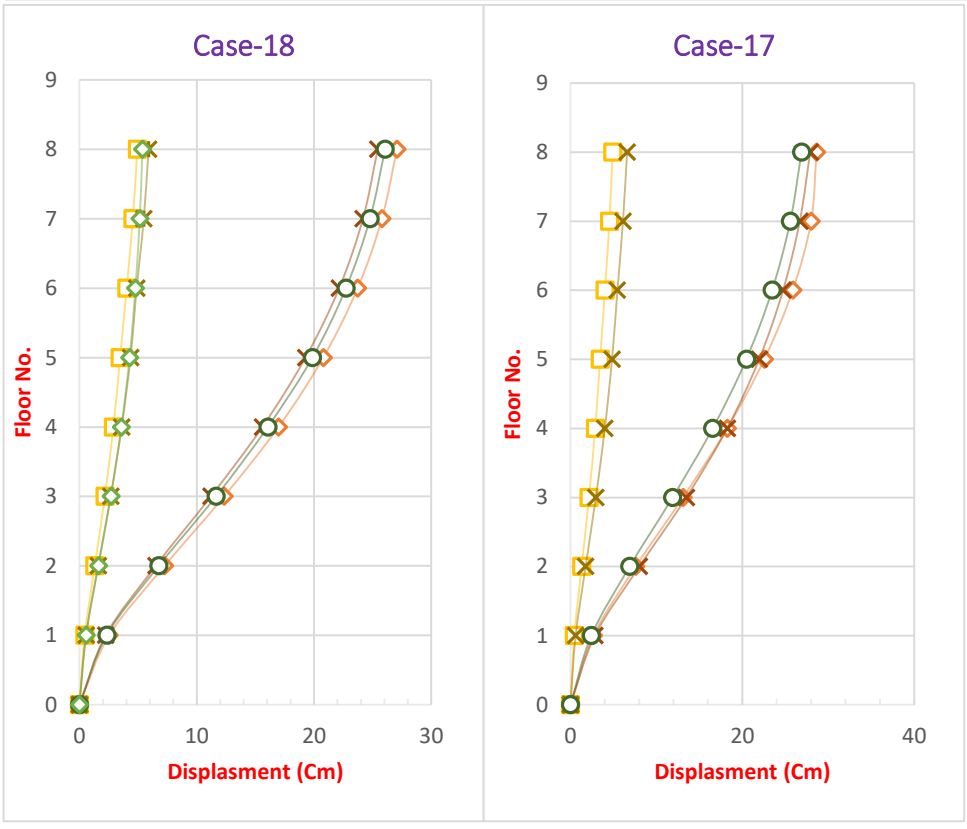
Case-18
Floor No.
Displasment (Cm)
0
10
20
30
Case-17
Floor No.
Displasment (Cm)
0
20
40

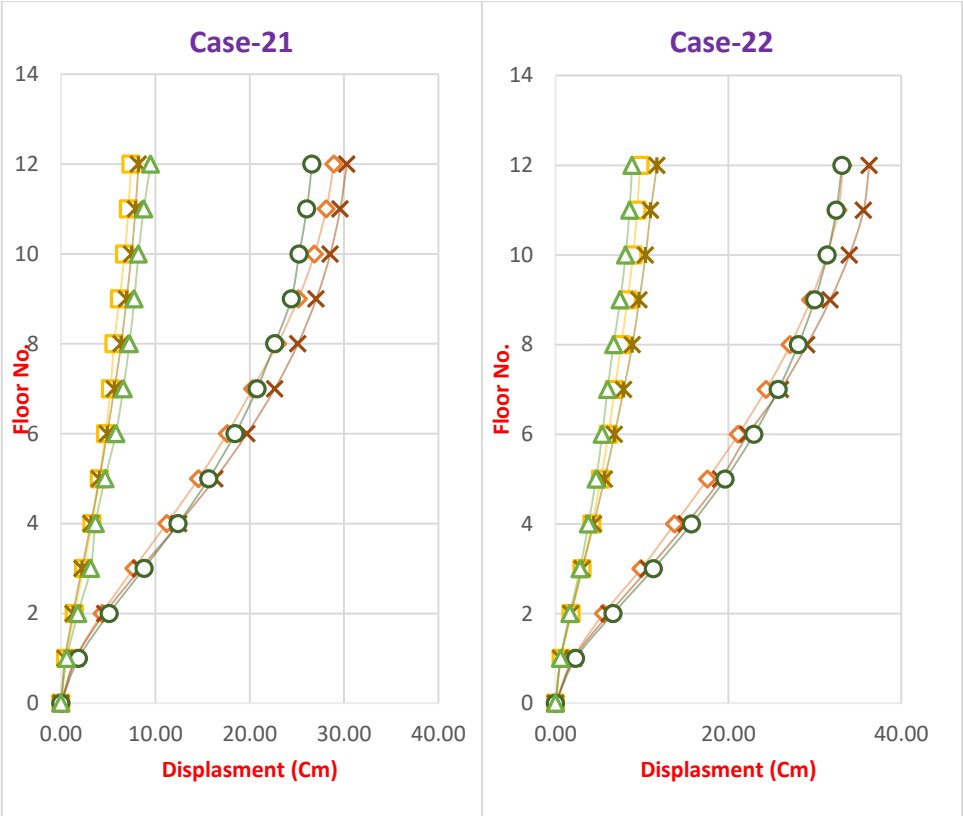
Case-21
Floor No.
Displasment (Cm)
0
2
4
6
8
10
12
14
0.00
10.00
20.00
30.00
40.00

Case-22
Floor No.
Displasment (Cm)
0
2
4
6
8
10
12
14
0.00
20.00
40.00

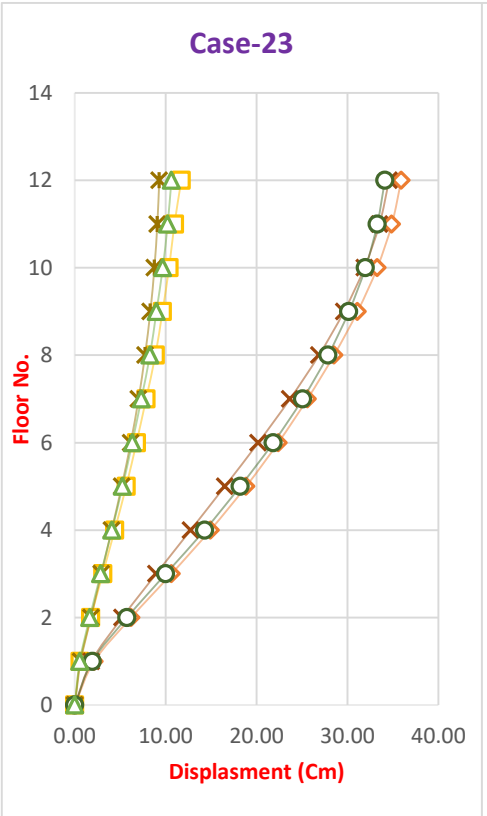
Case-23
Floor No.
Displasment (Cm)
0
2
4
6
8
10
12
14
0.00
10.00
20.00
30.00
40.00

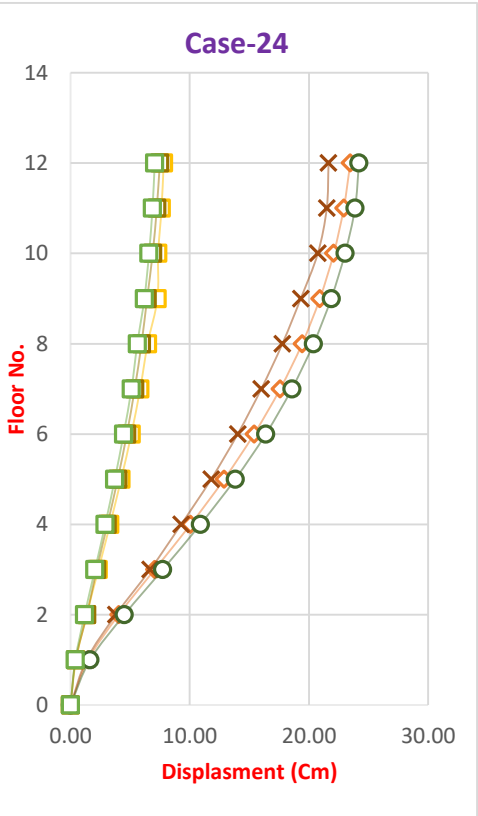
Case-24
Floor No.
Displasment (Cm)
0
2
4
6
8
10
12
14
0.00
10.00
20.00
30.00

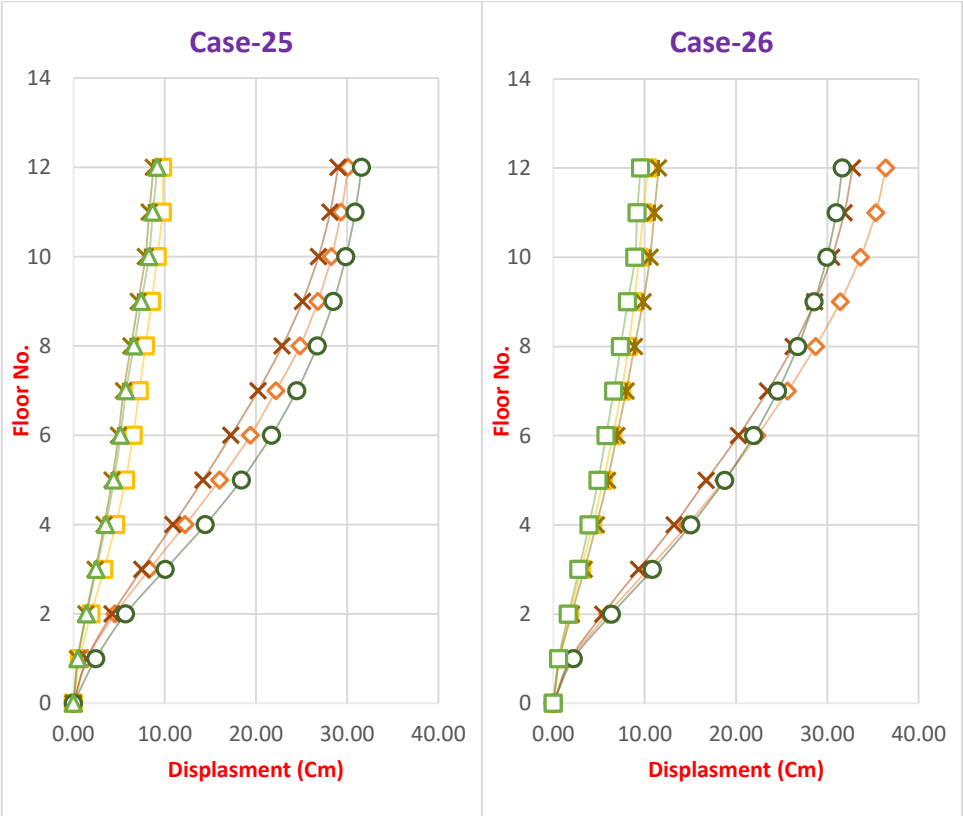
Case-25
Floor No.
Displasment (Cm)
0
2
4
6
8
10
12
14
0.00
10.00
20.00
30.00
40.00

Case-26
Floor No.
Displasment (Cm)
0
2
4
6
8
10
12
14
0.00
10.00
20.00
30.00
40.00

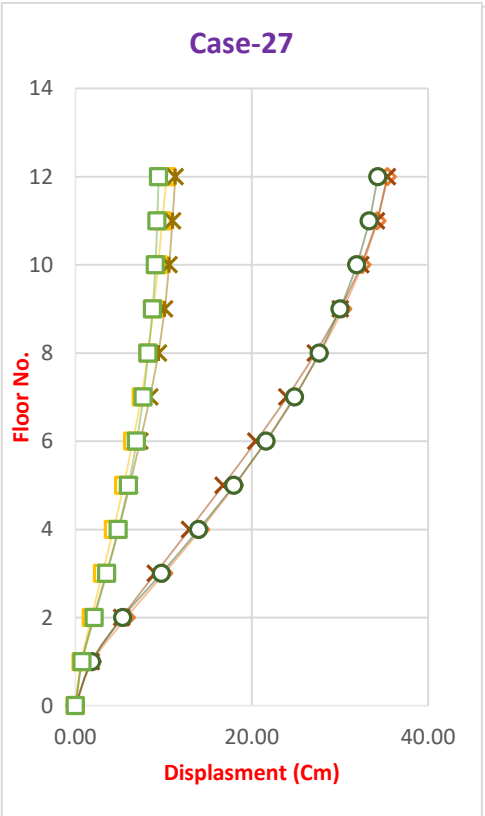
Case-27
Floor No.
Displasment (Cm)
0
2
4
6
8
10
12
14
0.00
20.00
40.00

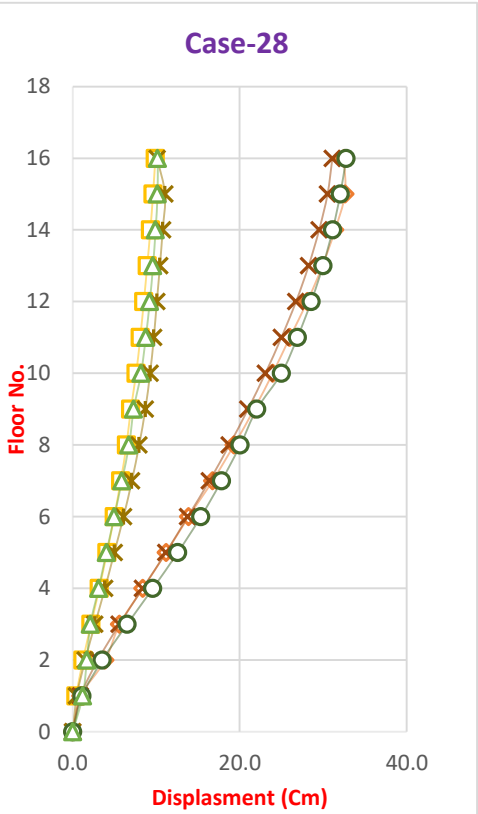
Case-28
Floor No.
Displasment (Cm)
0
2
4
6
8
10
12
14
16
18
0.0
20.0
40.0


Case-29
Floor No.
Displasment (Cm)
0
2
4
6
8
10
12
14
16
18
0
20
40
60

Case-30
Floor No.
Displasment (Cm)
0
2
4
6
8
10
12
14
16
18
0.00
20.00
40.00
60.00

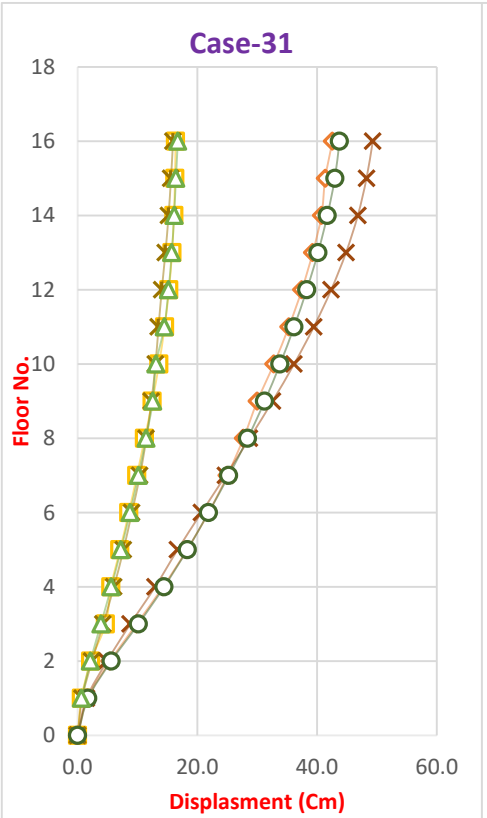
Case-31
Floor No.
Displasment (Cm)
0
2
4
6
8
10
12
14
16
18
0.0
20.0
40.0
60.0

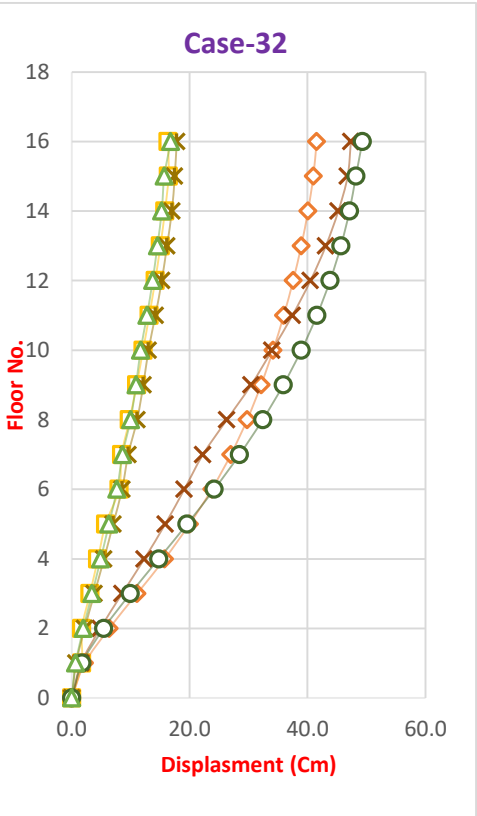
Case-32
Floor No.
Displasment (Cm)
0
2
4
6
8
10
12
14
16
18
0.0
20.0
40.0
60.0


Case-33
Floor No.
Displasment (Cm)
0
2
4
6
8
10
12
14
16
18
0.0
20.0
40.0

Case-34
Floor No.
Displasment (Cm)
0
2
4
6
8
10
12
14
16
18
0.0
20.0
40.0
60.0


Case-35
Floor No.
Displasment (Cm)
0
2
4
6
8
10
12
14
16
18
0.0
20.0
40.0
60.0

Case-36
Floor No.
Displasment (Cm)
0
2
4
6
8
10
12
14
16
18
0.0
20.0
40.0
60.0

Appendix C

Validation of the model for design

To validate the model for design, three checks are conducted :

1- **A compatibility check** is an essential step in structural analysis software such as ETABS to ensure the integrity of the model before applying loads. During this process, the software verifies that all elements within the model are properly connected at shared nodes, lines, and edges.

This verification is crucial because inaccuracies or errors in the model's geometry can lead to unrealistic or unreliable results when applying loads and performing analyses. By ensuring that all elements are correctly jointed and connected, the compatibility check helps to guarantee the structural integrity and accuracy of the model.

This process typically involves the software examining the connectivity of nodes, lines, and edges within the model, identifying any discrepancies or inconsistencies that may exist. If any issues are detected, the software may provide warnings or prompts for the user to address and correct these issues before proceeding with further analysis.

Figure C. 1

The deformed shape of the structure, indicating its compatibility, was obtained from ETABS

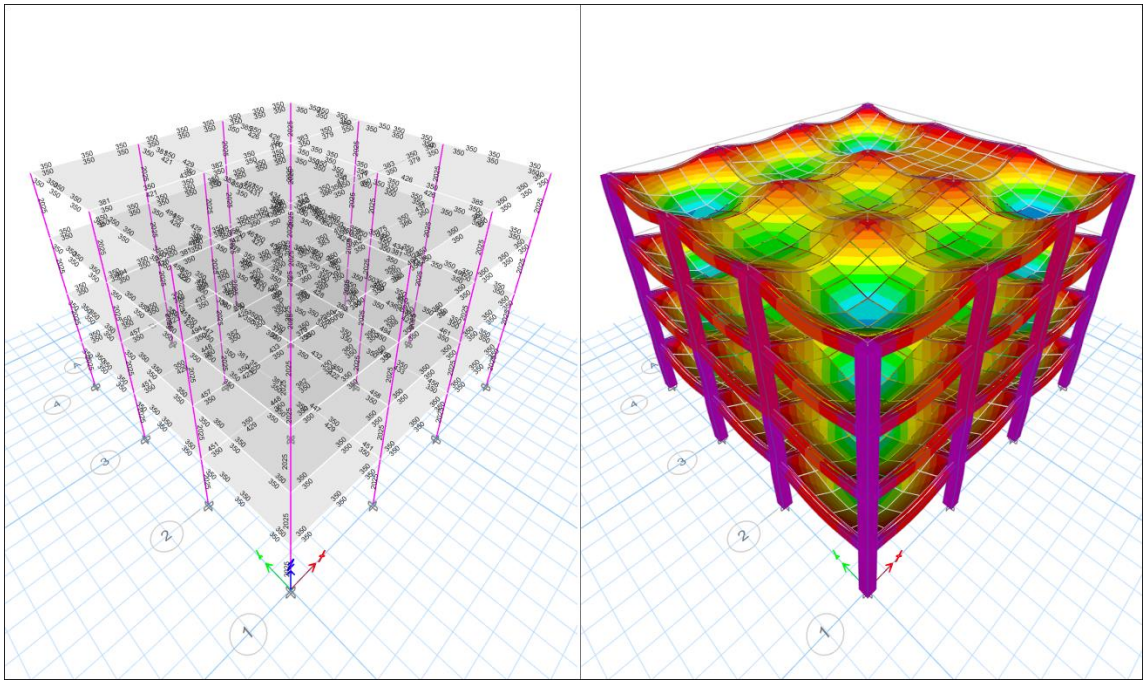

2- **Equillibrium check** is a fundamental aspect of structural analysis used to verify that the forces and moments acting on a structure are in balance. This check ensures that the structure is stable and that there are no unaccounted for or excessive loads that could lead to failure.

During an equilibrium check, the software calculates the sum of forces and moments acting on each element of the structure, as well as at various points or joints within the structure. The calculated forces and moments are then compared to ensure that they satisfy the principles of static equilibrium, where the sum of forces and moments in any direction or about any point equals zero.

If the calculated forces and moments are not in equilibrium, it indicates that there may be errors or inconsistencies in the structural model, such as missing loads, incorrect boundary conditions, or inaccuracies in the geometry or material properties. In such cases, adjustments may need to be made to the model to achieve equilibrium and ensure the accuracy and reliability of the structural analysis results.

Table C.1 provide the comparing between the manually calculated loads with the results obtained from the ETABS program for the loads acting on the supports.

Table C. 1

The equilibrium check

Loads	**Area**	**load (Kn/m2)**	**ETABS reaction (kN)**	**Manual (kN)**	**%error**
Live load	900	4	3600	3600	0%
Superimposed Dead load	900	3	2700	2700	0%
Dead load	density	Volume (m^3)	ETABS reaction (kN)	Manual (kN)	
1-Slabes	23.5631	180	4241.358		
2-Beames	23.5631	54	1272.4074		
3- columns	23.5631	34.02	801.616662		
total			6315.382062	6316.533	0%

3- **The internal force check** is performed to verify the accuracy of ETABS in calculating internal forces within a structure. This check involves analyzing the moments or bending forces present within structural elements such as beams, columns, and slabs. By comparing the calculated internal moments from ETABS with theoretical or hand-calculated values, engineers can assess the software's accuracy in predicting the distribution of forces within the structure. This validation process is crucial for ensuring the reliability and trustworthiness of ETABS 's analysis results, which are vital for designing safe and efficient structures.

To verify internal moment values, employ the Direct Design Method (DDM), a methodology tailored for calculating design moments in two-way slab systems under uniformly distributed loads and equally spaced column support. This method utilizes coefficients and ensures compliance with the constraints outlined in ACI Code 13.6.1.

Figure C. 2

Column and middle strips' width for the slab

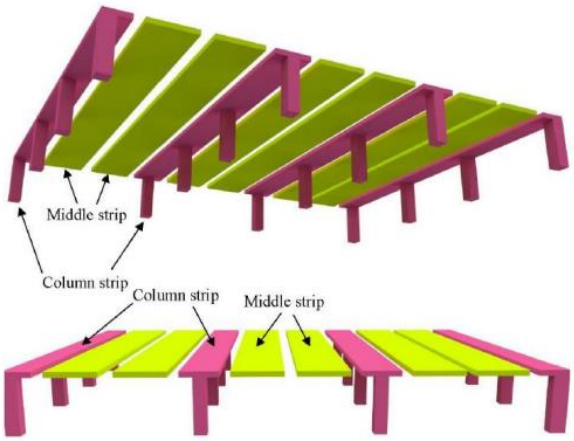

the DDM strategy hinges upon dividing the slab into distinct sections known as column strips and middle strips.

Column strips refer to the regions of the slab that are positioned directly above and adjacent to the supporting columns. These strips typically bear a significant portion of the load transferred from the superstructure to the columns. Consequently, they are subjected to higher bending moments and shears compared to the middle strips.

On the other hand, middle strips are the areas of the slab situated between the column strips. These sections typically experience lower loads and are characterized by relatively smaller bending moments and shears compared to the column strips.

The calculations below compare the manual solution with the results from the ETABS software.

Effective width of beam = 0.25m.

- Calculation of Ultimate Load

$$qu = 1.2\,DL + 1.6\,LL$$

$$qu = 1.2(3 + (0.2x23.5631) + 1.6x4) = 10.86$$

- Computation of Total Static Factored Moment (Mo)

$$Mo = \frac{qul_2{l_{n1}}^2}{8} = 140.46\,Kn.m^2$$

- Negative and positive moment values

  (L2 = 5m, L1 = 5m, MS width = 5m, CS width = 2.5m, ln1 = 4.55m).

$$\mathrm{M}_{+\mathrm{ive}} = 0.35\mathrm{x\ Mo} = 0.35 * 140.46\ Kn.m^2 = 49.159\ Kn.m^2$$

$$\mathrm{M}_{-\mathrm{ive}} = 0.65\mathrm{x\ Mo} = 0.65 * 140.46\ Kn.m^2 = 91.30\ Kn.m^2$$

- Negative and positive moment magnitudes within column strips of a slab and beams

$$M_{+ve}(CSslab) = \frac{49.159\ x0.75x0.15}{(2.5\ -\ 0.25\ )} = 2.46\ Kn.m^2$$

$$M_{-ve}(CSslab) = \frac{91.30\ x0.75x0.15}{(2.5\ -\ 0.25\ )} = 4.56\ Kn.m^2$$

$$M_{+ve}(CSbeam) = 49.159\ x0.75x0.85\ = 31.33\ Kn.m^2$$

$$M_{-ve}(CSbeam) = 91.30\ x0.75x0.85\ = 58.20Kn.m^2$$

- The percentage of error between Mu based on the (DDM)

$$ManuallyMu\ =\ 4.56\ kN.m^2\ for\ Slab\ and\ Nigative$$

$$ByEtabs\quad Mu\ =\ 4.08\ kN.m^2\ for\ Slab\ and\ Nigative$$

% of error 10.5 % < 25 % which is an acceptable error.

Appendix D

Model Design

1- **To design a structure for strength**, must analyze the loads the structure will face, such as gravity loads, wind loads, and seismic forces. Then, determine the suitable cross-section for the structural members, considering factors like the material strength, span of the member, and the applied loads. This involves selecting an appropriate shape (e.g., beam, column, or slab) and dimensions (width, depth, and thickness) to ensure the member can carry the required loads without failing.

Additionally, the requires area of steel reinforcement calculate to provide adequate tensile strength and ductility to the structure. This involves determining the amount and spacing of steel bars or mesh needed in reinforced concrete members or steel sections in steel structures. The goal is to ensure that the structure can withstand applied loads while also considering factors such as deflection limits and serviceability criteria.

Figure D. 1

design a structure for strength

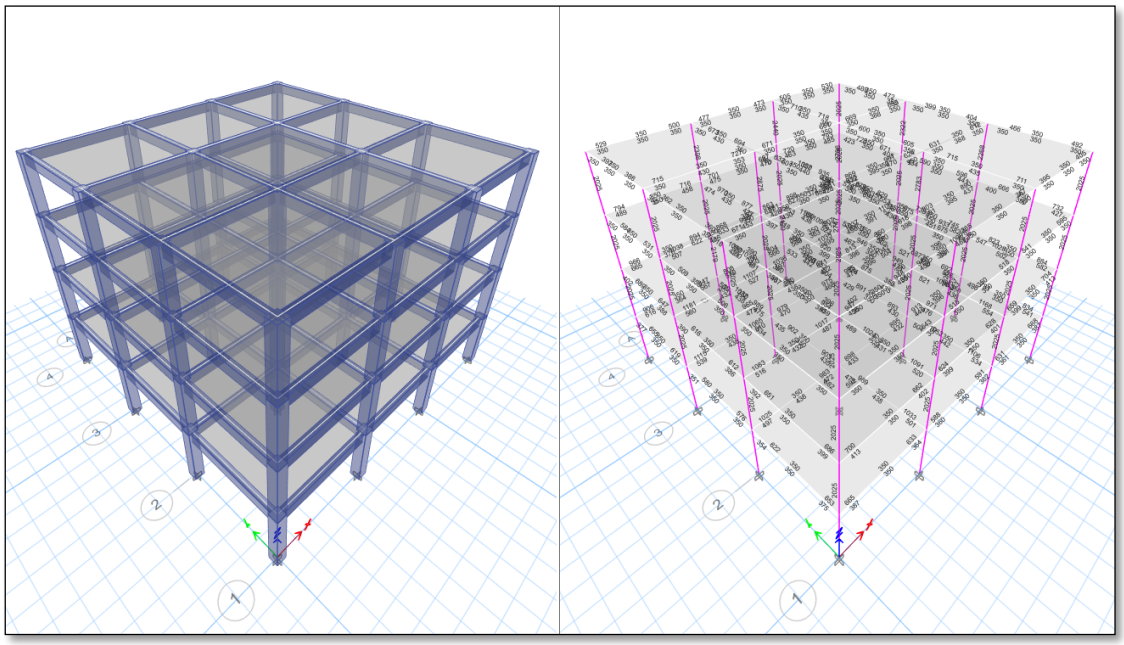

2- **Checking a structure for drift** involves assessing its lateral displacement or movement under various loads, such as wind or seismic forces. Drift is a critical consideration in structural design because excessive drift can lead to damage or failure of the structure and compromise safety.

To check a structure for drift according of ASCE7-16, need to analyze its response to lateral loads using structural analysis software or manual calculations. then assess factors such as building geometry, stiffness, and the distribution of lateral loads to predict the expected drift.

Once the drift is calculated, need to us table 12-12-1 in ASCE7-16 Code that to compare it against allowable limits specified in building codes or design standards. These limits are based on factors such as building function, occupancy, and structural materials.

If the calculated drift exceeds allowable limits, need to modify the structural design by adjusting member sizes, increasing stiffness through additional bracing or shear walls, or implementing damping systems to reduce drift.The table below illustrates the process of checking a structure for drift.

Table D. 1

Checking a structure for drift

Story	Drift	delta inelastic	MAX
Story4	0.002311	0.011555	0.02
Story3	0.003385	0.016925	0.02
Story2	0.003793	0.018965	0.02
Story1	0.002242	0.01121	0.02

3- **Checking a structure for P-Delta** effect involves considering the interaction between lateral loads and the resulting deformations due to axial loads. This phenomenon, known as the P-Delta effect, is particularly significant in tall or slender structures subjected to lateral loads like wind or seismic forces.

The P-Delta effect arises from the fact that lateral displacements induced by these loads can cause additional moments in the structure due to the resulting axial deformations. This additional moment can further amplify the lateral displacement, leading to a potentially significant increase in structural response .

Referred to Section 12.8.7 in ASCE 7-16 which describes check the P-Delta effect.

Table 3-9 provides how Checking a structure for P-Delta.

Table D. 2

Checking a structure for P-Delta effect

Story	P (Kn)	K	story height (m)	Ø	Ø max	Check
Story4	12927.9	183183.4	3	0.023525	0.1	OKAY
Story3	26899.1	293115.2	3	0.03059	0.1	OKAY
Story2	40870.2	367193.6	3	0.037101	0.1	OKAY
Story1	54841.4	415612.7	3	0.043984	0.1	OKAY

4- **ACI's reinforcement requirements for special frames :** aim to ensure that the frames can adequately resist lateral loads without excessive deformation or failure. These requirements typically include provisions for the design and detailing of reinforced concrete members, such as columns, beams, and shear walls.

ACI's reinforcement requirements for special frames encompass several critical aspects. Firstly, they focus on ensuring that reinforced concrete members possess adequate design strength to withstand lateral loads, factoring in material properties, geometry, and loading conditions. Additionally, these requirements emphasize promoting ductile behavior within the structure, allowing for force redistribution and energy dissipation during seismic events, often achieved through specified reinforcement ratios and detailed enhancements.

Figure A.1through **Figure A.36** Show 36 case study elastic and inelastic Displacement Vs floor Number

جـامعـــة النجاح الوطنية
كليـــة الدراســـات العليـــا

استكشاف العلاقة بين معامل تضخيم الانحراف والزمن الدوري في هياكل الخرسانية المسلحة من النوع النظام الإنشائي الإطارات المقاومة للعزوم

إعداد
مراد ربحي حسين بشارت

إشراف
د. منذر دويكات
د. منذر ابراهيم ذياب

قدمت هذه الأطروحة استكمالا لمتطلبات الحصول على درجة الماجستير في هندسة الإنشاءات، من كلية الدراسات العليا، في جامعة النجاح الوطنية، نابلس –فلسطين.

2024

استكشاف العلاقة بين معامل تضخيم الانحراف والزمن الدوري في هياكل الخرسانية المسلحة من النوع النظام الانشائي الاطارات المقاومة للعزوم

إعداد

مراد ربحي حسين بشارت

اشراف

د. منذر دويكات

د. منذر ابراهيم ذياب

الملخص

يعد عامل تضخيم الانحراف (C_d) عاملاً حاسماً في التصميم الزلزالي، خاصة عند تصميم الهياكل في المناطق المعرضة للزلازل. فهو يضمن قدرة الهيكل على تحمل القوى الديناميكية أثناء الأحداث الزلزالية مع الحفاظ على مستويات انحراف مقبولة. يعد المعامل C_d ضروريًا في التصميم الزلزالي وفقًا لمعايير الحد الأدنى لحمل التصميم للجمعية الأمريكية للمهندسين المدنيين ASCE7-16، خاصة عند تقييم الانجراف والفاصل الزلزالية بين المباني.

في ASCE7-16، يتم استخدام عامل C_d لحساب الإزاحة غير المرنة عن طريق ضربها في الإزاحة المرنة. يعد الإزاحة غير المرنة أمرًا بالغ الأهمية لحساب الفاصل الزلزالي (المسافة بين مبنيين متجاورين).

يبقى المعامل C_d ثابتًا لنفس النظام الهيكلي، وفقًا لـ ASCE7-16، بغض النظر عن طبيعة تردد للمبنى. والعوامل التي يرتبط بها (T_n). تهدف هذه الدراسة إلى إيجاد علاقة بين قيمة C_dالتردد المبنى.

الهدف هو تحسين الاستجابة الزلزالية وتقليل الفاصل الزلزالي خاصة بالنسبة للمباني الشاهقة، وهو ما يمثل دائمًا تحديًا أثناء التصميم والبناء. ولتحقيق هذا الهدف، تم فحص العوامل المختلفة المرتبطة بخصائص المبنى (ارتفاع المبنى، وطول الجسر، وارتفاع الطابق، وعدد الخلجان) التي قد تؤثر على قيمة C_d. بعد ذلك تم اقتراح معادلة يحدد من خلالها قيمة C_d لكل بمبنى بالاعتماد على خصائصه الفريدة.

ولتحقيق هذا الهدف البحثي، تم تحليل 36 دراسة حالة لنموذج بناء مربع الشكل بأعداد مختلفة من الطوابق (4، 8، 12، و16 طابقا)، وارتفاع الأرضية، وطول جسر، وعدد الخلجان، باستخدام كل من التحليل التاريخ الزمني الخطي وغير الخطي.

يتم استخدام برنامج ETABS للتصميم الهيكلي الشامل مع الأخذ في الاعتبار الاحمال الجاذبية والزلزالية (وهذا يشمل تصميم الهيكل للقوة، والتحقق من الانجراف، وP-delta، والالتزام بمتطلبات تفاصيل التعزيز المحددة في كود ACI 318).

تم إجراء استجابات التاريخ الزمني غير الخطي باستخدام برنامج SAP2000 للعناصر المحدودة من خلال تحليل البلاستيك المرن المتزايد، مع التركيز على اللدونة المركزة داخل العناصر الهيكلية.

إن عامل C_d هو قيمة ثابتة حسب ASCE 7-16، وقد ثبت من خلال النتائج التحليلية أنه يختلف باختلاف خصائص المبنى بما في ذلك طول الامتداد وارتفاع القصة وعدد الخلجان والفترة الزمنية (T_n). تم تطوير معادلة لتمكين حساب قيمة C_dخاصة كل مبنى.

الكلمات المفتاحية: عامل تضخيم الانحراف، C_d، SMRFs، التاريخ الزمني، طيف الاستجابة، غير الخطية، الفترة الزمنية، المفصلات الليفية.